ADDIS ABABA UNIVERSITY

ADDIS ABABA INSTITUTE OF TECHNOLOGY

SCHOOL OF MECHANICAL AND INDUSTRIAL ENGINEERING

PERFORMANCE ANALYSIS OF HYBRID PHOTOVOLTAIC THERMAL AND HEAT PUMP SYSTEM USING COMPUTATIONAL MODEL

Alemayehu Tenaw Eneyaw

Supervisor: Dr. Ing Demiss Alemu Ambie (Associate professor)

A Dissertation Submitted for the Degree of

Doctor of Philosophy (Ph.D.) in Mechanical

(Thermal and Energy Conversion Engineering)

October 21 2020

Addis Ababa, Ethiopia

ADDIS ABABA UNIVERSITY

ADDIS ABABA INSTITUTE OF TECHNOLOGY

SCHOOL OF MECHANICAL AND INDUSTRIAL ENGINEERING

PERFORMANCE ANALYSIS OF HYBRID PHOTOVOLTAIC THERMAL AND HEAT PUMP SYSTEM USING COMPUTATIONAL MODEL

Alemayehu Tenaw Eneyaw

Approved by bord of Examiners

Dr.Yilma Tadesse	_____	_____
Dean, School of mechanical and	Signature	Date
Industrial Engineering		
Dr. Ing Demiss Alemu	_____	_____
Supervisor	Signature	Date
Professor Feng C. Lai	_____	_____
External Examiner	Signature	Date
Dr. Tesfaye Dama	_____	_____
Internal Examiner	Signature	Date
_____	_____	_____
Post Graduate Director	Signature	Date

DECLARATION

I declare that "**Performance Analysis of Hybrid Photovoltaic Thermal and Heat Pump System Using Computational Model"** is the original work of my own, has not been presented for the requirement of graduation at any institute. All the sources that I have used are acknowledged and indicated through referencing. The document is submitted for partial fulfillment of the requirements for the degree of Doctor of Philosophy in Mechanical Engineering (Thermal and Energy Conversion Engineering) at Addis Ababa University.

_____ _____

Alemayehu Tenaw Eneyaw Date

This is to certify that the above declaration made by the candidate is correct to the best of my knowledge.

_____ _____

Dr. Ing Demiss Alemu Ambie (Associate Professor) Date

ACKNOWLEDGMENT

First of all, I would like to thank the Almighty God for safeguarding me up to this time and for giving me the courage to accomplish this dissertation.

Next, my gratitude goes to my supervisor, Dr. Ing. Demiss Alemu (Associate Professor) for his invaluable help and support during my stay in the Ph.D. program. His insightful, persistent guidance, full of readiness all the time to lend his hand and the tremendous effort he did on this research work is very special. Thus, I can consider myself as I am one of the fortunate advisees to work under his supervision.

I would like also to forward my great appreciation to the Ethiopian Metrological Agency and Numerous PV/T-heat pump manufacturers for giving me valuable solar data and quoting the good price of the equipment. It is my fortune to gratefully acknowledge Addis Ababa University School of Mechanical and Industrial Engineering for accepted as a student. I am very grateful to my home University, Woldia University, for the sponsorship and the Department of Mechanical Engineering staff members for their encouragement during my study in the program.

I would like to thank my dedicated sister; Mastewal Tenaw and my wife Mirtezer Zemene for their constant support and love. My father Aya Tenaw you are a reason for my motivation to join and to complete the Ph.D. Program through your priceless moral support. Dear beloved mother Anchatey you are the pillar of my life. I am not confident enough to express my feeling about your encouragement and effort in shaping my life from the time of my early childhood up to now. I would never be able to pay back your favor. I am also very grateful to all my family members; Brother Tamru Mersha, Mulutesfa Tenaw, Tadel Tenaw, HaileGiorges Tenaw, and my lovely and considerate sisters MelkaMariam Tenaw, AtsdeWork Tenaw, and FikerteSellase Tenaw. Thank you very much for all of you, for you are always with me when I need you either in a good or difficult situation.

Last but not least, I wish to express my thankful indebtedness to all my dear office comrades for giving and sharing me a good moment all the time. In fact, you are beyond an academic zone friendship; I suppose a chance to get a true brother in life and I am also very thankful to the

members of St.Giorgis Maheber (Our childhood's schoolmate) for simplifying my life in many ways and showing me the true direction for the academic and social life in general.

ABSTRACT

Renewable energy resources such as solar energy have great potential in meeting electrical and thermal energy demand in off-grid areas of developing countries. Working on this breakthrough and well-tried sector changing the lives of millions of people living in off-grid areas. In recent decades, enduring plenty of studies and development works on solar technology, specifically on the hybrid photovoltaic and thermal collector have been given attention. As a part of this global research and development trend, this research integrates photovoltaic, solar collector, and heat pump (PV/T-heat pump) to one system by combining to deliver both electrical and thermal energy simultaneously or thermal energy alone (hot water).

Cooling of photovoltaic panels by water improves the electrical conversion efficiency and produces warm water as a by-product. The photovoltaic thermal system is being used for the co-generation of electrical energy and hot water. In this study, the annual performance of a glazed photovoltaic thermal system (a combination of PV module and solar flat plate collector) with a storage tank was investigated at first by a dynamic computational model. The PV/T model was developed using MATLAB under the actual hot water demand condition for co-generation of electrical energy and hot water, and simulation was conducted for two locations in Ethiopia, Dire Dawa and Addis Ababa.

The computational model determines the electrical energy production and temperature of water at different points and other components of the PV/T system within a given time interval. Also, summaries of monthly and annual incident solar irradiance, electrical energy generation, thermal energy transported to storage, and thermal energy supplied as hot water to end-users are computed, considering the hourly hot water consumption pattern and storage size effect. The simulation, which is conducted for 20 m^2 PV/T system consists of 12 panels with each 1.65 m^2 module areas resulted in the generation of 803 kWh/year thermal energy and 310 kWh/year electrical energy. The annual average electrical efficiency, thermal efficiency, hot water end-use overall efficiency, and co-generation (PV/T) efficiency of the system were 15.4%, 50.4%, 38%, and 65.8%, respectively. Moreover, the maximum hot water temperature was below 50ºC; hence, the PV/T system can be used for water preheating and reach about half of the heating load in tropical areas besides electrical energy generation.

As the Photovoltaic-thermal system can only be used for preheating water, the warm water can be used as an input to the heat pump water heater to attend required water temperature by the end-user. The electrical energy required by the heat pump water heater will be covered by the electrical energy generated by the PV/T system. It shall be noted that the heat pump uses an average of 1 kW of electricity to generate 3 kW of thermal energy. The hybrid PVT-heat pump system is appropriate and capable to deliver thermal (hot water) and electrical energy to the user either on the domestic or institution scale without an additional alternative source of energy.

The performance of the hybrid PV/T-heat pump system was analyzed and compared in two Ethiopian cities, geographical and environmental representative zones of the highland and lowland regions, namely Addis Ababa and Dire Dawa respectively. The analysis was done on the system COP and outlet hot water temperature in both selected sites considering an illustrative month of the year regarding the solar irradiations availability. Besides, the end-use hourly hot water consumption pattern (variability effect in three dissimilar cases constant, restaurant, and motel) on the system performance was examined.

Eight different heat pump compressor electrical energy consumption scenarios with a constant hourly hot water consumption fraction pattern were analyzed. On those eight different energy consumption patterns cases have been comprehended the effect on the system; COP, hot water temperature delivery value, end-use efficiency, and heat generation capacity of the PV/T-heat pump system.

In those diverse situations, the heat pump system in most of the cases generated above 55℃ annual average hot water temperature, and the system come of an outcome 3 COP were analyzed. Finally, the economic analysis of the system was evaluated. The payback period and the cost of energy were leveled as 16.96 years and 2.16 ETB/kWh, respectively.

Table of Contents

Lists of Figures

Lists of tables

NOMENCLATURE

A: Area;

C_p: Specific heat capacity;

C_w: Specific heat of water;

D_e: External diameter of tube;

E: Electrical energy;

fw: Collector efficiency factor;

G_r: Grash of number;

h: Thermal heat transfer coefficient;

hf_i: Convection heat transfer of storage;

I: Hourly total irradiation;

k: Thermal conductivity;

k_T: Clearness index;

l: Length;

m : Mass;

$\dot{m}$: Mass flow rate of water;

n: Number of days in a year;

N: Number of tubes;

N_u: Nusselt number;

$\dot{Q}_u$: Useful heat;

Ra: Rayleigh number;

T: Temperature;

U_l: Overall loss coefficient;

V: Volume;

V_{wind}: Wind velocity;

Greek Symbols

δ: Declination angle;

φ: Packing factor;

$\emptyset$: Latitude angle of the location;

ρ: Density;

ρ_g: Ground reflection;

β: Inclination angle;

ϖ: Hour angle;

δ: Declination angle;

η_f: Fin efficiency;

η_r: Reference cell efficiency;

$\alpha\tau$: Effective absorptance;

σ: Stefan Boltzmann constant;

β_r: Temperature coefficient;

Subscripts:

a : Ambient Temperature;

b: Beam;

c : Convection, inclined surface collector

cd: Conduction;

d: Diffuse;

el, a: Annual electrical;

f: Fluid;

g : Glass;

hws, a: Annual hot water service;

i: Inlet, insulation;

o: Outlet, Extra-terrestrial irradiation;

p: Absorber Plate;

$p-$i: Between absorber and insulation;

P_{el}: Electrical power;

pv_t, a: Annual photovoltaic thermal;

r: Irradiation, Reference;

st: Storage;

t: Time, Thickness;

th, a: Annual thermal;

w: Water;

wt: Water tube;

Abbreviations:

DWC: Daily hot water consumption in litre;

FF_{ii}: Daily hot water consumption hourly fraction;

pv: Photovoltaic panel;

pvt: Hybrid photovoltaic thermal;

TRNSYS: Transient systems simulation;

PVsyst: Photovoltaic sizing software.

CHAPTER ONE

INTRODUCTION

1.1 Background

Electrical energy consumption has been increasing both in developing and developed countries. The increment of consumption of energy affects the environment due to the emission of a large amount of carbon dioxide into the atmosphere. In Ethiopia, a modern source of fuel covers only 10% of the total energy consumed; the rest is covered by biomass fuels[1], [2]. In the rural part of Africa, only 42% of the community uses modern fuels, which is less compared to 70% of the urban areas [1]. Figure 1-1 shows Ethiopia and world energy production and the supply trend of source diversity. This shows that Ethiopia has a high limitation on the production of diverse energy because the majority of the energy supply is limited to biomass and waste followed by oil and hydro sources [3].

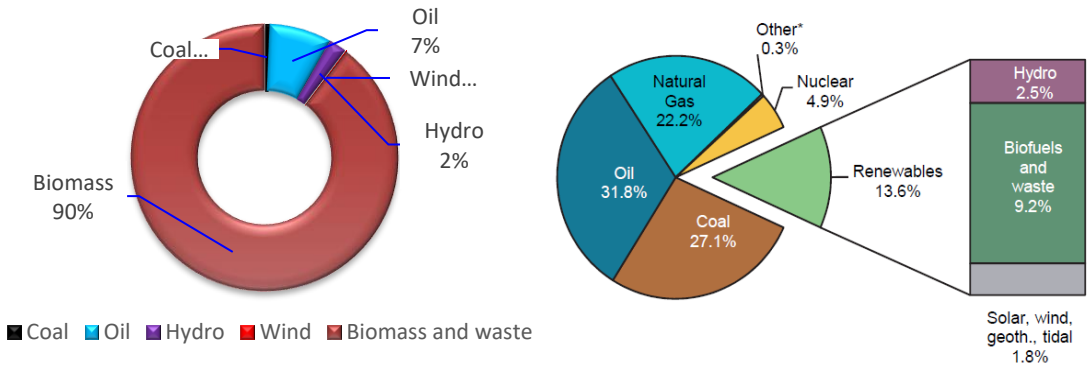

Figure 1-1 Energy supply trend by sources, Ethiopia (left) and the world (right)

Besides the problem of energy resource diversity of Ethiopia had had heaps of weakness on energy generation and supply to the end-user. Among those constraints price variability, preference, and familiarity with the technology, accessibility to the grid, and unreliable service provider organization are major ones. Due to this, household consumers most often choose the traditional sources of energy compared to the modern ones [1].

The Second Growth and Transformation Plan of the Ethiopian government set to increase electricity production to 17,208 MW in 2019/20 from a reference period 2014 of 4,180 MW capacity. The GTP II plan includes diversifying the source of energy in different sectors. A total of 17,208MW were planned to generate 13,817MW and 300MW from hydropower and solar energy, respectively. The production of this energy was supposed to increase electricity access coverage from 60 to 90% [4].

Specifically, it was planned to produce through solar energy 3,600,000 solar lanterns, 400,000 household solar PVs, 3600 institutional solar PVs, and 500 solar thermals. Besides, 3,600 solar cookers were also an integral part of the plan to be achieved in 2019/20[4].

Ethiopian households use mostly biomass and kerosene in the rural and urban area numerically 99% and 75% respectively for cooking [2]. As per the assessment made by International Energy Agency in 2018, Ethiopia's electricity access coverage rate of 45% with 11% of its population has access through decentralized grid connection, but the access to clean cooking only 7%[5].

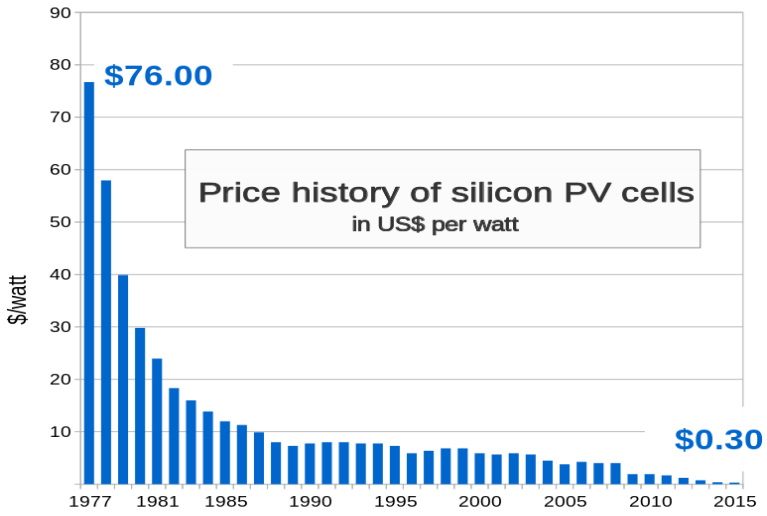

Figure 1-2 Global PV price trend per watt[6]

To avail electricity and thermal energy to off-grid areas, the use of renewable energy like wind, solar, and micro-hydropower with a relevant design solution and appropriate approach is necessary. Among renewable energy sources, solar technology is a better option for tropical areas due to the simplicity of installation and operation, and lower price per peak watt. The price of PV

modules declined by 20% in 2016 compared with 2015, with more aggressive prices in the range of USD 0.35-0.40/W quoted in some markets [7]. Figure 1-2 shows the trend of decreasing the price of the photovoltaic module globally[8].

Integrating the photovoltaic system to the thermal collector improves the PV conversion efficiency by reducing the temperature of the module using water as coolant and it simultaneously generates preheated water and electricity [9]. Around 3.5% of PV efficiency improvement was obtained by applying the PV/T system than the conventional PV system[10]. The increment of temperature in the PV without a cooling system stimulates two undesirable consequences: a drop in cell efficiency (typically 0.4% per ^{o}C rise for c-Si cells) and permanent structural damage of the module if the thermal stress remains for a prolonged period [11].

The integration of solar water heaters, photovoltaic, and heat pump improves the conversion efficiency and qualities of the co-generation of electricity and hot water for different applications [12], [13]. The integration of PV/T with heat pump is beyond the efficiency improvement of PV/T rather it builds the capability of delivering the hot water at the required temperature of the user. The global trend shows that most of the energy is consumed to fulfill the demand of cities for electrification and domestic hot water. Out of the total energy consumption in households, almost 20% is used for water heating for an average family[14]. This shows that the PV/T Heat Pump system has a huge potential in satisfying the large demand by delivering electrification and hot water. Also, such a hybrid photovoltaic thermal heat pump system is not only technically viable but also a feasible solution in the off-grid areas.

1.2 Problem statement

The demand for energy consumption is increasing alarmingly in Ethiopia and other developing countries from time to time. It has a direct relationship with population growth, urbanization, industrialization, and other related factors. Moreover, the cost of fuel is increasing alarmingly. In addition, the extension of the grid to sparsely located rural villages is expensive. Hence, decentralized energy conversion systems using renewable energy resources especially solar energy can be part of the solution. Also, the quest to mitigate climate change caused by the emission of large amounts of CO_2 and increasing energy use efficacy which is shifting from fossil fuel and biomass to solar renewable energy is very decisive.

Due to the falling price of PV modules and ease of installation and maintenance, it is highly probable that PV will be one of the main sources of electricity in off-grid areas of developing countries in the future. Whenever electricity and hot water have to be generated in off-grid areas, the PV/T system seems to be a natural solution. However, achieving the required hot water temperature is a challenge to the PV/T system. Therefore, it is necessary to examine the use of a hybrid PV/T air source heat pump water heater system for the co-generation of hot water and electricity. Optimize the system configuration according to the demand for electricity and hot water.

1.3 Objectives

The general objective of this study is to optimize the system performance of hybrid PV/T and heat pump systems for co-generation of electric energy and hot water for off gird health centers, lodges, and camps using a computational model.

The specific objectives are:

- Design and size the PV system based on the selected site and the demand for electrical energy use.
- Designing, simulating and optimizing the photovoltaic thermal system for the electrical and hot water user demand with maximum system performance efficiency.
- Integrating a heat pump system for boosting hot water temperature.
- Identifying the major components of the photovoltaic-thermal heat pump system and how it is going to be configured.
- Simulating the photovoltaic-thermal heat pump for optimizing maximum system efficiency using numerical computation tools.
- Evaluating the economic viability of the system and make comparative assessments with other energy sources.

1.4 Significance of the study

The study will benefit a country like Ethiopia which is economically underdeveloped, rich in solar energy availability, and with a huge population living in an off-grid part of the country. The

research project targeted to solve the electrical and hot water demand-supply limitation in the off-grid area using one integrated system. Institutes such as health centers, off-grid lodges, schools, and camps of megaprojects are beneficiaries of this research in the long-range.

The implementation of this integrated system will reduce deforestation and environmental pollution. It will improve the health and production capacity of the community. Also, different small-scale enterprises that participated in the production and supply of such technology can consider one option for product development.

1.5 Limitation of the study

This research deals only with the design, simulation, validation, and optimization of photovoltaic thermal heat pump system without experimental investigation. However, the validation of the method and results are done based on previously published peer-reviewed researches in the area. The daily hourly hot water consumption pattern used for the simulations in this work is done based on the western hot water consumption fraction standard was used due to the unavailability of standardized hourly hot water consumption patterns in Ethiopia and similar developing countries.

1.6 The novelty of the research

The research novelty from the system integration up to design consideration and optimization analysis are summarized as follows.

- PV/T system is simulated considering the end-use hot water consumption pattern. The limitation of the PV/T system is to heat water to a maximum temperature of 50^oC which could be observed even in tropical regions.
- The mathematical model to simulation a hybrid system of PV/T Heat Pump is developed.
- The simulation of a hybrid PV/T Heat Pump system can heat water to 60^oC by proper configuration of PV/T area and heat pump capacity.
- The developed model can be used to simulate hybrid PV/T Heat Pump system performance at different locations and climatic conditions even though the results presented in this work are for two places in Ethiopia.

CHAPTER TWO

RESEARCH METHODOLOGY

2.1 Literature review

Different sources were used to review the state of the art of the PV/T and heat pump system to prepare this dissertation. The review addressed different relevant scientific publications and the PV/T and heat pump system manufacturers' product manuals and documents. The collected peer-reviewed journals and manufacturing manuals on hybrid photovoltaic thermal and heat pump systems were ordered chronologically prioritizing the latest work. The review covers the development of photovoltaic thermal systems and heat pump water heaters in the last three decades.

2.2 Data collection

Climatic data consisting of hourly solar irradiation and ambient temperature were collected for the selected sites from Ethiopian Metrological Agency (EMA). The end-user electricity and hot water demand data collected from the site visit.

2.3 Conceptual model configuration

At the first photovoltaic module and balance of system, the device had been configured to meet the electrical energy demand. Then, a PV/T system (PV with a thermal collector at the back) were considered to generate electricity with an improved conversion efficiency and pre-heat water simultaneously. The PV/T physical model was configured so that electricity demand is met by the PV area and daily hot water consumption. Then, the hot water tank size was varied to see the maximum hot water delivery temperature and system efficiency.

Finally, the air source heat pump water heater module that uses part of the electricity generated by the PV/T is integrated with the system using PV/T warm water as input. The heat pump water heater capacity is selected so that the warm water from the PV/T storage tank can reach the temperature required by the end-user in the coldest month. The system configuration is further improved through parameter variation of PV/T area, PV/T warm water tank, daily hot water

consumption, and heat pump capacity until demanded electricity and the required hot water at the specified temperature are obtained.

In both cases, the principles of engineering design and parametric optimization principles were used.

2.4 Computational model

The computational analysis starts from solar irradiation of the site and develops an energy balance analysis for each component of both the photovoltaic thermal system and hybrid photovoltaic thermal and heat pump system at each time step.

The dynamic computational model solves the energy balance equation at each layer of the PV/T module. The system of ordinary differential equations is solved numerically with the finite difference implicit method. The model estimates the temperatures at discrete points of the PV/T collector and hot water tank every 5 minutes. The electrical and thermal energy output estimation by taking all affecting parameters using a computer program in MATLAB software.

In the case of a heat pump water heater, thermal energy input to the water is related to the input electrical energy of the compressor by the COP which is given by the heat pump manufacturer as a function of hot water and ambient temperature.

To find the optimized system efficiency, different influencing parameters were varied until the objective functions are satisfied.

2.5 Validation and verification

To verify the accuracy of the results of the computational model, experimental data of PV/T systems published papers from peer-reviewed journals were collected. A computer simulation was conducted with the same system design parameters and weather conditions as the experiment. A comparison of the results of the computational model was made with an experimental result to verify the accuracy of the computational model.

2.6 Methodology flow diagram

The summary of the methodology chapter is illustrated in Figure 2-1.

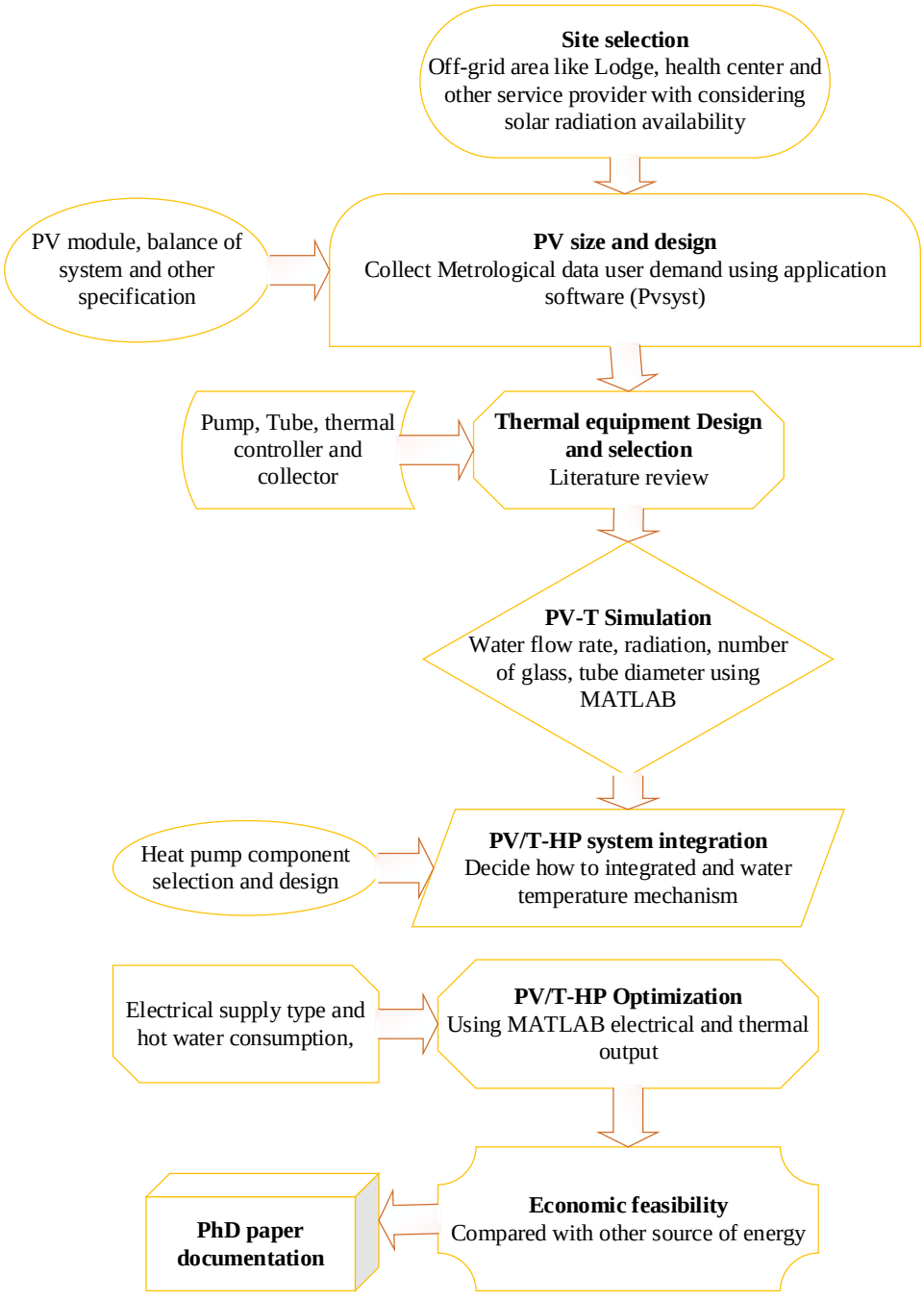

Figure 2-1 Flow diagrams for methodology

CHAPTER THREE

LITERATURE REVIEW

3.1 Energy background of Ethiopia

The growth of the population in the world has raised many issues. One of them is global warming caused by the emission of a large quantity of CO_2 into the atmosphere. Much of this gas is produced from electrical power plants that burn fossil fuels. The urgent need for reducing CO_2 emission in the atmosphere on one hand and the growing concern of the depletion of fossil fuel resources has resulted in a shift of focus to renewable energy resources.

Access to commercial energy in Ethiopia is relatively low. Biomass accounts for 88% of the total energy consumption of the country. In urban areas, 75.3% of the residents use electricity for lighting, while in rural areas, kerosene and firewood consumption stands at 80.1% and 18.5% respectively [15]. Access to commercial energy has been gradually improving, standing at 20% in 2007 by the efforts of the Ethiopian Electric Power Corporation in constructing new power plants.

In 2019, the national grid connectivity coverage was only 44.3%, which is by far lower than the electricity access plan of GTP II (90%)[16].

Ethiopia, known as the “Water Tower of East Africa”, has numerous rivers, lakes, and sufficient water resources. Ethiopian highlands are the origin of many North and East African rivers, most of which are the Blue Nile, Atbara, Sobat, Shebeli, and Jubba rivers, which flow in all directions. Hence, the country has a large hydropower potential. Especially, the Nile basin rivers, in particular, have the greatest potentials for hydropower in the north and east Africa[17].

Studies indicate that the yearly average daily solar irradiations of Ethiopia as a whole are 5.26 kWh/m^2. This varies significantly during the year ranging from a minimum of 4.55kWh/m^2 in July to a maximum of 5.55 kWh/m^2 in February and March. By region, the yearly average ranges from 4.25kWh/m^2 in Gambela, Western Ethiopia to 6.25kWh/m^2 in the Adigrat in Tigray [17].

3.2 Photovoltaic

Photovoltaic is a means of utilizing solar power by directly converting it into electricity. A PV cell is a semiconductor diode that can convert the energy from sunlight into direct current electricity[18]. The research in PV technology has made great advances over the last four decades in addressing issues related to cost reduction, efficiency improvement, building integration, and energy storage technology [19]. In a general sense, four types of PV installations can be identified and practiced. They are grid-connected centralized large power plants; grid-connected distributions (smaller rooftop and facade systems); off-grid non-domestic (power plants and industrial installations in remote areas); and off-grid domestic (mainly stand-alone rooftop systems for houses in remote areas)[19].

The working principle and energy conversion of the photovoltaic cell is a one-step process, which generates electrical energy from solar energy directly. The performance of PV panels is characterized by an I-V curve, at the standard value of $1000W/m^2$ solar irradiance with an operating panel temperature of $25℃$ with a relation between the output photoelectric current, I, and the potential difference, V, across the panel[20]. There are many affecting parameters on the photovoltaic module power output. Many factors to name some of them are irradiance, cell temperature, dust, and soiling of the solar panel[21].

PV modules can be made from different types of materials; however, crystalline silicon is the most significant one in domestic energy use [18]. From such materials, the following four types of PV modules are the most predominant in the commercial market.

Monocrystalline silicon (Mc-Si) module, which is made using cells saw-cut from a single cylindrical crystal of silicon. From a very pure molten silicon, they show effective growth of a slice of 0.2 to 0.3-mm thick. Mc-Si module has an average electrical efficiency of 10–17%, which is higher than that of other types of silicon. But it is slightly more expensive than others due to the time and energy required for the manufacturing process [22].

Polycrystalline Silicon (Pc-Si) module is made from cells cut from an ingot of melted and recrystallized silicon using a casting process. It is cheaper than Mc-Si due to the simpler manufacturing process. However, it tends to be slightly less efficient, with an average electrical

efficiency of 11–15%. It has a stippled crystal reflective look, where it ought to be mounted in an exceedingly frame.

Amorphous Silicon (A-Si) is non-crystalline silicon. A-Si module is composed of silicon atoms in a thin homogenous layer rather than a crystal structure. It absorbs solar irradiation more effectively than crystalline ones, so the module can be thinner. A-Si can be deposited on a wide range of substrates, both rigid and flexible, which makes it ideal for curved surfaces and 'fold-away' modules. A-Si module is, however, less efficient than Mc-Si and Pc-Si ones, with a typical efficiency of 4–7%, but it is easier and cheaper to produce, where its output is less affected by high temperatures [22].

A hybrid module is made from two different types of PV technologies. The advantage of this module is that it performs well at high temperature and it maintains higher efficiency than conventional silicon PV modules. However, a hybrid module always comes at a cost premium[22].

3.3 Solar thermal collector

The major part of the solar thermal collector system is a solar collector as shown in Figure 3-1. This is a device that absorbs the incoming solar irradiation thereby, converting it into heat, and transferring it through a fluid (usually air, water, or oil) for useful purpose/applications [23]. One of the most widely known solar thermal applications is the solar water heating system[24]. This technology particularly, the solar water heater has effectively entered the global market [25]. The use of a solar collector to recirculates the same water through the absorber panel in the collector raises the temperature to 80 °C (maximum) on a good sunny day[14]

The solar energy collected is carried from the circulating fluid either directly to the hot water or space conditioning equipment or a thermal energy storage tank[26]. Also, the solar collector is used as an air dryer/heater for drying agricultural products and/or heating/cooling applications in combination with auxiliary heaters for air conditioning of buildings.

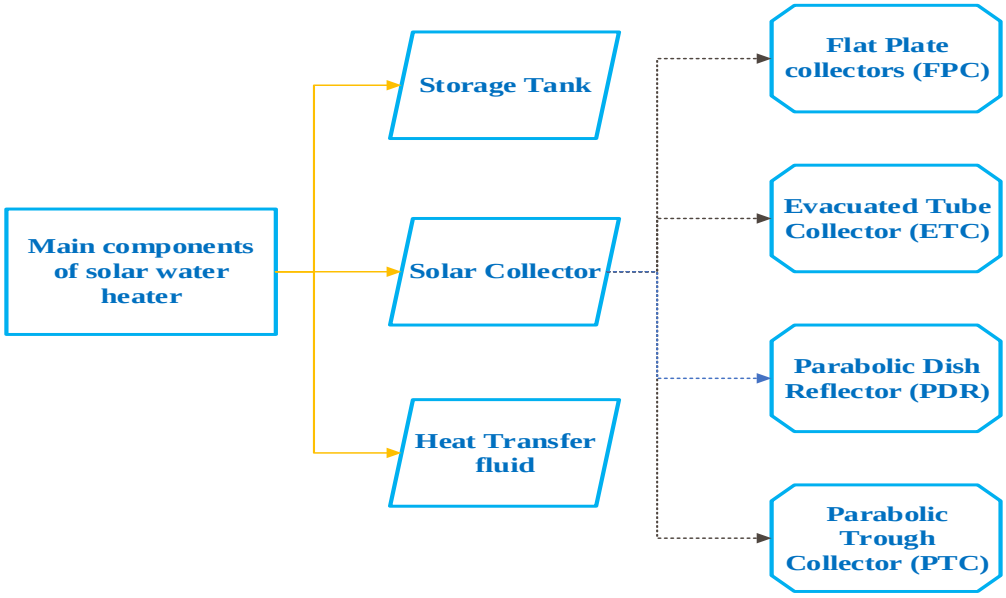

Figure 3-1 Components and classification of solar water heater

There are two types of solar collectors: non-concentrating or stationery and concentrating ones. Solar energy collectors can also be distinguished by their motion as stationary, single-axis, and two-axis tracking[27], [28].

3.3.1 Storage tank

One of the basic components of the solar thermal system is the storage tank, as illustrated in Figure 3-1 where the solar collector is linked by a pipe or integrated as one component[29]. In such technology development, a well-insulated storage tank is required to avoid heat losses. To this effect, most of the thermal storage tank is made of stainless steel and covered with insulated fiber and aluminum foil [30].

A storage tank is not only integrated with the solar collector but it is also combined with a heat pump to store hot water. A study on the characteristics of erratic thermal loads of the storage system was conducted for multi-purpose water heat pumps. By using the on/off controlling mechanism of the heat pump, the temperature of the hot water is maintained at 60℃, with the variation of the water flow rates in the heat pump. And this has resulted in better performance of the heat pump as compared with the constant flow rate[31].

3.3.2 Flat-plate collectors (FPCs)

When irradiation passes through a clear glass cover and impinges on the blackened absorbent material surface of high absorptivity, the major part of the irradiation is absorbed by the plate. The absorbed energy is transferred to the fluid within the tubes where it can be stored or directly used. The clear glass cover is used to scale back convection losses from the absorber plate through the restraint of the stagnant air layer between the absorbent material plate and the glass. Besides, it reduces irradiation losses from the collector as the glass is clear to the shortwave irradiation received by the sun and opaque to infrared irradiation[26].

The advantages of flat-plate collectors are inexpensive to manufacture; they both absorb the beam and diffuse irradiation, and they are permanently fixed in a position without the need for bidding the tracking mechanism. The collectors should be oriented directly toward the equator, facing south in the northern hemisphere and north in the southern hemisphere.

The optimum tilt angle of the collector varies according to the need of its applications. In general, the selection of the collector's tilt angle is done either by adding or subtracting a 10° - 15° on the site latitude angle. If the application is for solar cooling, then the optimum angle is less than 10^{o} from the site latitude. However, if the application is for space heating, the optimal angle is higher than 10°; Whereas for annual hot water production, its latitude is +5° to have relatively better performance during wintertime, when hot water is mostly required [26], [32]

Non-concentrated (Flat plate type) collector concept is more appropriate for this research because of its good compatibility with the photovoltaic module to make the hybrid system. The flat plate collector does not need to concentrate the solar irradiation in the focus area, which is helpful to improve the conversion efficiency of hybrid PV/T which then reduces the surface temperature[33].

3.4 Photovoltaic thermal

3.4.1 Introduction

The current popular technology enhances the conversion of solar energy into electricity and heat separately either using a photovoltaic module or solar collector. The photovoltaic thermal

(PV/T) system is designed to generate thermal and electrical energy simultaneously in one module [34]. Solar irradiations can be converted into either thermal energy or electrical energy or both[35].

The development of PV/T technology has emerged over the past three decades, coming up with several research outcomes. The first famous analytical model was developed with a simple modification of the flat plate collector design in the mid-1970s, making PV/T collectors [32]. After the development of the first simplified PV/T system model, the researcher prepared an elaborated analytical analysis as a reference to advance the PV/T technology [36]. Development effort has been made over the years on the work of PV/T performance analysis as reported in 1976[37]. Other studies have also been subsequently conducted on PV/T collector/systems.

Within a short time of research undertaking, the PV/T technology moved from analytical analysis to computer simulation and optimization for the improvement of the integration system. By using computer simulations, the flat plate PV/T collector was described to have shown better performance, improved solar absorptance, and reduced infrared emittance[38].

In 1995 a researcher conducted a theoretical examination of the flat plate solar collector model, by integrating it with solar cells to develop a hybrid system [39]. Through a transient analysis, another researcher pointed out that the air collector design is lower in thermal efficiency than the water collector due to, inferior heat transfer between the thermal absorber and the airflow stream[40].

The glazed and unglazed PV/T technology has been applied to understand their effect on electrical and thermal efficiency, and on the grade of energy rate through exergy analysis[41], [42]. In 2001, the modeling and simulation of a PV/T system showed the improvement of the standard PV system efficiency, increasing from 2.8 to 7.7% [43]. Various PV/T collectors simulation and testing proved that water heat extraction has resulted in a lower PV temperature than that of air heat extraction[44]. The same conclusion was drawn to establish the water PV/T system by implementing an experimental test on a different configuration of water and air-based PV/T system[45].

A different investigation was done on the hybrid PV/T system efficiency enhancement[46]. At zero reduced temperature, the evaluation of thermal efficiencies of the unglazed and single-glazed

sheet-and-tube collectors was found 52% and 58%, respectively, while the channel-above-PV design has 65% thermal efficiency [47], [48].

Subsequently, the development of an explicit dynamic model analyzed the transient performance of a single-glazed sheet and the tube collector by finite difference scheme[49]. Similarly, the transient dynamic thermal model analysis was carried out to simulate PV/T collector[50]. In the year 2007, PV/T technology was implemented in large projects throughout the world of both faced and roof-mounted integrated systems. However, the projects involved a more air-cooled PV/T system than water-cooled technology[51], [52].

After 2008, the PV/T project incorporated a water-cooled system at least on a small scale covering around 65% of the hot water demands at the household level[35]. The performance investigation continued on glazed and unglazed sheet-and-tube thermosiphon water-based PV/T through theoretical models and experimental tests[53]. A reflector adds to the system for efficiency improvement on the water-based PV/T system. Different research was conducted on a PV/T with a reflector to make a comparison with non-reflector PV/T how much cost incurred and energy gained due to the addition of the reflector [54].

According to recent reports, the computational analysis was carried out to optimize the parameters of the working fluid, in particular, nanofluid, to absorb selective solar infrared irradiation based on the concept of Direct Absorption Collection (DAC)[55]. The optimized arrangement of absorbers for the better efficiency of liquid-based PV/T with low cost and material usage was also recently investigated[55]. A concentrated PV/T system for application in both cooled and hot areas for high water temperature supply was investigated[56], [57].

Regarding the manufacturing and utility usage of the liquid-based PV/T collector, China is the leading country where it has employed PV/T technology as the main solar system in buildings [58]. But still, the market share of the PV/T system is small compared to the standalone photovoltaic and solar collectors. Due to the ounce of PV/T technology development i.e. for there is no standardization and certification, its market share is small [59].

A body of studies has been carried out worldwide to improve the system of competence and standardization by studying the PV/T system, and its compatibility for the different climatic conditions [60]. Over the past three decades, several improvements have been made on efficiency,

cost, technology, and accessibility to the end-user of the PV/T system. It is also expected that researchers will be conduct research over the coming years on the PV/T system to overcome the limitation of the technology for more efficient systems and cost-effectiveness.

3.4.2 PV/T classification

The basic types of photovoltaic-thermal systems can be classified depending on the heat extraction fluid used that is water and air type of PV/T collector. The classifications of flat-plate photovoltaic thermal collectors are shown in Figure 3-2 [34].

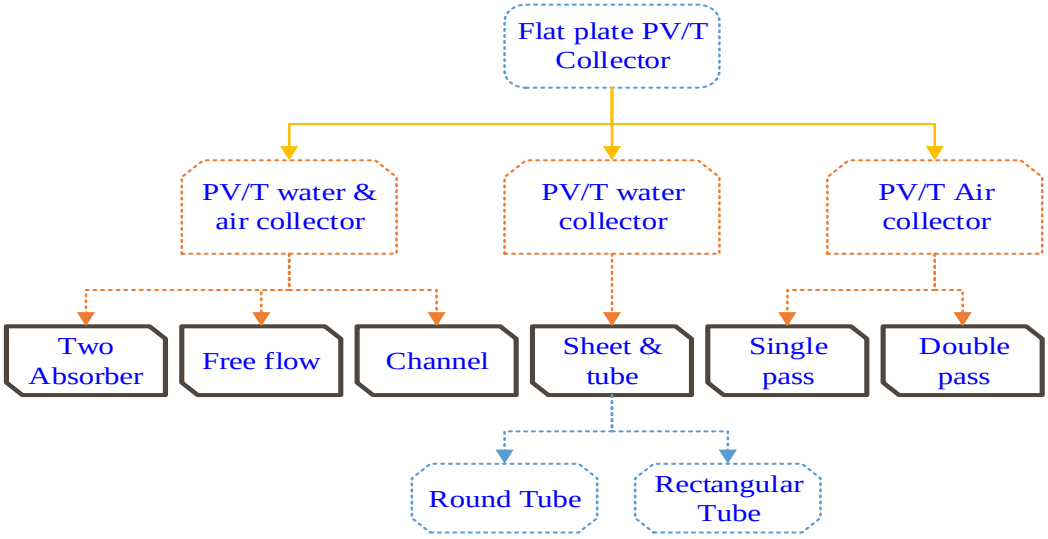

Figure 3-2 Flat-plate PV/T collector classifications

As depicted in the above Figure 3-2, PV/T collectors classification is based on the working fluid [61].

3.4.3 Air type PV/T collector

The air-type product style provides an easy and economical solution to PV cooling, and also the air will be heated to diverse temperature levels through forced or natural flow. Forced circulation is more efficient than natural circulation owing to better convective heat transfer, but the required fan power reduces the net electricity gain[62].

In the air PV/T, the cavity is formed behind a PV panel where the air is circulated; which cools the panel and heats the air as shown in Figure 3-3. The maximum thermal efficiency of the system was found to be 25% with a simple cavity; however, they found by adding an air gap and glazing

layer above the collector, almost doubling the thermal efficiency. Where air was circulated along the back surface of the module and the insulation layer, as well as along the top surface between the module and the glass cover, the air has given the best optimal functioning between electrical and thermal performance. In 1997 an unglazed PV/T collector had a maximum thermal efficiency of 38% [42]. It is also found that by the glazing system, or adding a static reflector, this efficiency could be increased to 60% which, in the meantime, has increased to 75% by adding both glazing and the reflector [63].

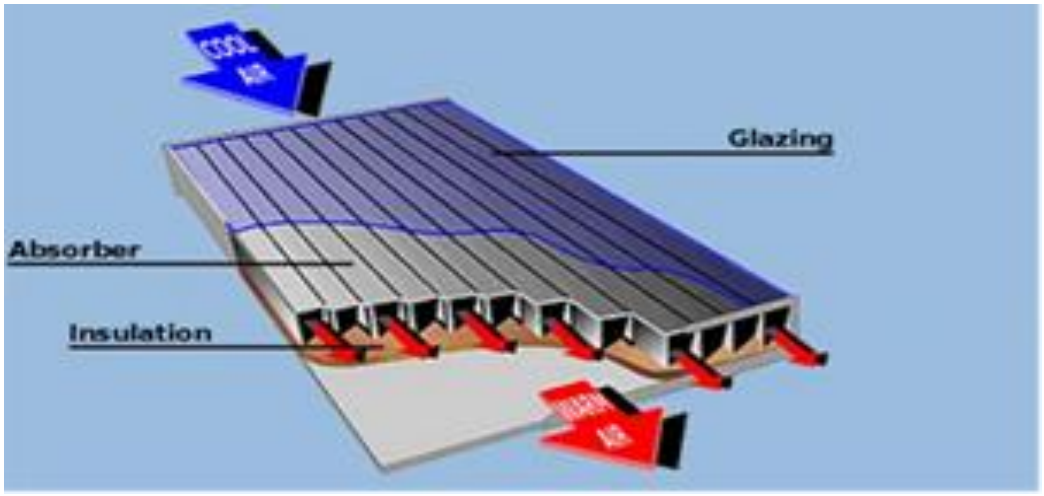

Figure 3-3 Air type PV/T module collector [64]

The air type PV/T systems are suitable for building applications in medium and high latitude countries. In low latitude countries, the ambient air temperature throughout the day is over 20℃ for pretty much half of the year [65].

3.4.4 Water/liquid PV/T collector

Here, water is used as heat transfer fluid. Furthermore, water, PV/T collectors are often divided into different groups in line with the temperature levels of the heat transfer fluid. It ranges from low to high-temperature applications, for example, swimming pool and heat pump applications have medium-temperature applications around 55°C for domestic hot water applications. PV/T collectors are recommended that such systems might be useful as pre-heaters for domestic hot water services and industrial applications [63].

As illustrated in Figure 3-4 nominated by letter (a) the collector components before the assembly, and (b) in the assembled position, and (c) the detailed dimensions of the module.

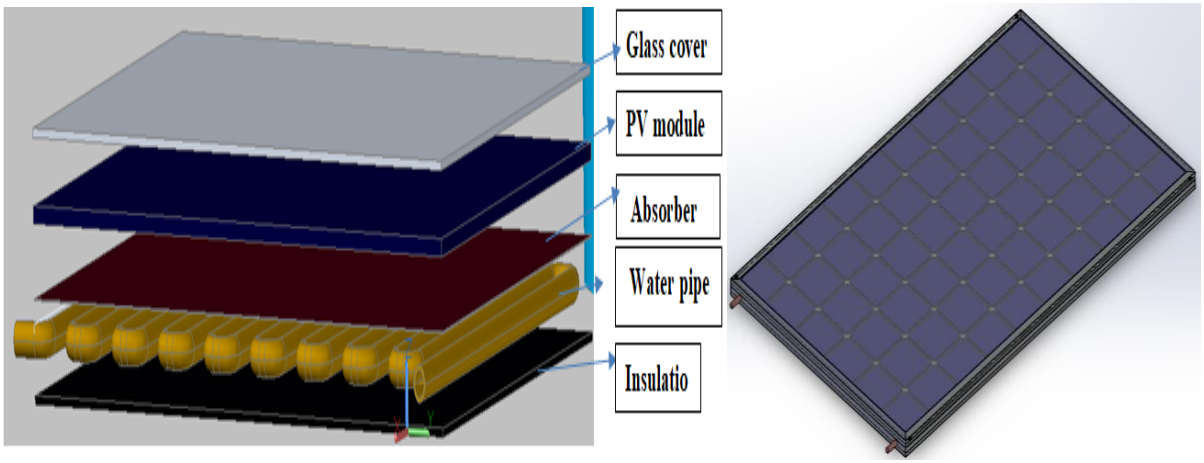

(a) (b)

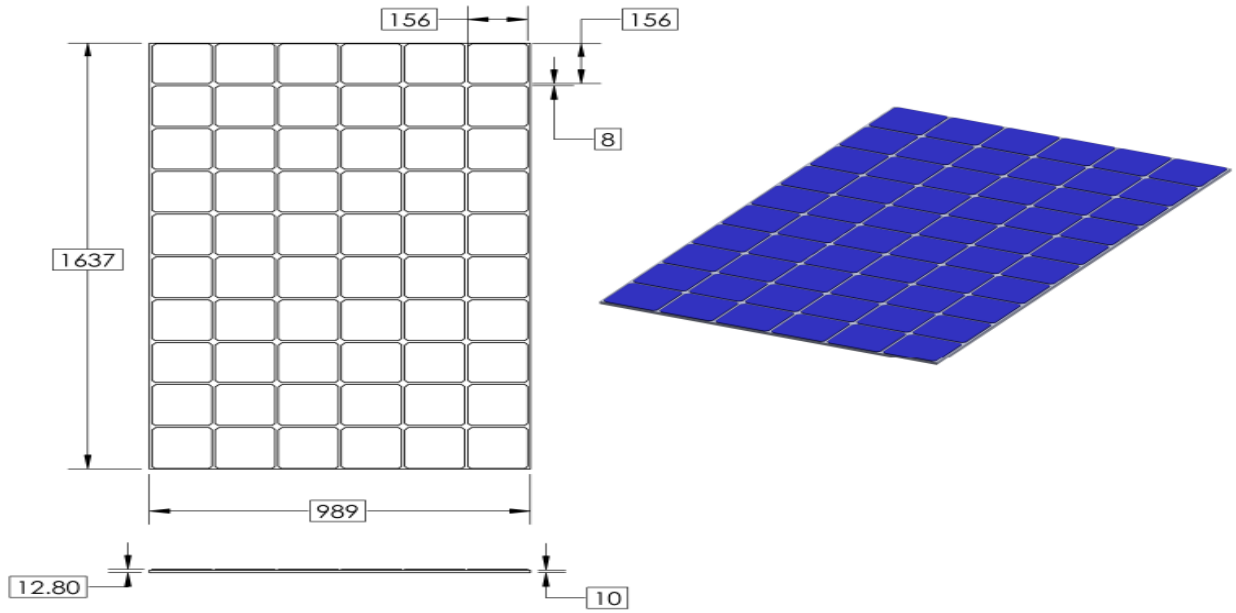

(c)

Figure 3-4 A proposed PV/T collectors for water heating

In the water type PV/T collector, PV cells are pasted directly on the absorber. Due to this direct contact between the absorber and the PV module, it will allow a high thermal gradient/transfer to

occur. The heat transfer fluid runs inside the tubes in the absorber and collects heat from the absorber. Due to continuous heat extraction and transfer to the working fluid from the PV cells, the PV module temperature is reduced, which helps the module to attain higher electrical efficiency conversion[66].

A water cooling PV/T system integrated with insulation improves the efficiency of the polycrystalline silicon PV cells up to 10%, with a 3% efficiency improvement in the case of a PV cooling by water without insulation [36]. It was also found that water cooling provides better cooling than air circulation. And the performance of the systems could be further improved through the use of reflectors or glazing in the same work.

In the PV/T collectors, glazing the collectors would improve thermal performance at the expense of electrical potency. Relative to the glazed system, the unglazed sheet and tube collector had the lowest thermal but highest electrical efficiency [42]. This work also showed that the glazed PV/T collectors had a maximum thermal efficiency of 65%. The heat transfer fluid can be circulated either by a pump or by the natural specific gravity difference of the heat transfer fluid. The water type PV/T systems can be used effectively in all seasons, mainly in low latitude countries, as water from the source is usually under $20^{o}C$[63], [65]

3.4.5 Building-integrated PV/T (BIPVT)

The multi-functional external facade/roof was identified as better for PV/T installation, which produces heat, light, and electricity simultaneously as demonstrated in Figure 3-5. Other than the use of airflow behind the PV modules, a PV/T system is designed for light transmission, requiring no additional system cost except for ambient light sensors to optimize the gain from day lighting[67].

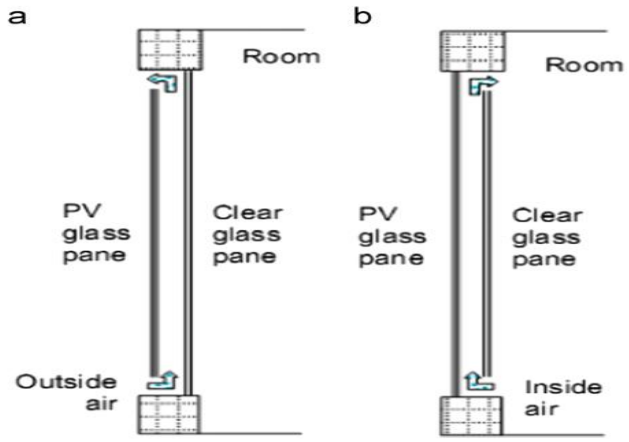

Figure 3-5 Ventilated PV/T for building integration (a) Cooling mode. (b) Heating mode[67]

3.4.6 Concentrator PV/T system

Concentrate photovoltaic (CPV) systems can operate at higher temperatures than those of the flat plate collectors. Collecting the rejected heat from a CPV system leads to a CPV thermal (CPV/T) system, providing both electricity and heat at medium temperatures. This approach is significantly promising due to the low cost of the reflectors relative to the solar cells. On the other hand, using "liquid" as a coolant is more effective than using "air" to obtain a better electrical output. For these reasons, the reflector-type of CPV/T systems is common from medium to high-temperature hot water systems applicable for cooling, desalination, or other industrial processes as illustrated in Figure 3-6 [67].

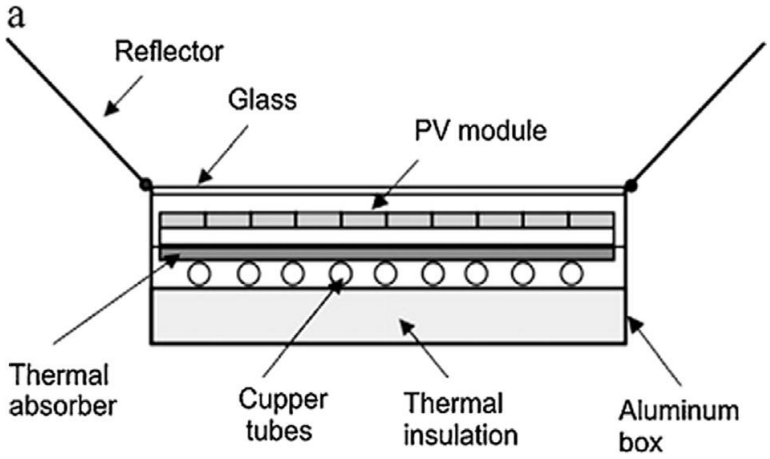

Figure 3-6 Concentrator photovoltaic thermal[67]

3.4.7 Heat pipe-based PV/T system

Heat pipes are considered efficient heat transfer mechanisms that combine the principles of both thermal conductivity and phase change transition. A typical heat pipe consists of three sections namely, the evaporating section (evaporator), adiabatic section, and condensing section (condenser) providing an ideal solution for heat removal and transmission as revealed in Figure 3-7 [67].

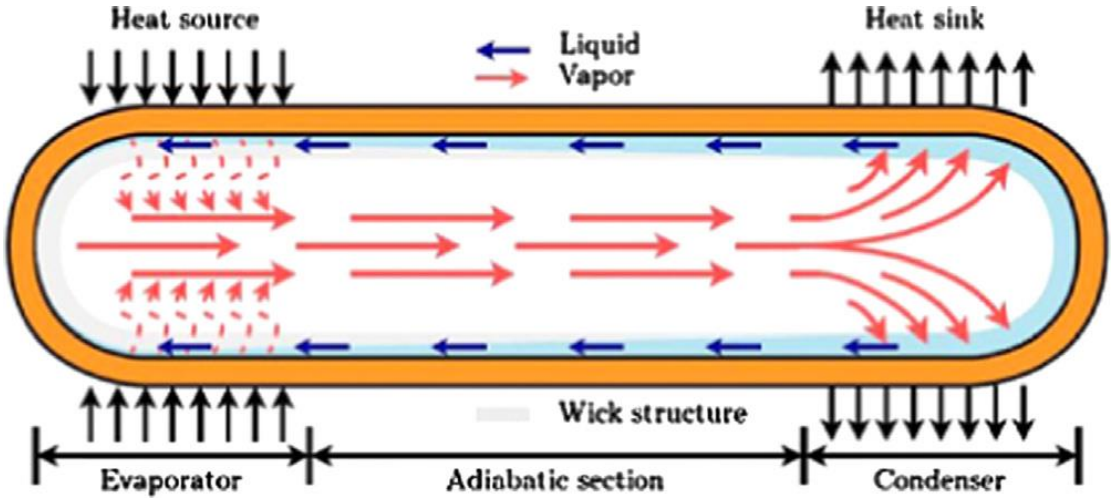

Figure 3-7 Schematic diagram of the PV/T heat pipe [67]

3.4.8 Glazing materials

Glass has been widely used for glaze solar collectors because it can transmit the maximum irradiation which is about 90% of the incoming shortwave solar irradiation while transmitting virtually none of the longwave irradiation emitted outward by the absorber plate. Window glass usually has high iron content, which is not suitable for use in solar collectors. Plastic films and sheets also possess high shortwave transmittance plastics that are generally limited in their application temperatures, without sustaining deteriorating or undergoing dimensional changes.

The commercially existing grades of window and greenhouse glass have standard incidence transmittances of about 0.87 and 0.85, respectively. Anti reflective coatings and surface texture can improve transmission significantly. The effect of dirt and mud on collector glazing could also be quite small, and therefore the cleaning effect of an occasional rainfall is typically capable to

maintain the transmittance within 2–4% of its maximum value. Dust is collected mostly during summer when rainfall is in a smaller amount.

3.4.9 Advantages of PV/T system

According to the reviewed literature, a photovoltaic thermal system as an alternative source of energy for the supply of heat and electricity simultaneously improves the conversion of the efficiency of the PV module. A PV/T system is developed using some additional components on a PV module array. Such technologies are good solutions to satisfy the energy demands for heat and electricity, especially in tropical areas. In general, the PV/T system has plenty of advantages relative to separate PV modules and solar collectors. And these are listed below[66]:-

- Minimized the usage of the installation area. It is proven that by combining the systems, the PV/T system produce more energy per unit surface area than the PV panel and solar thermal collector for the hot water system. This is more attractive in the case of rooftop and surface limited areas.
- It has the capability to replace the roofing material in addition to the production of energy that leads the system to a short payback period.
- The materials, transportation, and energy consumption may be better than the separate units.
- The cost of PV/T panels could be reduced by combining the two manufacturing processes into a single process.

3.5 Heat pump

3.5.1 Introduction

A heat pump is a device that transfers thermal energy from a source to a sink and has a higher temperature than the source[68]. Thus, heat pumps move thermal energy in a direction opposite to the direction of spontaneous heat flow. In other words, the ability to move thermal energy against the direction of natural heat flow requires an external source of energy, usually a mechanical compressor. The heat pump uses some form of high entropy denotes a low grade of energy to accomplish the desired transfer of thermal energy from the source to the sink. The name of the

system is by analogy driven from the standard fluid pump, which pumps a fluid against its natural flow, from lower to higher elevation[69].

Heat pumps use a refrigerant as an intermediate fluid to soak up heat where it vaporizes, within the evaporator, and then to release the heat where the refrigerant condenses, within the condenser. The refrigerant flows through insulated pipes in the middle of the evaporator and the condenser, allowing efficient thermal energy transfer at relatively long distances. If the heat pump is reversible, then a reversing valve is functioning to control the flow direction of the refrigerant. A heat pump can be classified based on the type of application delivered to the user: the heating mode and cooling modes.

Heating mode: the outdoor coil is an evaporator, while the indoor heat exchanger is a condenser. The refrigerant flowing from the evaporator (outdoor coil) carries the thermal energy from the environs air (or ground) to indoors, after the fluid's temperature has been amplified by the compressor. The indoor coil then transfers thermal energy (including energy from the compression) to the indoor air, which then moves to the inside of the building by an air handler. The refrigerant is then allowed to expand, cool, and absorb heat to reheat to the outdoor temperature within the outside evaporator, and the cycle repeats. This is a standard refrigeration cycle that saved the "cold" side of the refrigerator (the evaporator coil); so is outdoors where the environment is colder.

Cooling mode: the cycle is analogous, while the outdoor coil is the condenser and the indoor coil (which reaches a lower temperature) is the evaporator. This is a similar model to how the air conditioners operate[70].

3.5.2 Components of heat pump

a) Evaporator

A heat pump always has an outside heat source and an indoor outlet. Outdoor sources can be ambient air, exhaust air, ground rock, groundwater, river water, and others. The energy generated from these sources is infinite and hence, renewable. This energy makes up about 75% of the energy that is needed to drive the system. The outside heat exchanger an evaporator absorbs the thermal energy from the outdoor source to boil the refrigerant (the liquid in the heat pump) and drive it into a gaseous state.

b) Compressor

The refrigerant arrives at the main gates of a heat pump: the compressor. The compressor compresses the refrigerant which is in the gaseous state to high pressure, thereby increasing its temperature, which is a function of the pressure. Driving the compressor, which requires additional energy: from electricity, gas, or thermal. They make up 25% of the total energy needed to run the heat pump. If the electricity generated by photovoltaic is supplied to the heat pump, then the system is 100% renewable. Hence, it is CO_2 neutral.

c) Condenser

On the discharge side of the compressor, where hot and highly pressurized vapor passes through the second heat transfer device is called the condenser. This device allows the refrigerant to release the heat into the heating system for household appliances (air blower, floor heating, or radiators), and in connection with this, the refrigerant is condensed, changing from a gaseous state into a liquid state. The indoor outlet can be an air system (as the typical air conditioner units) or a hydronic (water-based) system.

d) Expansion valve

The condensed refrigerant then passes through a pressure-lowering device, the expansion valve. Then the low-pressure liquid refrigerant enters another heat exchanger, the evaporator, in which the fluid absorbs heat and boils, where the cycle repeats.

For the provision of sanitary hot water, the evaporator can either be in a hot water storage tank or can exchange heat with the water by circulation with a pump through a heat exchanger. The condenser can be air-cooled in ambient air.

3.5.3 Classification of heat pump

In general, a heat pump is classified into two basic categories based on the source of heat or output.

a) Ambient air source heat pump

Ambient air is by far the most popular heat source for heat pump applications worldwide. The reason for this is its unlimited availability, enabling an uncomplicated and quick installation. The performance of a heat pump reduces as the temperature of the heat source drops, leading to

unfavorable characteristics of heat pump performance. The performance of an ambient air heat pump will decrease as the heating demand is increasing.

At a certain point, the temperature difference between the heat source and heat sink will be too great for the heat pump to operate at all, immediately halting its operation. In most cases, ambient air heat pumps stop working at the temperatures range of $(-15\,℃) \sim (-20\,℃)$ [71].

b) Ground soil and bedrock source heat pump

The use of the ground as a heat source for heat pumps enables the use of renewable energy stored in the soil or bedrock. The use of ground soil as a heat source for heat pump applications has a negligible influence on the vegetation above it. The ground serves as the seasonal storage of solar energy. At a depth of 0.9-1.5 m, the amplitude of temperature changes due to changes in outdoor temperature, which then is damped and delayed. This results in very favorable working conditions for a heat pump extracting energy from the ground. The heat exchanger may either be designed for horizontal or vertical installation in the ground soil.

The coefficient of performance (COP), is not only reliant on the efficiency of the appliance. The same appliance will also generate quite different annual efficiency factors depending on the temperature levels of the heat source and the heat distribution system[71]. The ground features a stable temperature of between 10-12 °C throughout the year. This temperature is enough to heat the refrigerant because it has a very low boiling point. The Ground Source Heat Pumps (GSHPs) exchange heat with the ground and maintain a high level of performance even in colder climates[72].

On the other hand, the main limitation of the ground source of a heat pump is higher installation costs. Installing boreholes can create disruptions where the horizontal ground loop requires a large area and it is essential to size the ground collector accurately to avoid the difficulty of redoing it[73].

c) Based on the output of the heat pump

The second basic category of the heat pump is the output type system. The air to water heat pump: is the type of heat pump which uses air as a source of heat and generates hot water. Technically, air to water heat pump operates using the low temperature in the air to heat the

refrigerant first and then the water, where the hot water is carried to the end-user. This hot water will then be ready to heat the home or to pre-heat the water for the end-user[70].

3.5.4 Solar assisted heat pump (SAHP)

SAHP is a type of heat pump integrated with solar thermal collectors which supply heat directly or indirectly to the evaporator. SAHP systems can be classified into conventional indirect solar assisted heat pump (IX-SAHP) systems and direct-expansion SAHP (DX-SAHP) systems. The DX-SAHP system consists of a solar collector, a heat exchanger as a condenser, a thermostatic expansion valve, and a compressor. The solar collector is used as the evaporator of the heat pump system[12]. Due to the simplicity of direct-SAHP, the physical arrangement has the advantages of making the evaporator have a high heat transfer coefficient, reducing the overall system cost relative to conventional indirect-SAHP [74]. Both types are placed in series systems. In a parallel system, the conventional heat pump, typically air source (ASHP) is utilized in parallel with solar collectors as shown in Figure 3-9.

Figure 3-8 shows the series SAHP system i.e. a direct expansion (DX-SAHP) and indirect-expansion (IX-SAHP). The latter utilizes a water loop to absorb the heat from the collector where the heat pump is connected to the hot water produced by the solar collector and hot water storage tank. The heat collected by the solar collectors is transferred indirectly to the evaporator of the heat pump. With respect to DX-SAHP, two phases of solar collector/evaporator are used as an evaporator of the heat pump. The refrigerant is pumped directly by the compressor and eliminates the requirement of an additional water loop circuit, to transfer heat from the collector to the evaporator[68].

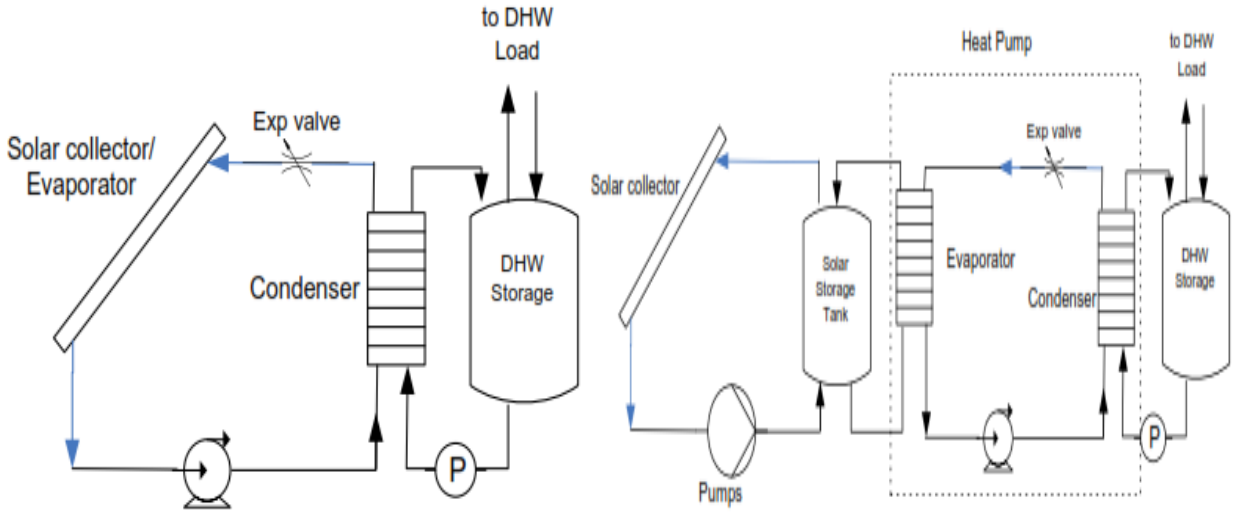

(a) (b)

Figure 3-8 Series SAHP direct expansion nominated by letter (a) and indirect expansion designated by a letter (b)[68]

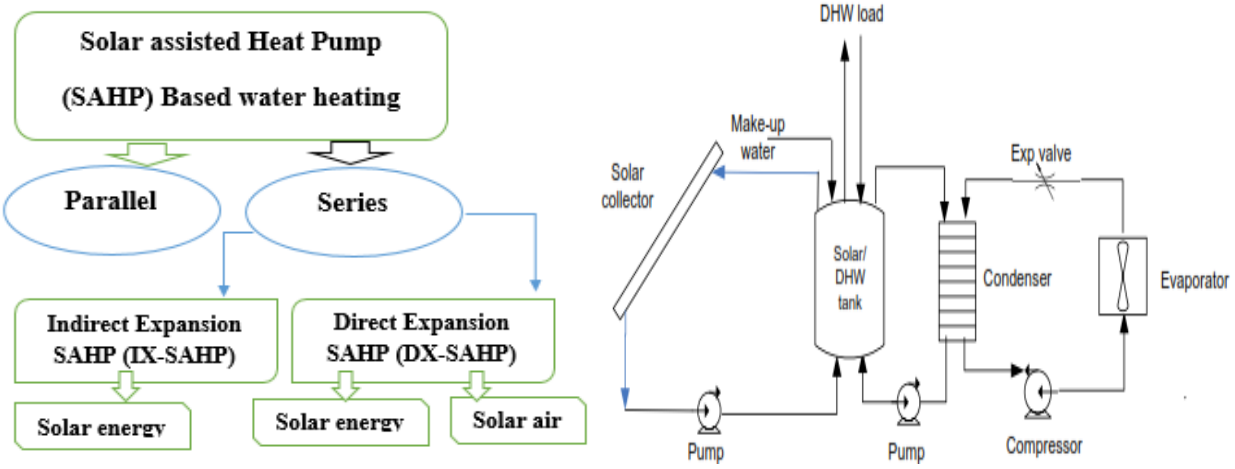

(a) (b)

Figure 3-9 Classification SAHP nominated by letter (a) and parallel SAHP system designated by (b) [68]

3.5.5 Refrigerants in heat pump

In identifying a refrigerant fluid for heat pump application, it requires a proper understanding of different characteristics of the refrigerant. One of the vital criteria for selection is the chemical stability of refrigerants, which quickly decomposes to harmless substances in the atmosphere. The

second consideration for selection is based on a thorough assessment of the environmental and health impact of the refrigerant on the user. The third selection criteria for refrigerant were thermodynamic properties i.e. freezing temperature, well below normal operating conditions critical point, and boiling point temperatures which are appropriate for the application. Also, reasonable operating pressures are preferred to keep costs at a minimum. Last but not least, a practical characteristic. In this regard, high oil solubility is generally preferred: compatibility with common construction material and low cost.

3.5.6 Advantages of air source heat pump water heaters

A heat pump by its nature is capable of working at different climatic conditions, generating a high coefficient of performance with minimum energy consumption. Below are some of the basic advantages of the heat pump.

- Heat pump water heaters with an average COP generate about 3 kWh of thermal for every 1 kWh of electric energy consumption by the compressor because 75% of the energy comes from the ambient air through the evaporator.
- When electricity is generated by solar/wind/hydropower greenhouse gas emission is reduced to zero. Hence, it is environmentally friendly
- No emission of toxic gasses.
- Compared to boilers, it is simple to operate and maintain.

3.5.7 The proposed heat pumps

From the above theoretical detailed description of the heat pump, the moderately high ambient temperature air source heat pump water heater has been identified. Such a heat pump has a low cost and systematically simple to integrate with the proposed PV/T type.

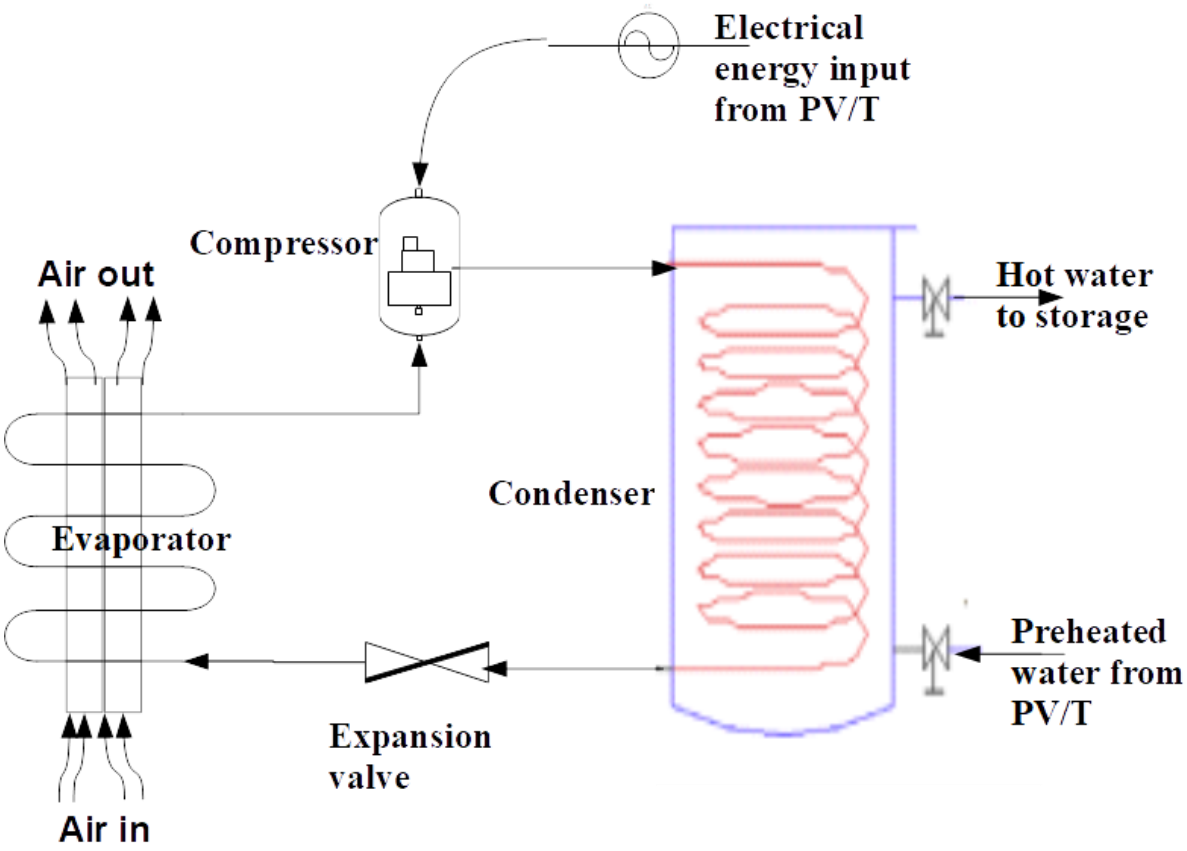

Figure 3-10 Proposed air source water heating heat pump schematic diagram

Figure 3-10 illustrates the heat pump system integration arrangement connected through a working fluid circulating pipe. As can be seen from the figure the evaporator (on the left side of the figure) absorbs heat from the atmospheric air to start heating the circulating refrigerant fluid.

3.6 Hybrid photovoltaic thermal and heat pump system

3.6.1 Introduction

A combination of solar energy and heat pumps can improve the quality of the energy delivered, providing a high potential for different applications. Hybrid PV/T Heat Pump is the combination of heat pump and hybrid photovoltaic thermal system. Both direct and indirect solar assisted heat pumps can be integrated with photovoltaic thermal systems to develop a hybrid PV/T Heat Pump system.

Over the past two decades, the concept of a hybrid PV/T Heat Pump system, developed in 1999 assembled a PV/T Heat Pump system integrating solar-assisted heat pump with PV/T collector,

which serves as an evaporator to the heat pump[75]. Correspondingly, the long term performance of a solar-assisted heat pump for water heating application was investigated in 2003[76]. Likewise, extensive research on PV/T Heat Pump was carried out, including the theoretical and experimental model development [77], [78].

The refrigerant-based PV/T operates in conjunction with a heat pump. A higher temperature of the heat is provided to the system user. The refrigerant-based PV/T can achieve 10% electrical efficiency and thermal efficiency of around 65%. The system is used as a heat exchanger where heat yielded by the PV/T panel is transferred from the absorber, which acts as an evaporator, to the high-temperature condenser by circulating the refrigerants[79]. The condenser then heats the water.

The PV/T Heat Pump had different categories from the most commonly practiced one; the PV/T collector functions as an evaporator i.e. PV/T-SAHP. The other type of PV/T Heat Pump whose PV/T collector is directly used as an evaporator with heat pipe in the system is called the PV-SAHP/HP. And this has got two circulation loops, namely, the water-circulation and refrigerant-circulation loops. The PV/T collectors are arranged parallel to one another at the water/refrigerant-circulation loop. The PV/T collectors/evaporators and the air-cooled heat exchanger are also connected in parallel at the refrigerant-circulation loop. When solar irradiation is sufficient, the hybrid system operates in the heat-pipe mode. The thermal energy of the collectors is transferred by the heat pipes to the water flowing through the collectors. The water pump then circulates the water between the storage tank and the collectors, such that the thermal energy of the collectors is removed by the circulating water and it is stored in the storage tank. However, when solar irradiation is insufficient, the hybrid system operates in the SAHP mode[80].

A new concept of COP analysis of PV/T Heat Pump including the electrical output of the PV/T collector integrated into the PV-SAHP was developed[78]. The PV/T-SAHP is not limited to domestic application, its high potential for different industrial applications was also stated in some works [79].

The PV/T-SAHP starts operation by circulating low-temperature refrigerant through the PV/T collector or evaporators that absorb the thermal energy and become refrigerant vapor. After the vapor passes through the compressor and becomes high-temperature/pressure refrigerant gas,

which is subsequently condensed in the condenser: while the thermal energy is simultaneously transferred from the refrigerant to the water in the storage tank.

Finally, the condensed liquid refrigerant passes through an expansion valve and returns to the evaporator. During rainy days or when solar irradiation is weak, the water is heated by the air source heat pump. In this case, the PV/T collector will not operate as a source of heat [80]. As the collector temperature will be lower than the ambient temperature during rainy days, the collector will not be able to supply heat and thus the system switches the air source to a heat pump or auxiliary heat pump.

Figure 3-11 describes the general working principle and integration of the photovoltaic thermal heat pump system. The solar preheating system mainly consists of an array of hybrid PV/T collectors, a plate type heat transfer device, and solar storage tanks. On the hot side of the heat exchanger, the fluid in the thermal collector circulates according to the temperature differential between the collector outlet and the bottom of the storage tank, which was monitored by an on-off differential controller at upper and lower dead bands. However, on the cold side of the exchanger, cold water is taken from the bottom of the storage tank and delivered to the heat exchanger connected to the collector where it gains solar energy and returns to the tank at a higher temperature. The water circulation is controlled by the on-off differential controller according to the temperature difference between the entrance of the heat exchanger on the hot side and the bottom of the tank.

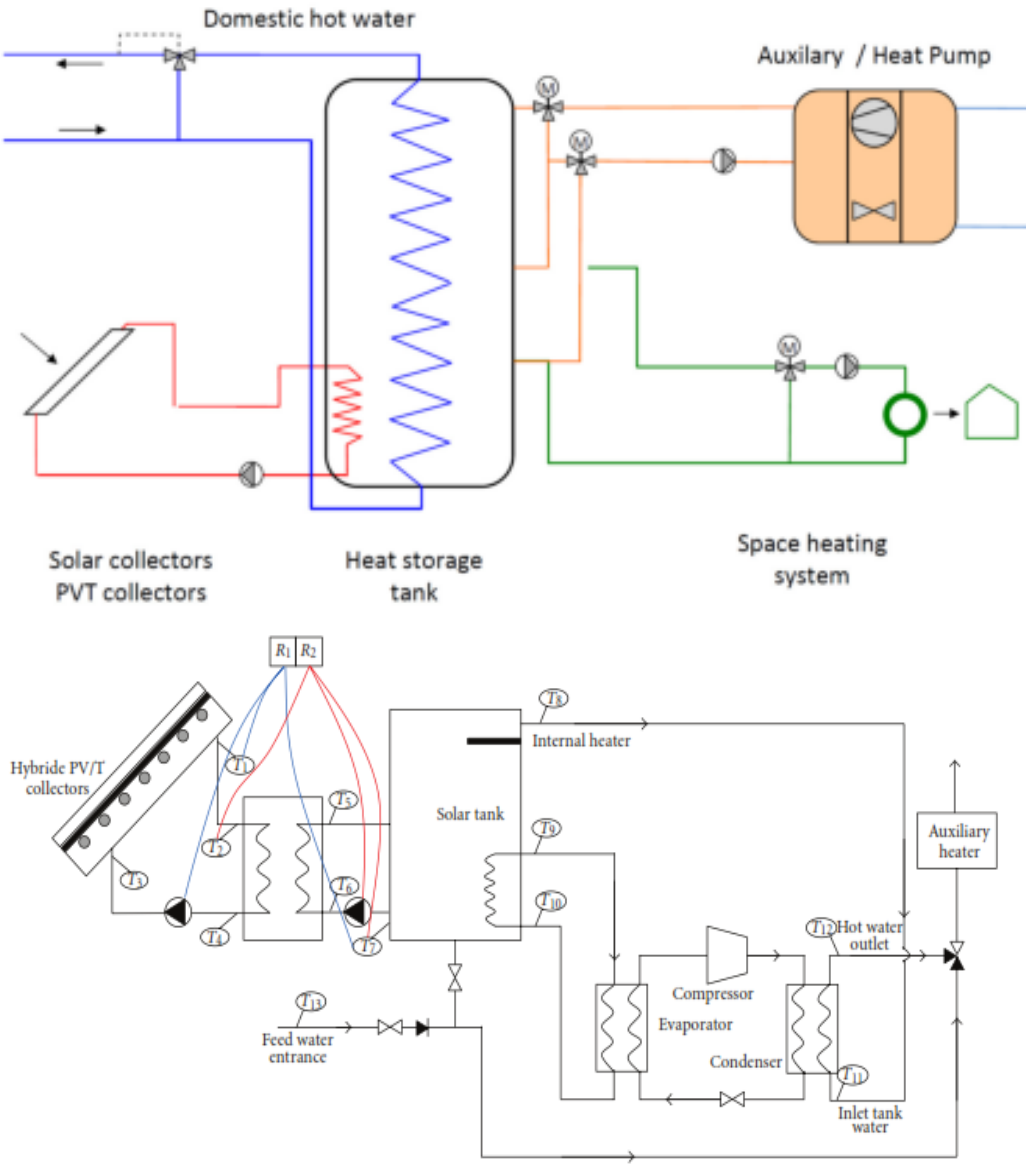

Figure 3-11 PV/T Heat Pump /space heating (top) and direct hot water system integrations (Bottom) [81]

In this work, the system integration of PV/T and air source heat pump water heater were done, considering the application to supply water, ranging from 50 ^{o}C to 60 ^{o}C in all seasons. Thus, the PV/T collector generates pre-heated water which is used as an input to the heat pump for further heating, to deliver to the end-user at the required temperature. The proposed PV/T Heat Pump arrangement is shown in Figure 3-12.

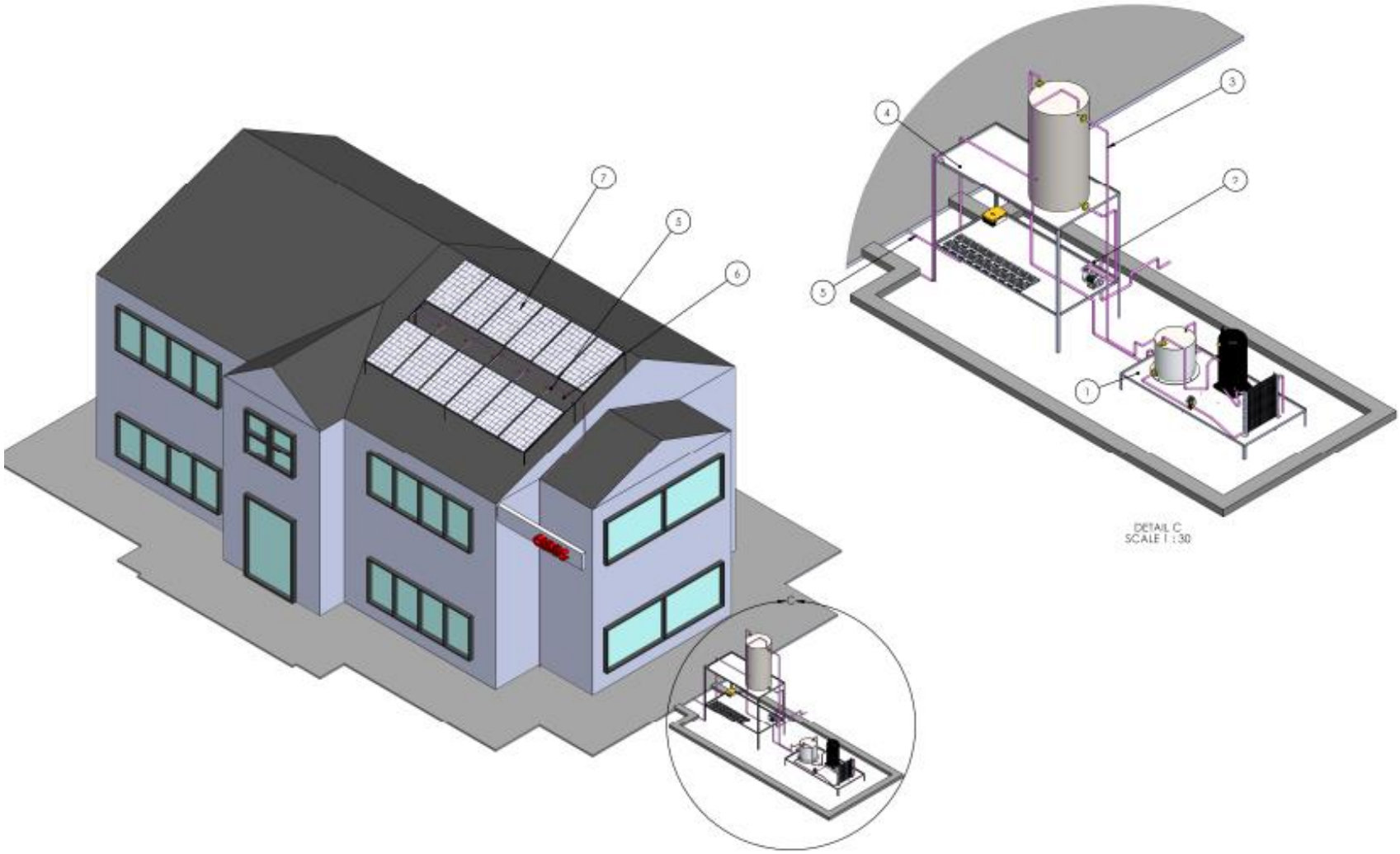

Figure 3-12 The Proposed PV/T Heat Pump integrated into the building in full assembly

CHAPTER FOUR

DEMAND ANALYSIS AND INITIAL SYSTEM DESIGN PARAMETERS

4.1 Introduction

This chapter is the main gate for the following subchapters on system performance analysis. In this chapter, the end-user demand or system sizing parameters will be specified based on the application. In this work, the application of the PV/T system and hybrid PV/T Heat Pump system is considered for lodges, health centers, and restaurants in the off-grid area of Ethiopia. For conducting electrical energy and hot water demand analysis, a lodge with 20 bedrooms is considered. More than eight scenarios of electrical energy supply options from PV/T to the heat pump were considered to be optimized and meet the end-user hot water temperature and hourly consumption. The investigation of hot water hourly consumption patterns was a constant fraction, restaurant, and motel patterns.

4.2 Electrical demand analysis

The calculation of the electrical load was done by determining the electrical appliances at the site, taking into account their daily operating hours as listed in Table 4-1. Most of these data were collected from interviews undertaken at the site. On the other hand, some acceptable standards have been used to determine some of the consumption of gadgets.

Table 4-1 Appliance electrical power usage

Name of appliance	**Power per appliance(w)**	**Number of Appliance**	**Consumption per day**		**Annual ($kwh/year$)**
			Tim (hr)	**Energy (kwh/day)**	
Fluorescent	12	30	12	4.32	1576.8
TV/PC/CD	80	5	6	2.4	876
Deep Fridge	100	1	24	2.4	876
Standby device	-	-	24	0.054	19.71
Total Sum				**9.2**	**3348.56**

Table 4-1 lists the electrical energy consumption of the appliances used as an input for the PVsyst software for sizing the PV area and balance of system (BOS) component. The detailed electrical energy hourly consumption pattern of the site is given in appendix A. beyond the supply of electrical energy, a photovoltaic/thermal-heat pump system was identified as an appropriate solution for supplying hot water.

Three different cases of hourly consumption fraction patterns were used in the simulation. The first one is a constant hourly consumption fraction pattern for 8 working hours (for the clinic), consuming all of the stored hot water. The second and third types of hourly fraction patterns are taken from standards of restaurant and motel cases[82].

4.3 Solar irradiation data analysis

Table 4-2 Recommended average days of the month, values and declination [32]

Month	n **for** i^{th} **day of month**	**Average days of the month**		
		Date	n	δ
January	i	17	17	-20.9
February	$31+i$	16	47	-13.0
March	$59+i$	16	75	-2.4
April	$90+i$	15	105	9.4
May	$120+i$	15	135	18.8
June	$151+i$	11	162	23.1
July	$181+i$	17	198	21.2
August	$212+i$	16	228	13.5
September	$243+i$	15	258	2.2
October	$273+i$	15	288	-9.6
November	$304+i$	14	318	18.9
December	$334+i$	10	344	23.0

In this work, the solar irradiation data on the horizontal surface recorded in short intervals for several years were taken from the Ethiopian Meteorology Agency (EMA). The hourly total average irradiation of the horizontal surface was determined for the 8760 hours of the year. And

simulations are conducted for the representative days of the months given in Table 4-2. The irradiation on the inclined surface has to be determined for these days from the beam and diffuse irradiation.

Figure 4-1 Addis Ababa and Dire Dawa solar irradiation on March and November respectively show the plot of solar irradiation on a horizontal surface, March, and November for Addis Ababa and Dire Dawa the month selected because the two cities scored good solar radiation in those months.

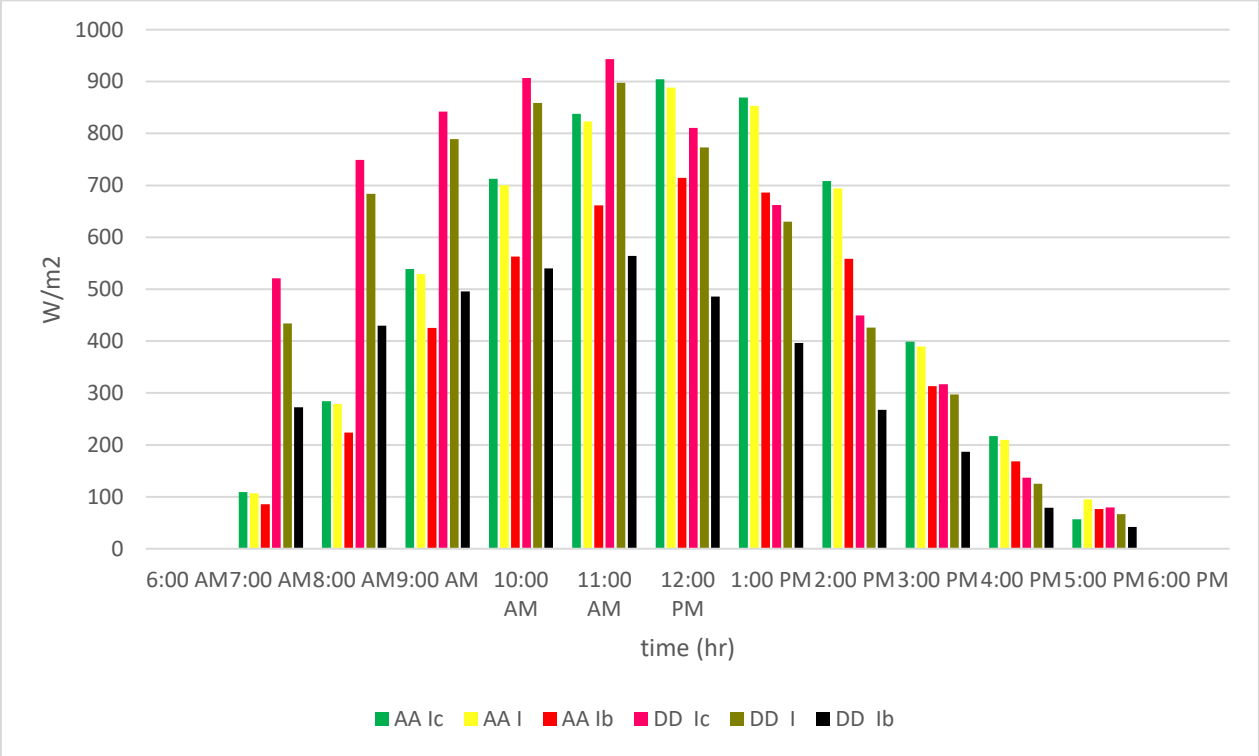

Figure 4-1 Addis Ababa and Dire Dawa solar irradiation on March and November respectively

4.4 PV System sizing

The sizing of PV and balance of system are done using PVsyst 5.74 well-customized application software for grid-connected, stand-alone, pumping, and DC grid sizing software[83]. As per the electrical energy demand, the PV size (PV/T) area is determined without considering hot water energy demand. The comprehensive procedure of system sizing under discussion is described in the flow chart in Figure 4-2.

4.5 PVsyst sizing flow chart

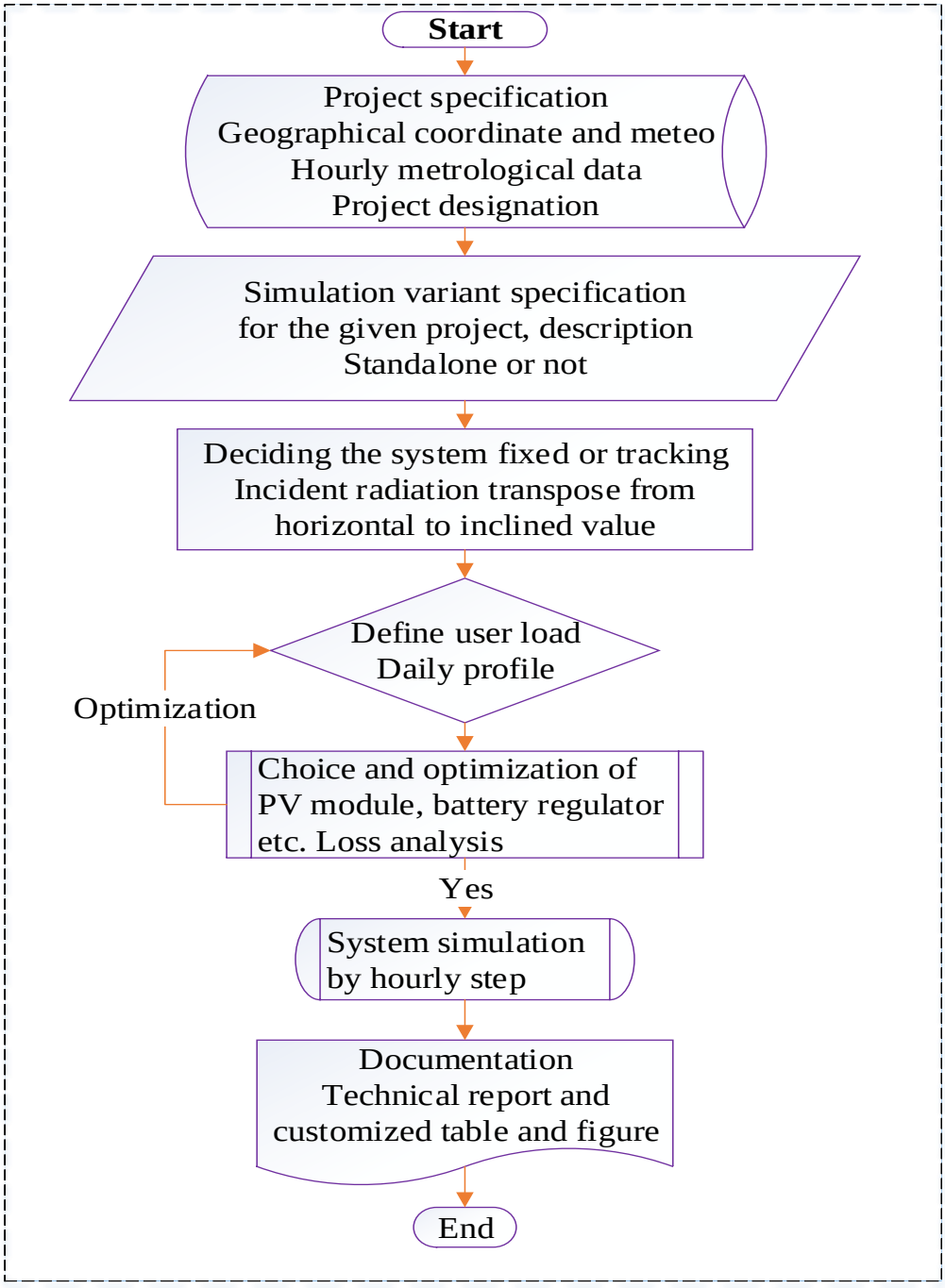

Figure 4-2 PVsyst system sizing flow chart

The generated electrical energy has to meet the demand for end-users electrical appliances and the heat pump. The detailed electrical energy profile supply distribution to the heat pump and other

appliances is quantified in appendix A. The electrical energy demand (load) pattern is given in Figure 4-3.

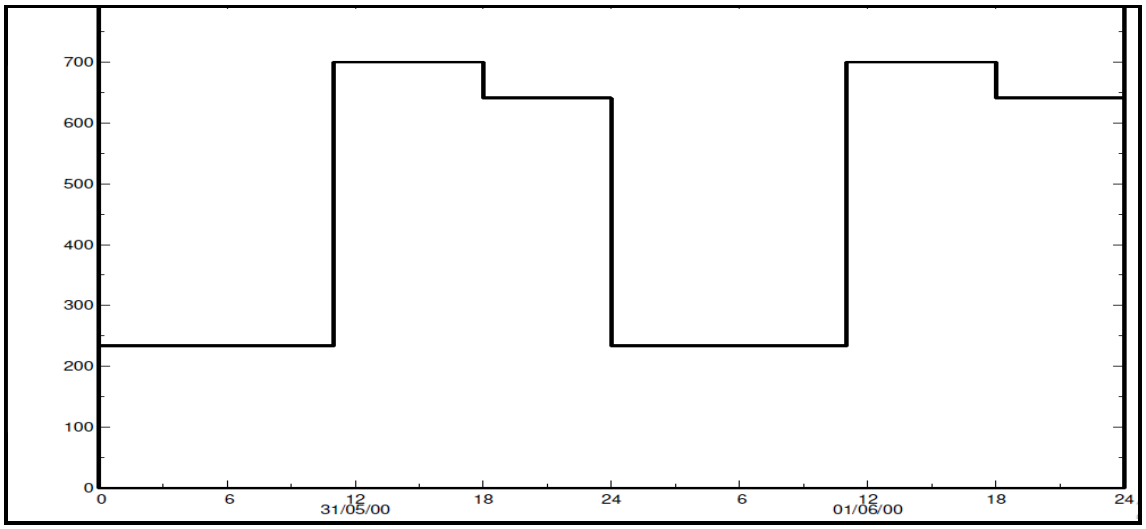

Figure 4-3 User's needs: the daily profile, constant over the year for two sites

The software sized the PV area to meet the electrical load curve which is given in Table 4-3 for two sites to compare a similar energy user demand and other conditions. Dire Dawa and Addis Ababa, respectively. Due to high irradiation, Dire Dawa has a lower number of modules compared to Addis Ababa. However, the PV conversion efficiency is less for Dire Dawa due to high ambient temperature.

Table 4-3 Two site's comparison for a similar energy user demand and other condition

Site Name	**Module Area** m^2	**No module**	**Battery stored**	**Missing energy**	**PV loss due to Temperature**	**Battery loss**	**Solar fraction**
Dire Dawa	20.1	15	58.1%	6.7%	12.7%	9.6%	0.933
Addis Ababa	24.1	18	61.2%	9.2%	9.1%	20.4%	0.908

From the energy generated by the PV system, only 38.8% and 41.9% were obtained from Addis Ababa and Dire Dawa, respectively for direct use without storing in a battery. So, all cases have

used similar battery storage, PV module, and balance of the system. The detailed specification of the PV module and battery specification is indicated in Table 4-4.

Table 4-4 PV module and Battery specification

Description	**PV module**	**Battery**
Model	STK-180P6-A	Solar PV 8G22NF
Manufacture	3E	Deka
Operating condition	$T_{amb} = 20^0 C \;\; at \;\; G = 800 w/m^2$	$20^o c(fixed)$
Unit Nom power	180Wp	
Operating Cha	$64v \times 38A$	$48V \times 1034Ah$
Number of Modules	Total 15, 3 In series x 5 in parallel	Total 88, 4 in series x22 in Parallel

4.6 Different load profile scenario effect

Different scenarios of the hourly load supply profile from the total electrical energy generated by PV/T to the heat pump system are necessary to see the overall performance of the PV/T Heat Pump system. These scenarios are shown in Table 4-5.

Table 4-5 Different electrical usage percentage comparison

The two main category case	**Energy supply (%)**	**Solar fraction SF (%)**	**Missing energy (% &kwh)**	**Battery efficiency loss (%)**	**Battery stored**	**Gassing current /electrolyte dissociation/ loss**
16 and 8 hours	5/90	93.4	6.6/275	1.9	24.4	1.5
Non-working and	10/90	93.7	6.3/259	1.7	25.7	1.5
working of the day	15/85	93.5	6.5/269	1.7	27.4	1.5
energy percentage	20/80	93.9	6.1/253	1.6	29.2	1.5
consumed	25/75	93.8	6.2/259	1.7	32.1	1.6
respectively						
The 12 hours night	10/90	93.6	6.4/264	2.3	36.8	1.1
and day percentage	25/75	93.4	6.6/273	2.5	45.3	1.2
	50/50	93	7/288	3.2	60.8	1.2

consumed
respectively

4.7 Design parameters of the PV/T system

PV/T module: The Dual Sun manufacturer is used in this study. The Dual Sun PV/T module area is 1.654 m^2 [84].

As described in Table 4-6, the detailed size and property of the PV/T module system have been used during this research undertaking.

Table 4-6 PV/T Property and size are used as inputs for the simulation

Name	Symbol	Description	Value
Glass	δ_g	Thickness (m)	0.003
	c_p	Specific heat (J/kg k)	670
	ε_g	Emissivity	0.88
PV module	δ_{pv}	Thickness (m)	0.00035 [85]
	c_p	Specific heat (J/kg k)	677 [86]
	k_{pv}	Thermal conductivity (w/m k)	148
	ε_{pv}	Emissivity	0.83[87]
	η_{pv}	Nominal efficiency	16.87[84]
	β	The inclination of the module	Location latitude
	ρ_g	Ground reflectivity	0.2
	ϵ_{pv}	Absorptivity of cell	0.75 [87]
	d_o	Outer diameter (m)	0.015
	d_i	Inner diameter (m)	0.013
	l_t	Length (m)	1.6
	N	Number per module	10
Tube and Absorber	c_p	Specific heat (J/kg K)	903 [88]
	W	Centre to centre (m)	0.98

	δ_a	Thickness (m)	0.002
	k_a	Thermal conductivity	310
		Material	Copper
Water	$c_{p,w}$	Specific heat (J/kg K)	4186
	k_w	Thermal conductivity (W/m k)	0.608
	V	Volume capacity per module (L)	8.49
	$\dot{m}$	Mass flow rate (kg/s)	0.00138
Insulation	δ_i	Thickness (m)	0.05
	$c_{p,i}$	Specific heat (J/kg k)	
	ϵ_i	Emissivity	
	k_i	Thermal conductivity (W/m2 ^oC)	0.045
Storage	V_t	Total volume (m^3)	0.48
Tank	δ_i	Insulation Thickness (m)	0.05

CHAPTER FIVE

MATHEMATICAL AND COMPUTATIONAL MODELLING OF PV/T SYSTEM

5.1 Introduction

Due to the concern of global warming and the emission of pollutants, environmentally friendly energy resources such as solar energy are becoming popular. While solar energy can be directly converted into electricity by a PV module [89] hot water can be generated by converting solar energy into thermal energy by a solar collector [90]. The photovoltaic thermal (PV/T) system is a superimposition of PV panels with glazing on a flat plate solar collector to generate thermal and electrical energy simultaneously [91]. PV is considered as one of the best options for rural electrification for off-grid areas of developing countries like Ethiopia. Due to falling module unit price, it might be necessary to use a PV/T system where hot water is required in addition to electricity such as off-grid rural clinics and lodges.

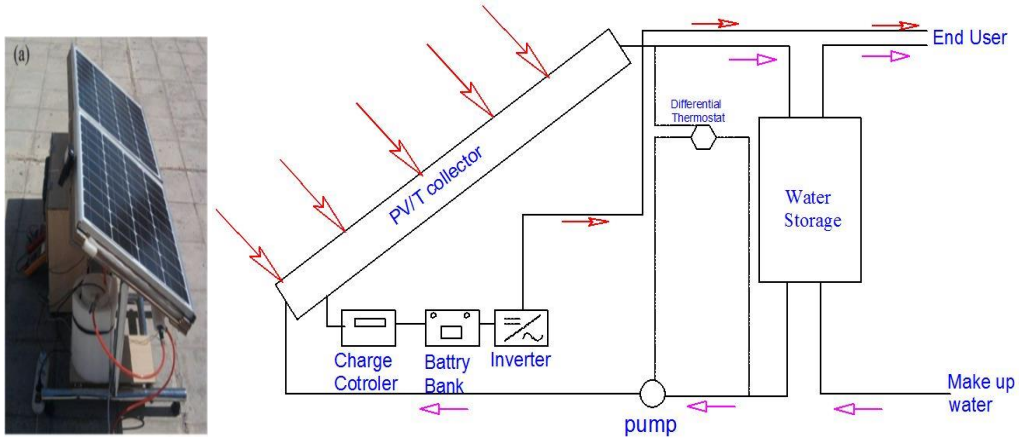

Figure 5-1 Experimental prototype (left)[92] and PV/T system schematic diagram (right).

A PV/T system consists of a PV/T collector, the balance of system (BOS), and a hot water storage tank as shown in Figure 5-1. The PV/T collector has glazing from the top and insulation at the back. In between a superimposition of a PV-module with plate and tube absorber is placed. The PV-module converts part of the incident solar irradiance into electricity and converts most of

the remaining energy into heat. Hence, heat is transferred to water in the absorber tubes increasing the water temperature and cooling the PV-module. As the water from the storage continuously circulates through the PV/T collector, the water in the storage will be heated and hot water will continuously flow from the tank to end-users.

Several researchers have investigated the performance, optimum design parameters, and efficiency of the PV/T system [91]. The performances of the unglazed, single glazed, and double glazed PV/T systems were compared and it was concluded that the unglazed system has the highest electrical efficiency and the lowest thermal efficiency [93]. Another investigation showed that the double glazed system has the lowest electrical efficiency and the highest thermal efficiency [94]. Hence, the single glazed PV/T can be considered as a cost-effective solution for optimum co-generation efficiency. Glazed and unglazed PV/T collectors were built and tested with water and air as working fluid, and thermal efficiency of about 58% and electrical efficiency approximately equal to 11% were obtained [95].

Effect of the mass flow rate of water on performance of PV/T system was investigated and the recommended optimum value was 25 kg/h [43], while 20 kg/h was stated as optimum mass flow rate in another work [96]. These are in agreement with the range of optimum mass flow rates given (as 0.001–0.0085 kg/s) [11]. The electrical, thermal, and PV/T (combined) efficiencies were investigated by a dynamic model under different conditions for a limited duration [49]. The performance of the 1.44 kW unglazed PV/T system was investigated for different locations in Taiwan using TRNSYS software as a simulation tool and electrical efficiency of 11.7–12.4% and thermal efficiency of 26.78–28.41% was obtained [97].

CFD based dynamic analysis of PV/T collectors was also carried out by several researchers [88], [98] But these analyses were performed for limited durations due to the long computational time required by multidimensional dynamic models. However, many researchers used TRNSYS software for predicting the long-term performance of PV/T systems [97]. TRNSYS uses the steady-state or quasi-dynamic model to compute the outlet water temperature. In this case, the collector loss coefficient is considered to be constant, it could lead to overestimation of thermal efficiency and underestimation of electrical efficiency.

Dynamic models of the PV/T system were also developed based on the solution of the transient differential equation obtained from energy balance using an explicit finite difference method for time stepping[49], [88]. However, most of these applications do not consider the effect of end-user hot water consumption patterns and the size of the storage on hot water end-use efficiency.

The proper use of hybrid solar technology requires a tactful balance between the low-temperature requirement of the water stream to serve as a coolant, and at the same time, the high-temperature requirement for satisfying the hot water need of the end-user [99]. Thus, the PV/T system should be considered and designed to preheat water for a maximum of 45–50 ℃ [49].

Current researches in PV/T technology focused on increasing the overall output energy and development of this technology in terms of novel design and high performance [99]. For example, the investigation of the PV/T system with the new configuration in Malaysia gave an electrical efficiency of 13% and a thermal efficiency of 61%. Similarly, investigation on the concentrated photovoltaic thermal collector (CPV/T) with a concentration ratio of 8.5 has shown 4.7 times electrical energy output to conventional PV/T although the electrical efficiency dropped to 8-9% due to high temperature of the PV-module [100], [101]. CPV/T collectors provide incomparably greater thermal and electrical outputs compared to stand-alone PV or PV/T systems as incoming solar energy is maximized inside the unit via energy-efficient concentrators [102].

In this work, the capability of the conventional PV/T system is shown in Figure 5-1 to generate electricity and preheat water using a dynamic computational model based on non-linear transient differential equations. The integrated PV/T collector, storage tank, and end-use system to estimate the amount of thermal and electrical energy generated, considering the hourly hot water consumption pattern and storage size for tropical areas in Africa, particularly for Dire Dawa, Ethiopia.

5.2 Mathematical model of the PV/T system

5.2.1 Estimation of solar irradiance on PV/T surface

The isotropic diffuse model irradiation on a tilted surface, which considers three components: beam, isotropic diffuse, and solar irradiance reflected from the ground are derived as follows [32].

$$I_T = I_b R_b + I_d \left(\frac{1+cos\beta}{2}\right) + I\rho_g \left(\frac{1-cos\beta}{2}\right) \quad (5.1)$$

To calculate the beam and diffuse component for Eq 5.1, a clearness index k_T shall be determined from hourly total irradiation and extra-terrestrial irradiation on the horizontal surface.

$$k_T = \frac{I}{I_o} \tag{5.2}$$

The data *I* is from a measurement of total solar radiation on a horizontal surface, that is, obtained from the Ethiopian Metrological Agency, and the hourly extra-terrestrial irradiation on a horizontal surface for a given hour angle ϖ is given as follows.

$$I_0 = I_{sc}\left(1+0.033\cos\frac{360n}{365}\right)x\left(\cos\phi\cos\delta\sin\omega+\sin\phi\sin\delta\right) \tag{5.3}$$

Where, the declination, (δ) is given as

$$\delta = 23.45\sin\left(360\frac{284+n}{365}\right) \tag{5.4}$$

The diffuse components of solar irradiance on a horizontal surface are determined from the total irradiation on the horizontal surface via k_T value range with the following correlation [32].

$$\frac{I_d}{I} = \sum\begin{bmatrix} 1-0.09k_T & \text{for } k_T \le 0.22 \\ 0.9511-0.1604k_T+4.338k_T^2-16.638k_T^3+12.336k_T^4 & \text{for } 0.22 < k_T \le 0.8 \\ 0.165 & \text{for } k_T > 0.8 \end{bmatrix} \tag{5.5}$$

5.2.2 Transient non-linear ordinary differential equations of PV/T system

For the energy balance analysis, some scientifically accepted assumptions were made for flat-plate PV/T collectors. The energy analysis should start from top to bottom components, from the glass cover up to the bottom insulation. For all parts, energy balance was made considering the rate of change of energy stored in the component, energy transferred into it, and leaving the component.

5.2.3 Glass cover

In analysing the glass cover, the heat transfer by radiation and convection were considered, by neglecting the conduction heat transfer within the glass. In this case, at the top of the glass heat is transferred by convection and radiation to the atmosphere. On the other hand, at the bottom convection and radiation heat transfer occurs between the PV module and the glass cover. Thus,

the rate of change of energy stored in the glass cover is obtained from the difference between solar irradiance absorbed by the glass plus the heat received from the PV module and the heat leaving the glass to the ambient as follows [88], [103].

$$m_g C_g \frac{\partial T_g}{\partial t} = A_{pv}\left[I_c(\alpha)_g + U_{pv-g}\left(T_{pv} - T_g\right) - U_{g-a}(T_g - T_a)\right] \quad (5.6)$$

Where $U_{PV-g} = h_{r,PV-g} + h_{c,PV-G}$ *and* $U_{g-a} = h_{r,g-a} + h_{c,g-a}$

5.2.4 PV module

In the PV module, heat is transferred by conduction to the absorber plate and water tubes in the backside and by natural convection and radiation to the glass cover at the front side. The energy equation of the PV module is obtained by equating the variation of the stored thermal and electrical energy. In the PV module, consider the difference between solar irradiance absorbed by the PV module, and the heat transferred from the PV module to glass and absorber, also electrical energy generated by the PV module [104].

$$m_{pv} C_{pv} \frac{\partial \mathrm{T_{PV}}}{\partial \mathrm{t}} = \mathrm{A_{PV} I_c \tau_g \alpha_{PV} - P_{el} - A_{PV} \frac{k_{PV}}{\delta_{PV}} (T_{PV} - \eta_f T_p) - A_{PV} h_{(PV-g)_c} (T_{PV} - T_g) - A_{PV} k_{(PV-g)_{cd}} (T_{PV} - T_g)} \quad (5.7)$$

The electrical power output of the PV module is given as follows [105].

$$E = I_c \times pf \times \tau_v \eta_0 \left[1 - \varphi_c \left(T_{pv} - 25\right)\right] \quad (5.8)$$

5.2.5 Absorber plate

The absorber plate, which is in direct contact with the back of the PV module at the top and the insulation at the back, has the function of removing heat from the PV module to the water in the tubes. The rate of change of energy stored in the absorber is equated from the difference between the heat transferred to and from the absorber to the PV module. The sum of heat transferred from the absorber to the water in the tubes and the ambient through the back of insulation, where the following transient energy differential equation of the absorber plated is obtained [90].

$$m_p C_p \eta_f \frac{\partial T_p}{\partial t} = \left(A_{pv} \frac{k_{pv}}{\delta_{pv}} (T_{pv} - \eta_f T_p\right) - A_{wt} U_{p-w} \left(f_w x T_p - \frac{T_{w,o} - T_{w,i}}{2}\right) - A_{pv} U_{i-a} (\eta_f T_p - T_a) \quad (5.9)$$

It shall be noted that η_f is fin efficiency of absorber plate to the tube, T_p is the maximum absorber temperature, $\eta_f T_p$ mean absorber temperature and $f_w = (2\eta_f - 1)$ is a factor that is used to determine water tube temperature from maximum absorber temperature.

5.2.6 Water stream

From the energy balance for the water in the tube, the rate of change of energy stored in the water inside the tube is equal to the difference between the heat transferred from the absorber to the water in the tubes and heat transported with water from the tube to storage. As a result, the following transient differential energy equation of the water in the tubes is obtained [104].

$$m_w c_w \frac{\partial T_w}{\partial t} = A_{wt} U_{p-w} \left(f_w \times T_p - \frac{T_{w,o} + Tw,i}{2} \right) - \dot{m}_w c_w \left(T_{w,o} - T_{w,i} \right) \quad (5.10)$$

5.2.7 Storage tank

In a similar manner with Eq 5.10, the rate of change of energy stored in hot water in the tank is obtained from the difference between energy transported from the collector to the tank and energy transported with hot water to the end-user plus the heat losses through the insulation of the tank as follows.

$$m_w c_w \frac{\partial T_{st}}{\partial t} = m_w n c_w (T_{w,o} - T_{w,i}) - dhwc \times c_w \times FF_{ii}(T_{st} - T_{ws}) - U_{st-a} A_{st} (T_{st} - T_a) \quad (5.11)$$

5.3 Computational model

The above transient ordinary differential equations are solved by an explicit finite difference time-stepping scheme. The temperature of the glass, the temperature of the PV module, and temperature of absorber as well water outlet temperature and water storage temperature are obtained by updating the values of the current time step from the previous time step by approximating time derivatives of temperature by forwarding finite difference technique.

5.3.1 Glass cover

Expressing the overall heat transfer coefficient in terms of convective and radiative components, the glass temperature at the current time step is solved as follows.

$$T_{g,i+1} = T_{g,i} + \frac{\Delta t}{m \times c_p} A_c \left(I_c \alpha_g - \left(h_{c,g-a} + h_{r,g-a} \right) \times \left(T_{g,i} - T_{a,i} \right) + \left(h_{c,pv-g} + h_{r,pv-g} \right) \times \left(T_{pv,i} - T_{g,i} \right) \right) \quad (5.12)$$

The radiation and convection heat transfer coefficients at the top and bottom parts of the glass are given as follows [106].

$$h_{r,g-a} = \sigma \varepsilon_g \left(T_{sky}^2 + T_g^2 \right) \left(T_{sky} + T_g \right), h_{r,pv-g} = \frac{\sigma \left(T_g^2 + T_{pv}^2 \right) \left(T_g + T_{pv} \right)}{1/\varepsilon_{pv} + 1/\varepsilon_g - 1} \text{ and } h_{c,g-a} = 2.8 + 3V_{wind} \quad (5.13)$$

Where $T_{sky} = T_a - 6$ taken as per the reference [106] quantified in what way the two temperatures functioned.

The convection heat transfer coefficient Eq 5.13 depends on wind velocity [107].

For the convective heat transfer between the PV module and the glass cover, the correlation of the Nusselt number with the Rayleigh number suggested by [88] is used.

$$N_u = 1 + 1.44 \left[1 - \frac{1708 \sin(1.8\beta)^{1.6}}{R_a \times \cos\beta} \right] \left[1 - \frac{1708}{R_a \times \cos\beta} \right]^+ + \left[\left[\frac{R_a \times \cos\beta}{5830} \right]^{1/3} - 1 \right]^+ \quad (5.14)$$

5.3.2 PV module

The recursive formula for updating the PV module average temperature at the new time step is obtained as follows.

$$T_{PV,i+1} = T_{PV,i} + \frac{\Delta t}{(m_c)_{PV}} A_c \left[I_c - P_{el,i} - \frac{k_{PV}}{t_{PV}} A_{PV-P} \left(T_{PV,i} - \eta_f T_{P,i} \right) - \left(h_{c,PV-g} + h_{r,PV-g} \right) \left(T_{PV,i} - T_{g,i} \right) \right] \quad (5.15)$$

5.3.3 Absorber plate

The maximum temperature of the new time step of the absorber plate is expressed by the following recursive formula.

$$T_{P,i+i} = T_{P,i} + \frac{\Delta t}{\eta_f (m_c)_P} \left[\frac{k_{PV}}{t_{PV}} A_{PV,i} \left(T_{PV,i} - \eta_f T_{P,i} \right) - \frac{\Delta t}{\eta_f (m_c)_P} \left(A_{wt} U_{P-w} \right) \left(F_w \left(2\eta_f - 1 \right) T_{P,i} - \frac{T_{wo,i} + T_{wi,i}}{2} \right) - U_{P-i} A_P \left(\eta_f T_{P,i} - T_{a,i} \right) \right] \quad (5.16)$$

5.3.4 Water outlet

The outlet temperature of the water from the collector for the new time step is given as follows.

$$T_{wo,i+1} = T_{wo,i} + \frac{\Delta t}{(m_c)_w}\left[A_{wt} U_{p-w}\left((2\eta_f - 1) T_p - \frac{T_{wo,i} + Twi,i}{2} \right) - \dot{m}_w c_w \left(T_{wo,i} - T_{wi,i} \right) \right] \quad (5.17)$$

The useful heat is evaluated as follows as per Duffie and Beckman [32].

$$Q_u = \dot{m}_w c_w \left(T_{wo} - T_{wi} \right)$$

(5.18)

5.3.5 Storage

The water temperature in the storage is updated at every time step as follows.

$$T_{stw,i+i} = T_{stw,i} + \frac{\Delta t}{C_w \rho_w V_{st}} \left[m_w n c_w \left(T_{wo,i} - T_{wi,i} \right) - \left[U_{st-a} A_{st} \left(T_{stw,i} - T_{a,i} \right) + \right. \right.$$

$$\left. \left. \rho_w V_{st} dhwc \times FF_{ii} \left(T_{stw,i} - T_{ws} \right) \right] \right] \quad (5.19)$$

5.4 Program flowchart

The developed dynamic computational model of PV/T integrated with storage was programmed in a MATLAB environment. The main input to the program is the beam, diffuse irradiance, and ambient temperature for the 8760 hours of the year, as well as PV/T collector design parameters, location data, hot water storage, and consumption pattern data, are input as demonstrated in Figure 5-2. The incident irradiance on the PV surface is computed and determined at every hour and the useful thermal energy, glass temperature, PV temperature, and absorber temperature collector outlet temperature and, hot water temperature in the storage tank and energy of hot water supplied to the end-user are determined for every time step.

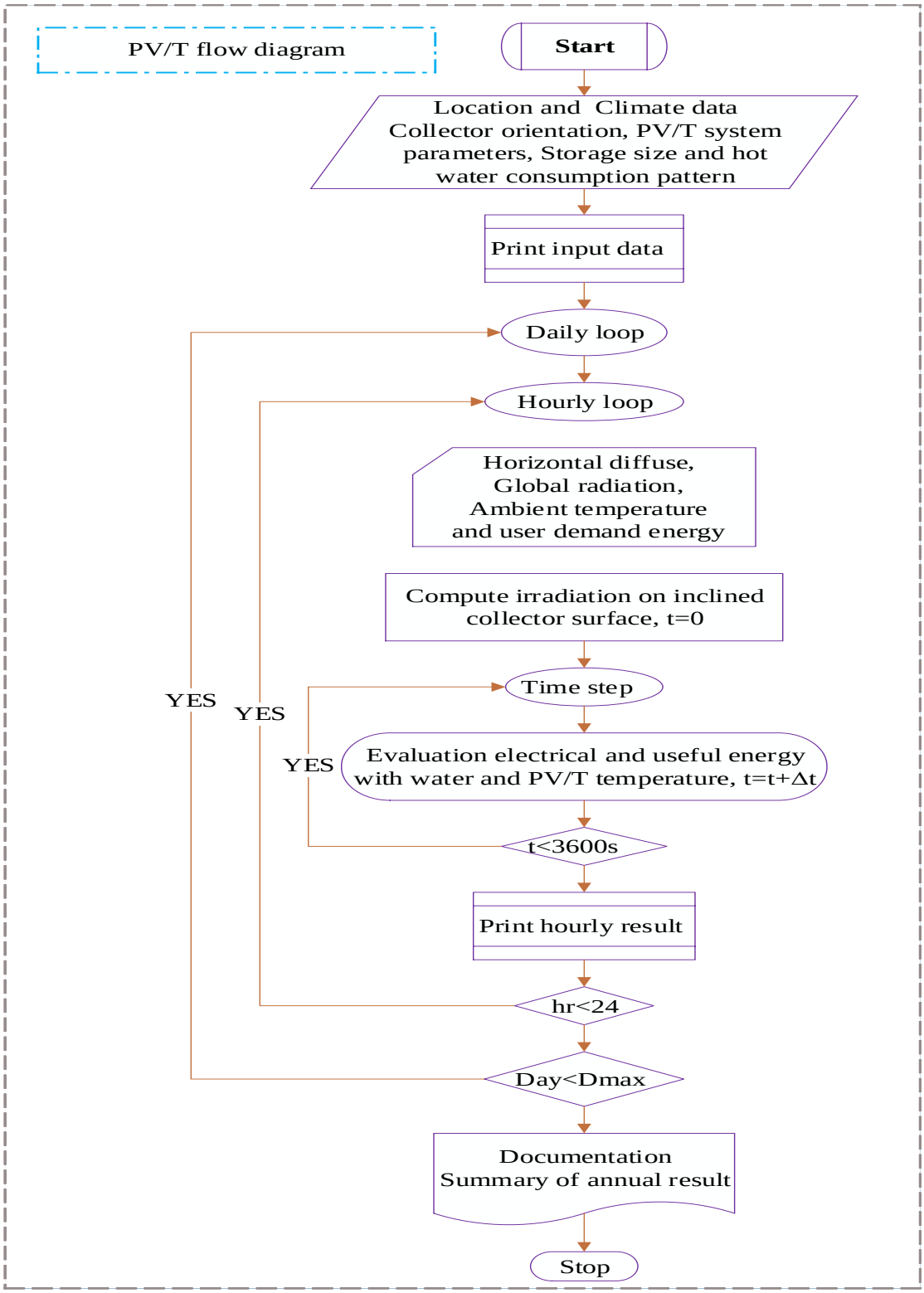

Figure 5-2 PV/T dynamic simulation program flowcharts.

5.5 Verification with the experimental result

The verification of results of the dynamic computational model of this work was done by comparison with the experimental work of a similar PV/T system [92]. The input parameter of the experimental work is given in Table 5-1. Using the weather data of the experimental site and PV/T parameters, a simulation was conducted by the MATLAB program of the dynamic computational model of the PV/T system and the simulation results were compared with the experimental result for validation.

Table 5-1 Experimental validation input parameters

Parameters	**Value**
Collector area	0.3
Collector fin efficiency factor	0.55
Fluid thermal capacity	4.174kJ/kg.k
Collector plat absorbance	0.9
Collector loss coefficient	$17W/m^2.k$
Cover transmittance	0.95
Temperature coefficient for solar cell	0.0045
Reference temperature for cell	25^oC
Packing factor	1
Cell efficiency	14%
Mass flow rate	30kg/h

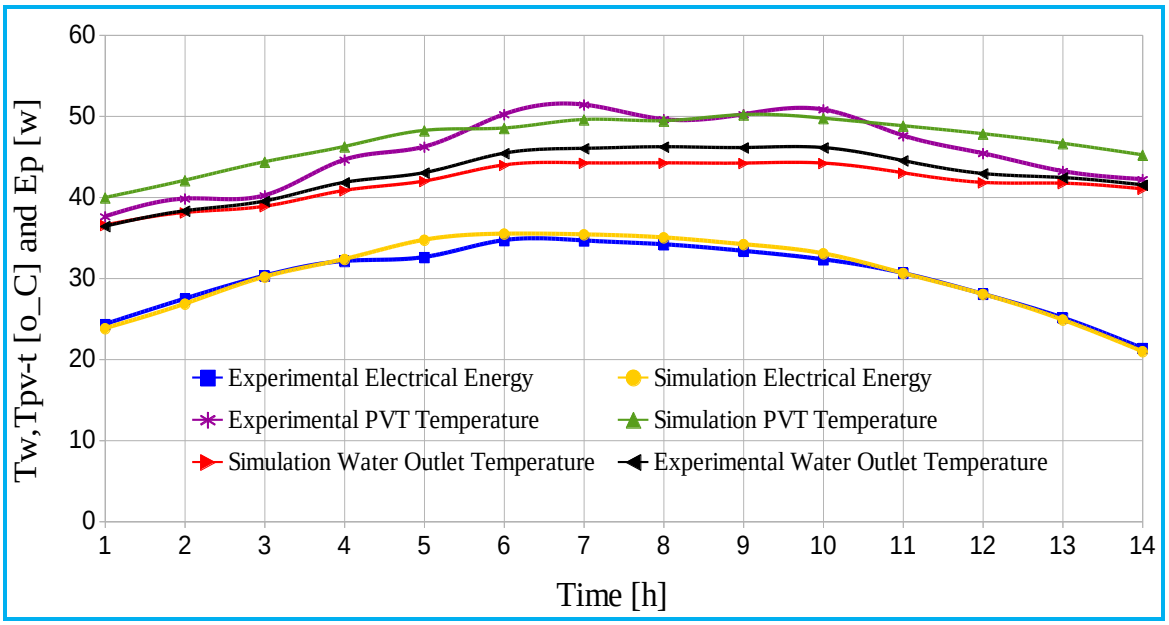

Figure 5-3 Comparison of the PV/T experimental and the simulation results

Figure 5-3 compares the experimental and simulation results for electrical energy generation, water outlet temperature, and PV/T surface temperature. In all cases, simulation and experimental results are in good agreement with an average error of 1.77%, 2.3%, and 3% for electrical energy, water outlet, and PV/T surface temperature, respectively. The computational model has low accuracy compared to experimental investigation due to simplifications in model formation, discretization error in numerical approximation, and rounds off error during computing. Hence, the errors are in an acceptable range.

A comparison was also done with other experimental results [100], [101] doing the simulation using similar solar irradiance on the collector surface and ambient temperature, and mass flow rate of water. The result shows electrical power out-put and the PV panel temperature have a similar trend with slight variation.

5.6 Result and discussion

Using the PV/T system simulation program, co-generation of hot water with 1 kW of electricity was investigated for an off-grid rural clinic near Dire Dawa, Ethiopia. Hourly ambient temperature and total irradiation on the horizontal surface were averaged for 5 years as input to the simulation. The initial size or area of the PV/T system was predicted using PVsyst, which is PV design

software. As per the result of PVsyst, 12 PV/T panels with each module area of 1.65m^2 and a capacity of 250 Wp are sufficient to yield an average of 1 kW during the working hours. Hence 12 PV/T collectors with a total area of 20 m^2 are interconnected for cogeneration of electric power and hot water.

5.6.1 Hourly solar irradiance incident on the collector surface

The hourly solar irradiance incident on the inclined PV/T collector was determined using Eq 5.1 after the clearness index was evaluated from total irradiation obtained from meteorology and extra-terrestrial irradiation on a horizontal surface by Eq 5.2 [32]. Figure 5-4 shows the hourly solar irradiance on the PV/T cover during the day for different months considering the geometrical orientation of the collector and location data of Dire Dawa.

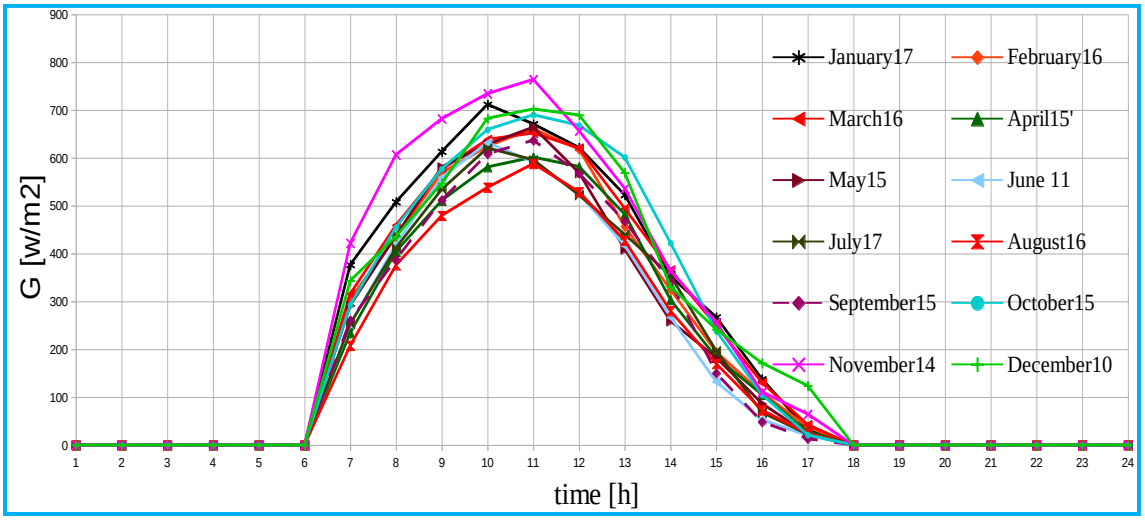

Figure 5-4 Solar irradiances on the collector surface for each month in W/m^2

As shown in Figure 5-4 the solar irradiance reached a maximum of 780 $\frac{w}{m^2}$on an average day of November and a minimum solar irradiance in August.

5.6.2 Glass temperature

Figure 5-5 shows the average hourly temperatures of the glass cover for the representative days of the months. The maximum temperature of the glass cover reached 37℃ in June and the minimum temperature in February and January.

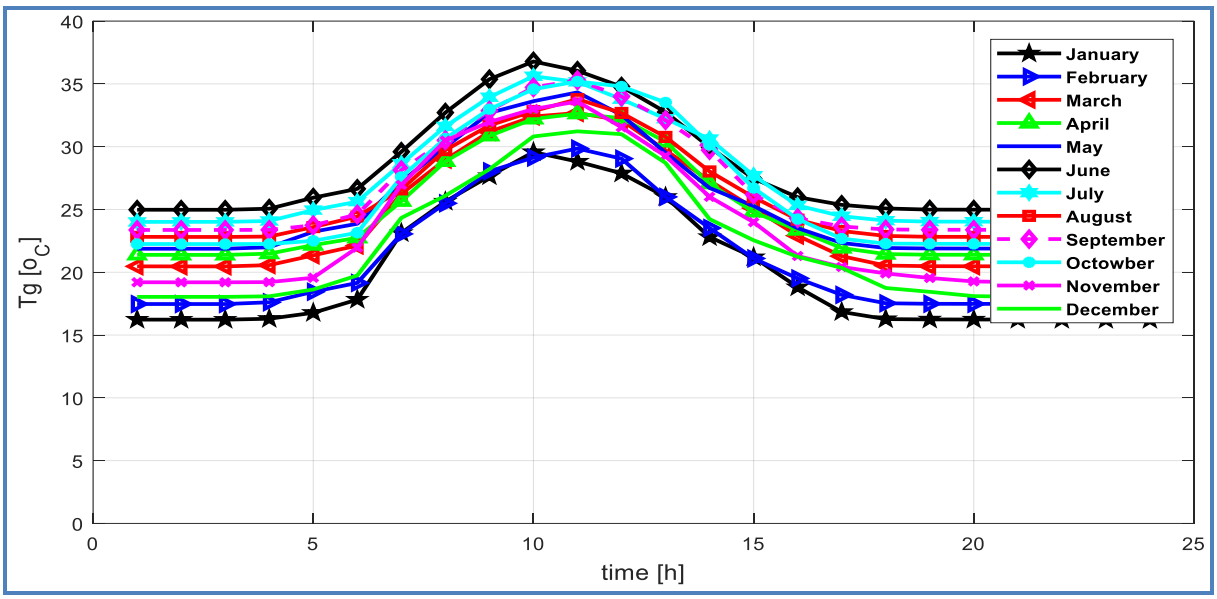

Figure 5-5 Glass temperatures on the representative day of the month

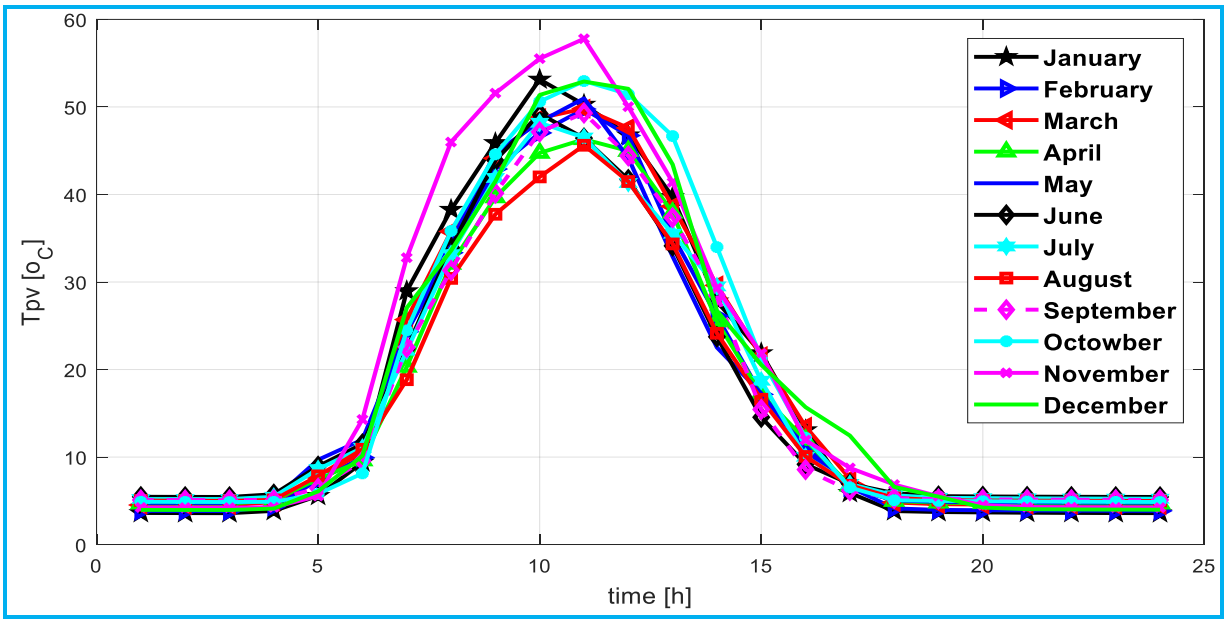

Figure 5-6 Photovoltaic module temperatures on representative days of the month.

5.6.3 Photovoltaic thermal module temperature

The PV module generates electrical energy and transfers heat to the absorber and subsequently to the water in the tubes. Figure 5-6 shows the maximum temperature of the PV-module, which reached 57 ^{o}C in November, and the minimum temperature in August. The PV-module temperature is highly dependent on solar irradiance, the mass flow rate of water, and many other parameters. It is possible to decrease or increase the temperature of PV by varying these parameters. As the mass flow rate of water increases, the PV module temperature decreases. Hence optimum mass flow rate is required to keep the PV module temperature under a given value and generate hot water at the required temperature.

5.6.4 Electrical output

The results of the annual performance simulation indicated that PV/T System simulation can generate 3720 kWh electrical energy per year, which is 10.2 kWh per day on average. This result is above the prediction of PV design software (9.22 kWh per day) for the cooling of the PV module resulted in higher PV efficiency. Figure 5-7 illustrated the daily generation of electrical energy in each module.

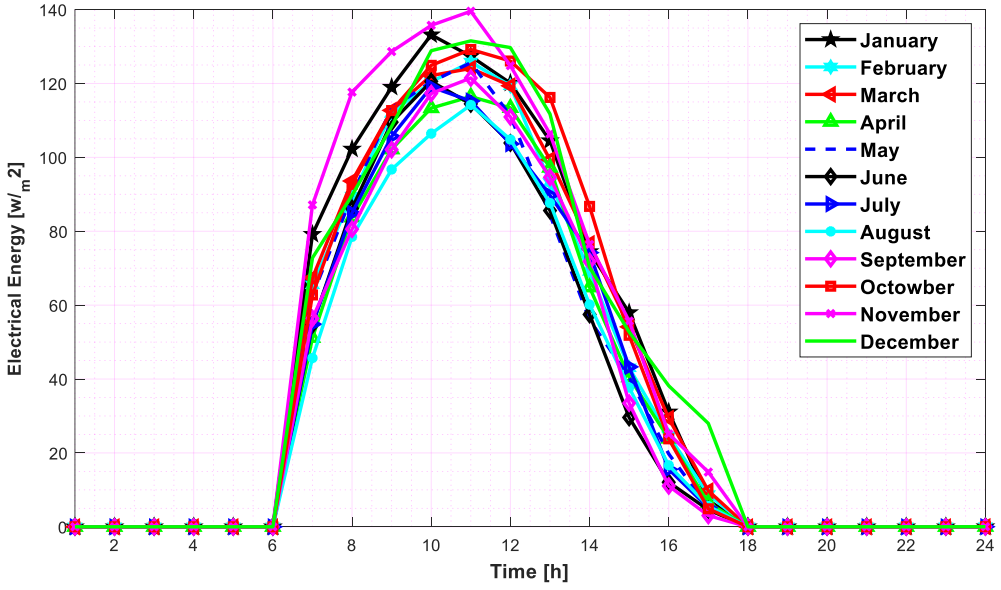

Figure 5-7 Electrical Energy generated by PV/T in one module

5.6.5 Absorber temperature

Figure 5-8 shows the maximum temperature of the absorber plate (in the middle between tubes). The maximum hourly temperature of the absorber reached 53°C in June.

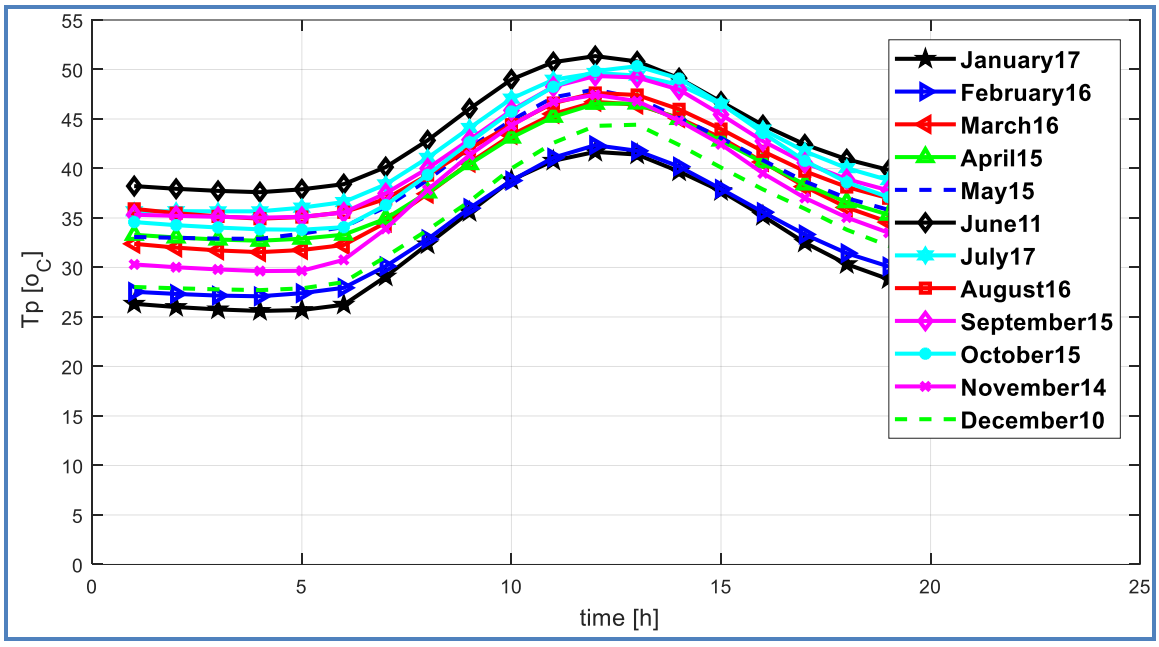

Figure 5-8 Absorber temperature on representative days of the monthly

5.6.6 The hot water outlet temperature of the PV/T collector

The hot water outlet temperature from the PV/T panel depends on several parameters among which the end-user hot water consumption pattern, storage tank size, and cold-water supply temperature are the most important ones.

Figure 5-9 shows the outlet temperature of the PV/T collector for constant hot water consumption patterns during the working hours of a rural clinic with total daily water consumption of 0.48 m^3 per day and a storage capacity of 0.48 m^3.

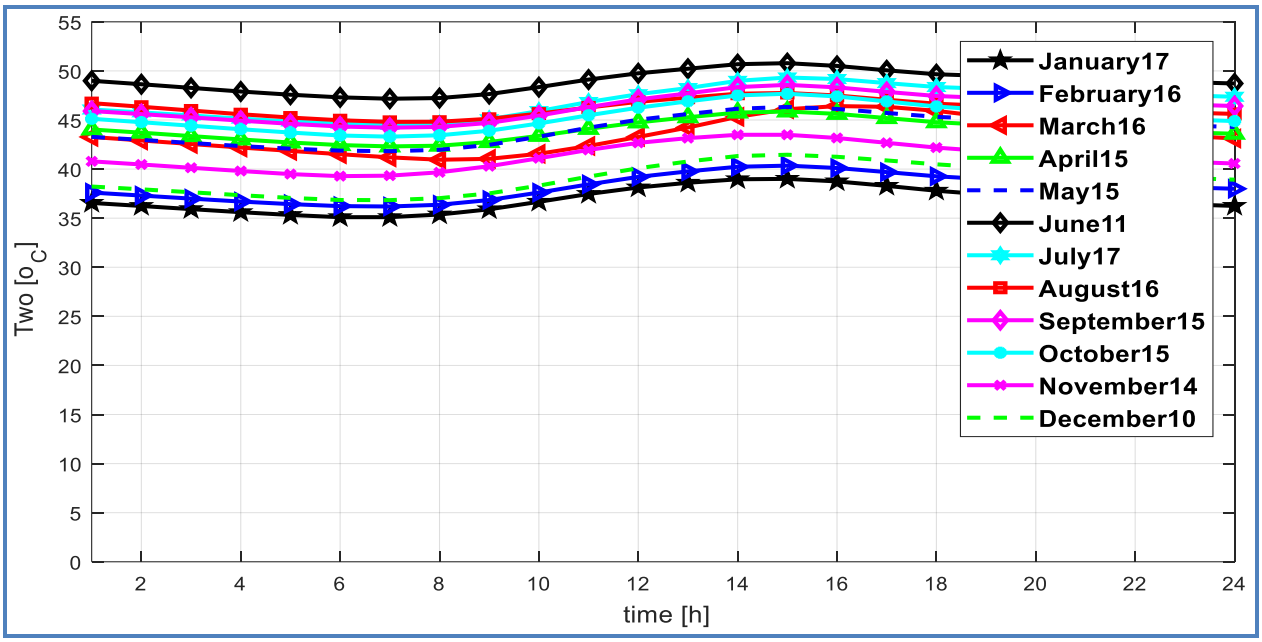

Figure 5-9 PV/T water outlet temperature on representative days of the month at Vs = 0.48m3

The outlet temperature showed a slight increment when the storage volume is decreased. The hot water outlet temperature is highly dependent on the mass flow rate with the other parameters kept constant. Comparing the circulation mass flow rate of 0.00138 kg/s per PV/T panel with 0.00164 kg/s, the PV/T water outlet temperature decreased. Table 5-2 shows that useful heat obtained from the collector increases slightly as the mass flow rate increases.

Table 5-2 Mass flow rate comparison (energy is given in kWh).

Item for comparisons	$\dot{m}_w$ **= 0.00138kg/s**	$\dot{m}_w$ **= 0.00164kg/s** [49]	**Result Difference**
Annual elect. Energy	3684	3694	+10
Annual useful heat	10094	10621	+527
Annual sol. Energy	13464	13464	0
Elec efficiency	15.4%	15.4%	0
Thermal efficiency	50.4%	50.89%	+0.49%
Hot water efficacy	37.99	37.72%	–0.27%

5.6.7 Hot water temperature in the storage tank

The computer program requires an input of daily hot water consumption, storage tank size, insulation thickness, and an hourly fraction of daily hot water consumption, which affects the hot water temperature in the tank, which is affected by the climate data and PV/T collector parameters.

Figure 5-10 shows the hot water temperature in the storage tank for the case of 0.48 m^3 size tank, 0.48 m^3 daily, hot water consumption with constant hot water consumption during the working hour for a rural clinic. Sensitivity analysis of the system for different tank sizes of 0.48 m^3, 0.6 m^3, and 0.72 m^3 resulted in a storage tank temperature of 43.45 ℃, 43.19 ℃, and 42.93 ℃, respectively.

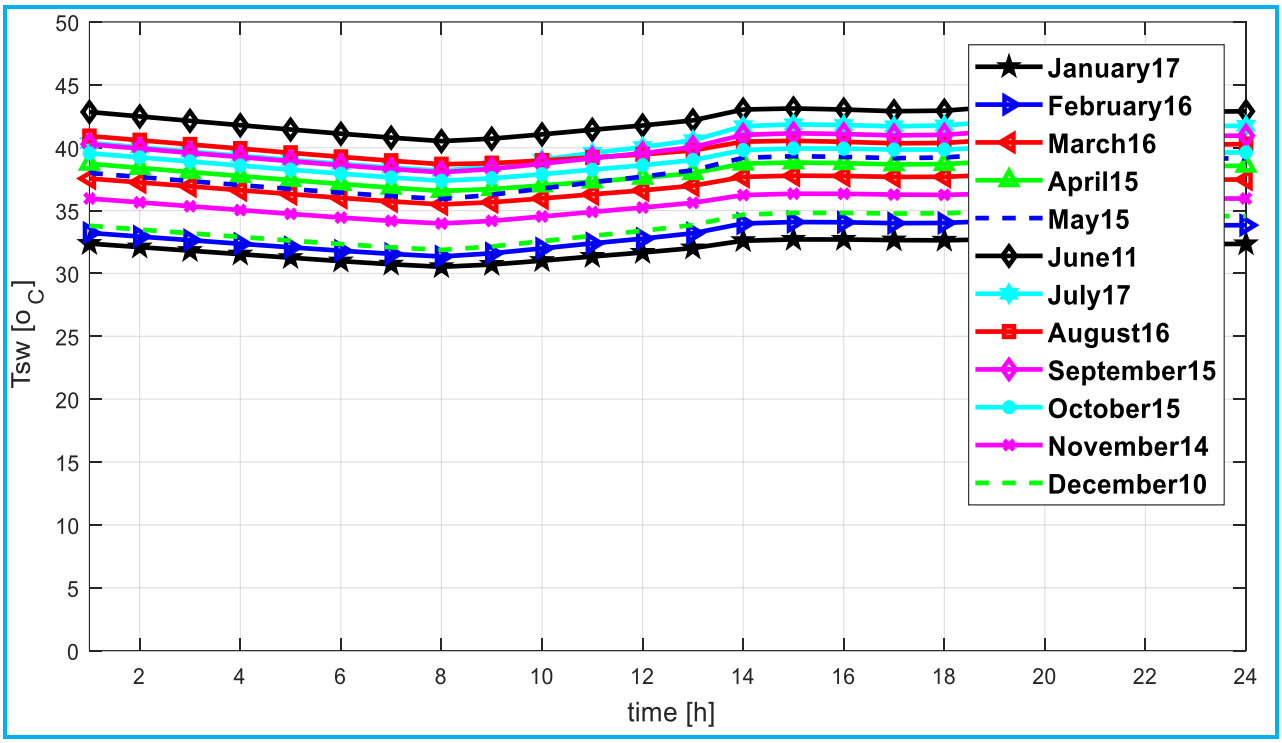

Figure 5-10 Water temperature in the storage tank on the representative days of the month at Vs = 0.48 m^3

5.6.8 PV/T system efficiencies

PV/T generates concurrently hot water and electrical energy within one component, so it has electrical, thermal, and cogeneration efficiencies. As shown in Figure 5-11 cogeneration efficiency (thermal plus electrical) of the system is illustrated for each month of the year. The cogeneration efficiency ($\eta_0 = \eta_{th} + \eta_{ele}$) evaluates the combined output by taking the yearly total output of the system [108].

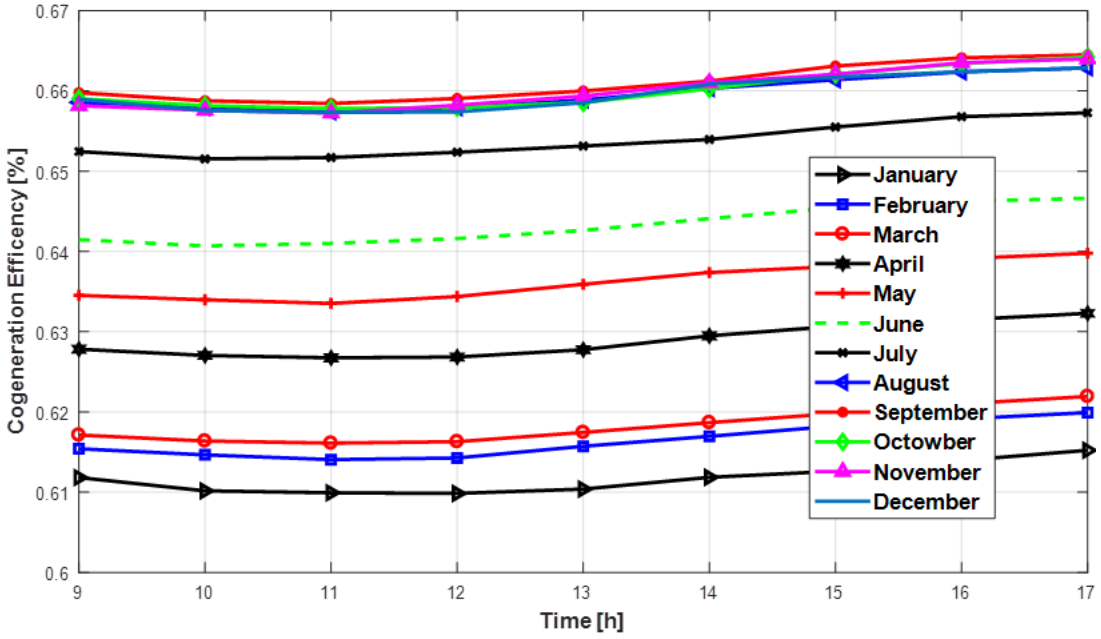

Figure 5-11 Cogeneration efficiency of the PV/T system.

a) Electrical efficiency

$$\eta_{elc} = \frac{E_{el,a}}{G_{pv-t,a}} = 15.4\% \tag{5.20}$$

b) Thermal efficiency

$$\eta_{th} = \frac{Q_{th,a}}{G_{pv-t,a}} = \frac{1.012 \times 10^3}{2.007 \times 10^3} \times 100 = 50.4\% \tag{5.21}$$

c) Hot water end-use overall efficiency

$$\eta_{th,end} = \frac{Q_{hws,a}}{Q_{pv-t,a}} = 37.9\% \quad (5.22)$$

d) Cogeneration efficiency

$$\eta_o = \frac{E_{el,a} + Q_{th,a}}{G_{pv-t,a}} = 65.8\% \quad (5.23)$$

5.6.9 Comparison with selected researches of PV/T system

Table 5-3 shows the comparison of the other four previous works with the results of this study. While article 1 and article 2 give higher thermal efficiency and slightly higher maximum water temperature, the results of these investigations are based only on one sunny day investigation moreover the hot water use pattern is neglected. The channel type of absorber can have higher thermal efficiency compared to the tube and plate absorber considered in this study, the average thermal efficiency of article 4 and maximum water outlet temperature is also less than that of this work.

Hence, it can be concluded most of the studies conducted so far are based on the results of short-term duration without considering the actual hot water storage and use pattern. Even there are few long-term performance simulation results, does not consider the effect of daily hot water use pattern by the end-user.

Table 5-3 Comparison of different papers.

Comparison criteria	**1st paper** [109] **Published 2014**	**2nd paper** [87] **Published 2015**	**3rd paper** [110] **Published 2015**	**4th paper** [111] **Published 2012**	**5th Current research paper**
Location and types of collector	Malaysia 4.2° N,101.9° E Glazed PV/T	Algeria 32.4° N, 3.6° E Glazed PV/T	Sydney 33.8° S,151.2° E Both glazed and unglazed PV/T	Lyon 45.7° N,4.8° E Both glazed and Unglazed	Dire Dawa 9.6° N,41.8° E Glazed PV/T
Types of analyses	Numerical Analysis only	Numerical and Experimental	Simulation and Validation with experimental	Simulations using TRNSYS	MATLAB Simulation

	sunny and cloudy days				with validation
The outlet water temperature of PV/T	Sunny 54 ℃ and cloudy 41 ℃ days	Not given	Max of 38 ℃ Tested for 3 days	Max 45 ℃ with axillary heater	Max 50 ℃
Efficiencies	$\eta_{el} = 12.9\%$ $\eta_{th} = 61.3\%$ at sunny days	$\eta_{el} = 11.1\%$ $\eta_{th} = 54.5\%$ Sunny day in September	Not given	$\eta_{el} = 11\%$ $\eta_{th} = 72\%$ at zero reduced temperature	$\eta_{el} = 15.4\%$ $\eta_{th} = 50.4\%$ Annual efficiency
Daily hot water Consumption Pattern	Not considered	Not considered	Not considered	Not considered as a variable	Considered
Mass flow rate	No specified	No specified	0.217 kg/s m^2	0.0125 kg/s m^2	0.0013 kg/s
Hot water Storage	Heat up in one day	No description	Yes The temperature of storage is set equal to that of main water every morning	Yes	Yes Storage temp. at every morning is obtained from the previous day

Note: The reduced temperature corresponds to the difference between the fluid mean temperature and the ambient temperature, divided by the solar irradiation [111].

5.7 Conclusion on PV/T performance

A dynamic computational model of a PV/T system integrated with a storage tank and hot water end-use was developed and the accuracy of the computer program was checked by comparing the model with experimental results. Simulation result of cogeneration of electricity and hot water for rural clinic around Dire Dawa was investigated. The results indicated that a PV/T system can supply hot water up to a maximum of 45 ℃, attaining the following achievements PV efficiency of 15.4%, thermal efficiency of 50.4%, hot water end-uses overall efficiency of 37.9%, and

cogeneration efficiency of 65.8%. The fraction of the PV/T system in meeting the hot water energy demand was 44.5% when the hot water supply temperature is 60 ℃. There is more than a 10% difference between the thermal efficiency and overall end-use efficiency of hot water generation due to the time shift between generation and consumption of hot water.

The research indicated that the PV/T system has good PV and cogeneration efficiencies. The effect of considering daily hot water demand fraction variability and storage size effect resulted in hot water end-use overall efficiency close to the reality and a maximum hot water supply temperature becomes below 45 ℃. Hence, a PV/T system can be used only as a preheater for hot water generation systems even in tropical African areas meeting at maximum up to 50% of the energy demand. Moreover, the time shift between hot water generation and consumption as well as dilution of hot water by cold make-up water causes degradation of thermal energy and lower end-use efficiency and hot water temperature.

CHAPTER SIX

HYBRID PHOTOVOLTAIC THERMAL HEAT PUMP SYSTEM

6.1 Introduction

The proposed integrated hybrid photovoltaic thermal and heat pump water heating system for this research consists of a PV/T system that generates warm water and electricity and an air-to-water heat pump that uses the warm water from PV/T and generates hot water. The heat pump boosts the temperature of warm water to 50-70 ^{o}C running with the electricity supplied by PV/T. The system can be configured in such a way only to supply hot water or both electricity and hot water. In the first case, the PV/T will generate sufficient electricity in the critical month to run the compressor of the heat pump so that it can boost the warm water from the PV/T storage tank to the minimum required temperature. In the second case, it will generate electricity not only to run the air source heat pump water heater but also it will supply additional electricity for different applications such as lighting, refrigeration, etc.

Compared with a fuel hot water boiler or electrical water heater, a heat pump water heater is a more efficient and environment-friendly system[112]. Air source heat pump (ASHP) is a state of art heating system with many advantages, such as low energy consumption and relatively stable performance with huge energy-saving potential[113]–[115]. A heat pump water heater supplies water at the required temperature using an on/off or modulating control system of the compressor and it can have also an electric heater back-up heater integrated with the storage tank[31].

Air sources heat pump water heater using grid electricity are widely used for domestic water heating, swimming pool heating, and commercial water heating. Following the international trend, several air source heat pump water heaters were installed in 2-4-star hotels in Ethiopia in the last decade.

In the hybrid photovoltaic thermal heat pump system mentioned in the literature, PV is used as a source of electrical energy to the heat pump compressor, PV/T thermal collector is used as an evaporator and the condenser is used for water or air heating [116]–[118]. However, such a system

is complex and will not function in months of very low solar irradiation. As PV/T collectors and air source heat pump water heaters are available in the market, the two units can be configured in the right proportion to construct a hybrid PV/T Heat Pump system to meet a specified hot water and electricity load.

The main novelty of this work is that the PV/T system is used as a source of electrical energy to the compressor of the heat pump and used PV/T collector as water pre-heater for the heat pump water heater rather than an evaporator (refrigerant fluid circulated in the PV/T collector). The pre-heated water by the PV/T collector is circulated through a heat pump condenser for further water temperature increment to the required level. The main motivation to use PV/T electricity heat pump mainly lies in that heat pump can have a COP of 2-5 and PV price per peak Watt has been drastically falling.

6.2 System description

As shown in Figure 6-1, the PV/T collector absorbs solar irradiation and converts it into electrical and thermal energy. While part of the irradiation is converted into electricity, some are lost to the ambient and the rest is converted into heat and transferred to the absorber plate below the PV module and eventually to the water in absorber tubes generating water up to 50 ℃. The pre-heated water is accumulated in the PV/T warm water tank from which it is transported to the heat pump hot water tank to make the hot water supplied to the end-user.

The hot water in the heat pump hot water tank enters into the heat pump circulation loop and is heated by the refrigerant in the condenser while the refrigerant vapor condenses at high pressure. The heated water conveys thermal energy from the condenser into the hot water storage tank from which hot water is delivered to the end-user. As hot water is consumed by end-use, make-up warm water will flow from the PV/T tank to the heat pump hot water tank. And make-up cold water enters from water supply main into PV/T warm water tank. The flow of make-up water to the two tanks are controlled by level controllers. Small pumps are used to circulate the water through the PV/T thermal collector and the heat pump condenser.

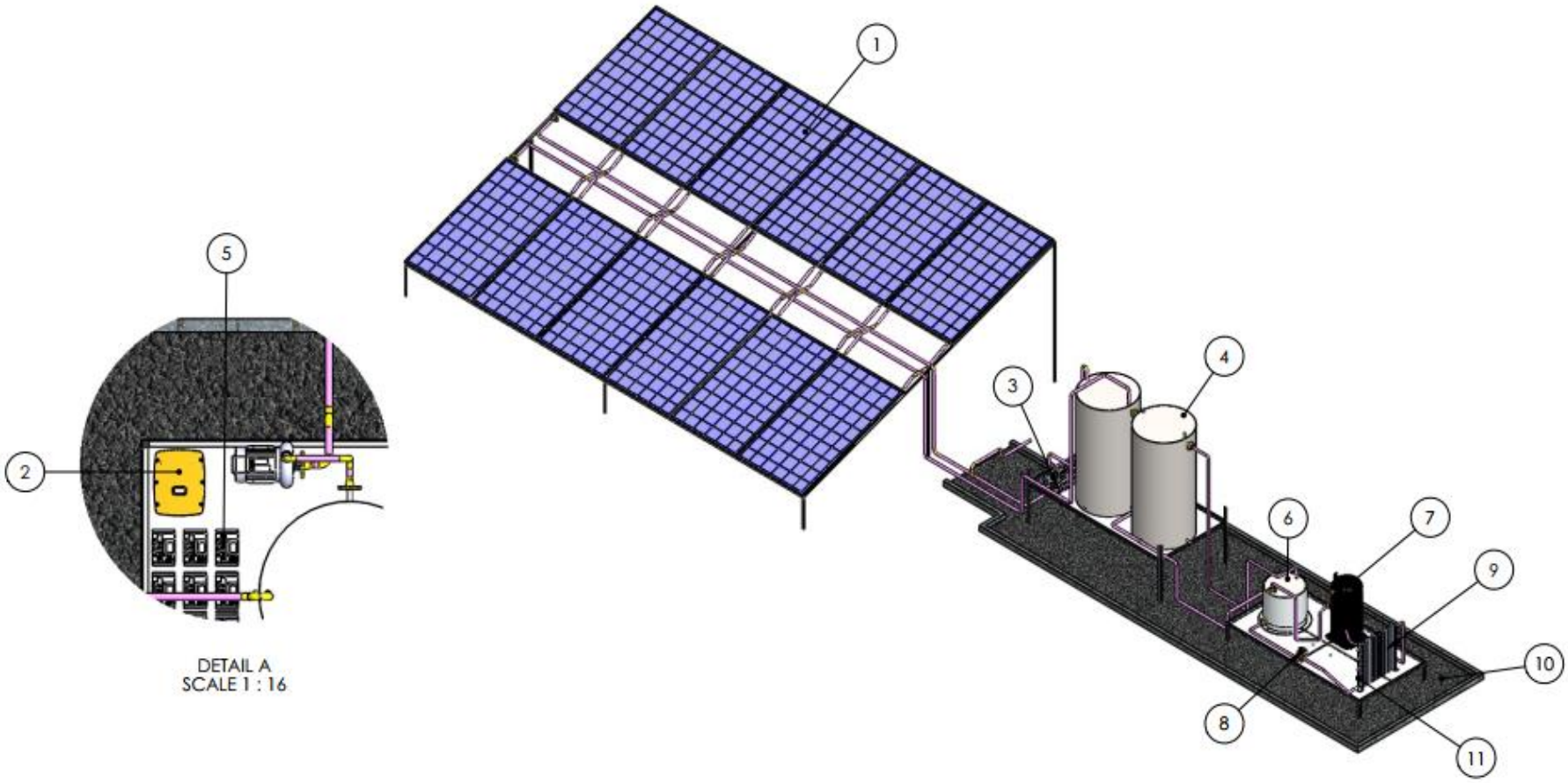

Figure 6-1 PV/T HEAT-PUMP system description layout

In Figure 6-1 the numbers represent the following (1) PV/T collectors; (2) inverter; (3) solar battery (4) Water storage tanks (5) pump (6) Condenser (7) Compressor; (8) Expansion valve (9) Evaporator (10) Basement (11) piping.

In smaller-capacity heat pump water heaters, the condenser coil can be placed in the hot water tank for compactness as shown in Figure 6-2. Heat pump water heater with integrated hot water storage and condenser.

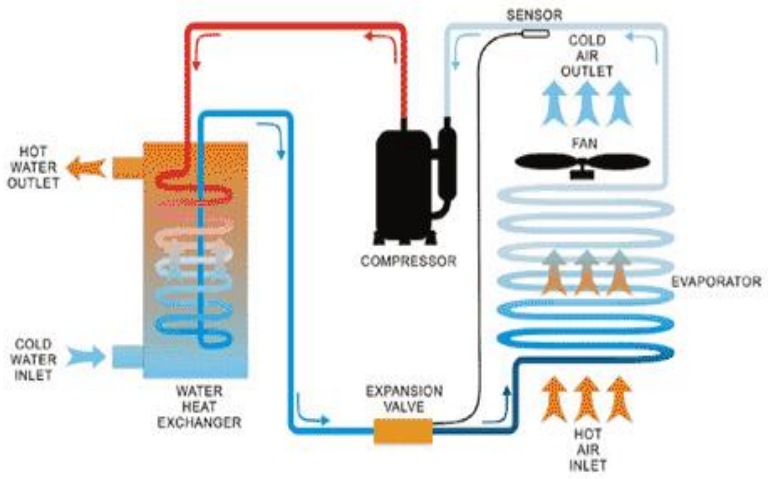

Figure 6-2 Heat pump condenser coil in the water storage tank

The air source heat pump water heater thermodynamic cycle is illustrated in Figure 6-3 described as follows.

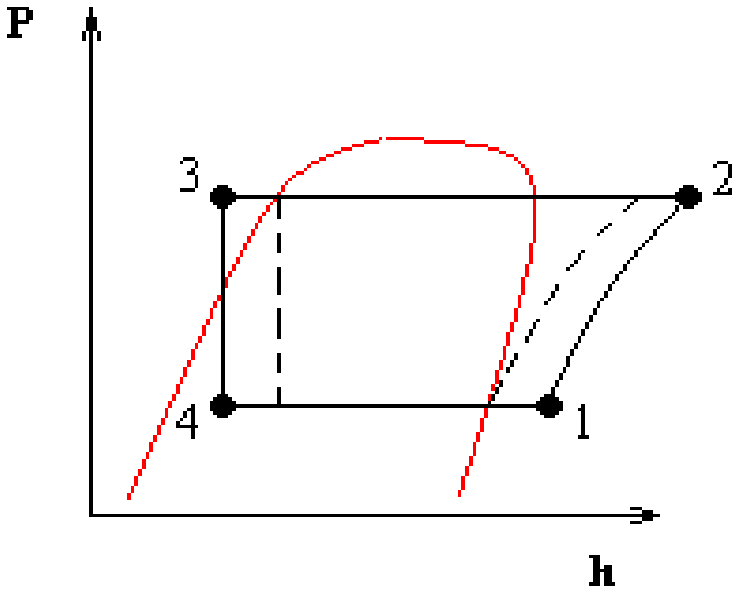

Figure 6-3 Heat pump thermodynamic cycle

a) Evaporation (4-1): - The refrigerant evaporates in the evaporator absorbing heat from ambient air at low pressure and temperature either naturally or using a fan to blow ambient air across fined evaporator tubes.
b) Compression (1-2): -The refrigerants is compressed in the compressor. As a result, the temperature and the pressure of the refrigerant are increased.
c) Condensation (2-3): - As the refrigerant temperature is above hot water temperature at the outlet of the compressor, the refrigerant condenses at high pressure rejecting heat to the hot water as it enters the condenser. As a result, the increment of hot water temperature in the storage tank is obtained.
d) Expansion (3-4): - Finally, the refrigerant enters into the expansion valve and expands to the evaporator pressure, and a fraction of the refrigerant flashes into vapor.

6.3 Computational model and analysis

6.3.1 Introduction

One possible path in the determination of the performance of the PV/T Heat Pump system happens is to use the PV/T computational model described in Chapter 5 to determine instantaneous electrical power generation and hot water temperature. The PV/T warm water tank and electrical energy at every time step generated. Then input the electric power to the compressor and use the warm water in the PV/T tank as make-up water for heat pump hot water tank from which hot water is supplied to end-use. The heat input from the condenser of the heat pump will be determined using the COP of the heat pump and compressor input power. The COP of the heat pump is dependent on ambient temperature (that governs heat absorption by the evaporator) and hot water temperature (that governs heat rejection by the condenser to hot water)

Thus, the heat pump module is added to the existing PV/T simulation model. Input parameters for dynamic simulation of the heat pump operation are hourly values of the ambient temperature for a year, daily hot water consumption volume, hourly hot water consumption pattern, hot water storage tank volume, heat loss coefficient of storage and surface area, instantaneous electrical power generation by PV/T and PV/T water tank temperature and COP general relation from the manufacturer of a heat pump.

6.3.2 Useful thermal energy

Eq 6.1 states the heat transported by the heat pump system from ambient to the hot water storage tank without electrical battery storage when the power generated by PV/T is directly consumed by the heat pump [119]. Similarly, Eq 6.2 evaluates the heat transported by the heat pump to hot water using battery storage. In this case, an hourly schedule for electric energy consumption is necessary for the simulation.

$$\dot{Q}_{HP} = COP_{HP} \times P_{el} \quad (6.1)$$

$$\dot{Q}_{HP} = COP_{HP} \times P_{el} \times f_{HP} \quad (6.2)$$

The end-user annual overall PV/T Heat Pump system efficiency is calculated by taking the final hot water (thermal energy) of the heat pump and solar energy incident on the PV/T surface. The general equation equated as follows in Eq 6.3.

$$\eta_{sys,eff,a} = \frac{Q_{hp,a}}{G_{PVT,a}} \quad (6.3)$$

6.3.3 Hot water storage tank temperature

The temperature of hot water in the heat pump storage tank is determined by the net heat gain of the hot water tank. The net heat gain of the storage tank is equal to thermal energy transported by the heat pump from ambient to the hot water tank subtracting the difference of enthalpy of thermal energy of hot water supplied to the end-user and warm make-up water from PV/T water tank and the heat lost to the ambient across the wall of the storage tank.

$$T_w^{n+t} = T_w^n + \frac{Q_{hp} - (DWC \times C_w \times ff(j)) \times (T_{,w}^n - T_{s1}) - U_{ls} \times A_{st} \times (T_w^n - T_a))}{\rho_w \times V_{dot} \times C_w} \quad (6.4)$$

6.4 Computer program flow chart

The flow chart of the computer program is given in Figure 6-4 comprising the two sub-systems: the hybrid photovoltaic thermal and air source heat pump water heater. As we can see in the flow chart, the primary target of the PV/T system module is to determine electrical and thermal (hot water) energy generation by PV/T which are used as inputs to the heat pump water heater.

The computational analysis starts by converting the solar irradiation at a horizontal surface on the inclined PV/T surface at every time step. Then, using the generated PV/T electrical

energy and warm water temperature, the ambient temperature of the site, manufacturer performance data of heat pump, daily hot water consumption volume, and end-user hourly hot water consumption pattern, the hot water supply temperature is determined. The computer program can be used to see whether a given system configuration meets design requirements or not. As shown in the flow chart, the developed MATLAB program delivers the heat pump generated thermal energy, hot water temperature, and COP at every time step. Year-round or 8760 hours of simulation has to be conducted to determine the annual performance of the system.

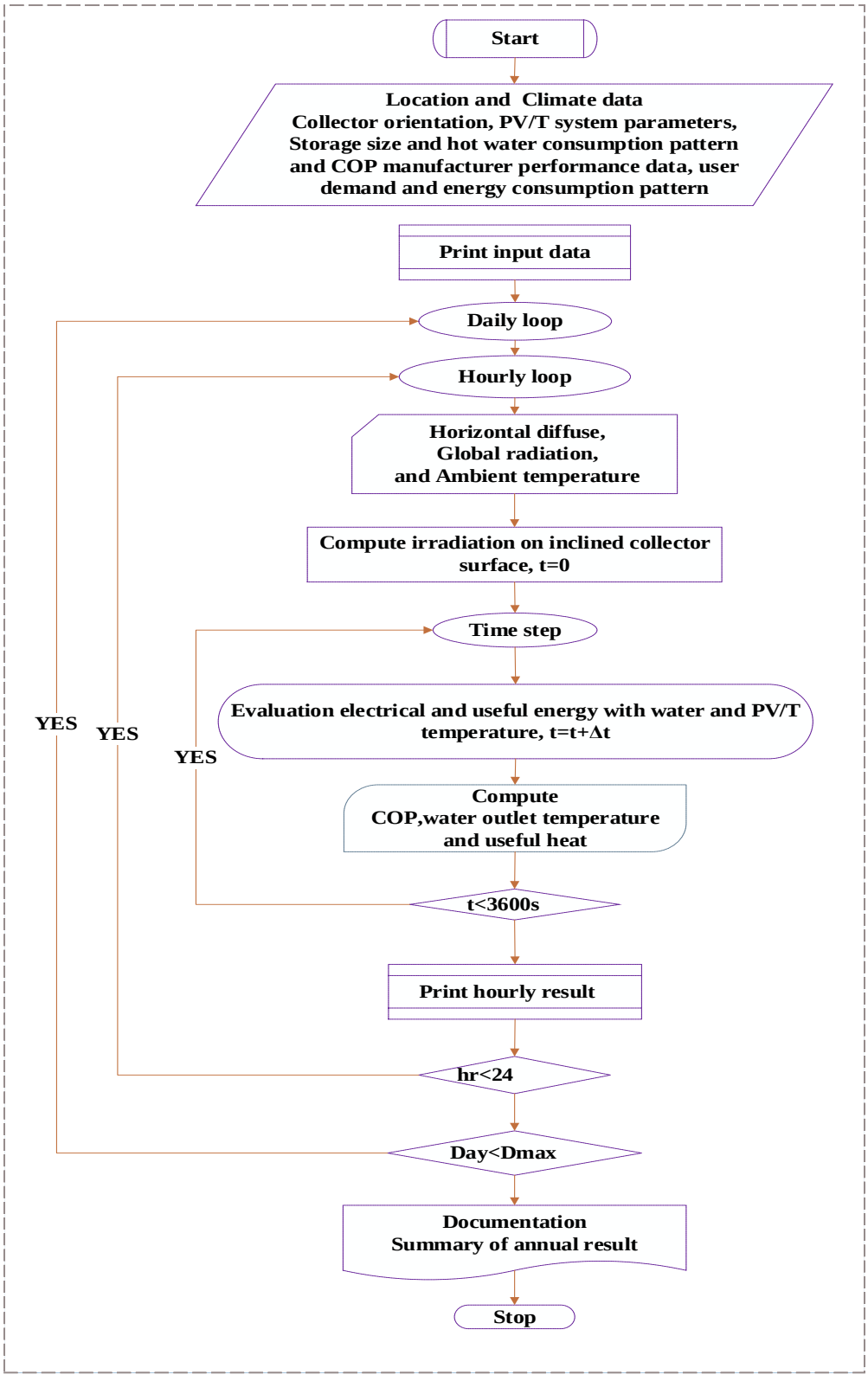

Figure 6-4 Hybrid PV/T Heat Pump system algorithm

6.5 COP formula of heat pump

The coefficient of performance of heat pump relates to the output or the heat transported by the condenser per unit time for water heating divide by the input which is the electrical power input into the compressor stated in Eq 6.5. As stated below COP value of heat pump water heaters is given as a function of ambient air temperature and hot water temperature by manufacturers. For the heat pump used for simulation, the manufacturer tabulated value of COP is given in Table 6-1.

$$\mathrm{COP_{HP}} = \frac{\mathrm{Q_{HP,out}}}{\mathrm{P_{el,in}}} \tag{6.5}$$

Table 6-1 COP of the heat pump as a function of ambient and hot water temperature

		Inlet water temperature				
		25	32	40	43	50
Ambient Temperature	7	4.05	3.5	2.92	2.7	1.98
	15	4.76	4.22	3.62	3.32	2.68
	25	5.82	3.36	4.41	3.36	3.1
	35	---	---	4.72	4.31	3.4

Using parameters in Table 6-1, a 3D surface was developed as shown in Figure 6-5 using curve fitting application, and the following equation of COP was developed as a function of hot water temperature and ambient temperature. From the surface generated the COP relation is presented in Eq 6.6.

$$COP = \begin{pmatrix} 0.4641 - (0.36538 \times T_{s2i}) - 0.13596 \times T_a - 0.01164 \times T_{s2i}^2 + 0.004564 \times T_a \times T_{s2i} \\ + 0.008122 \times T_a^2 + 0.00009655 \times T_{s2i}^3 + 0.0003286 \times T_{s2i}^2 \times T_a - 0.2829 \times T_{s2i} \times T_a^2 \end{pmatrix} \tag{6.6}$$

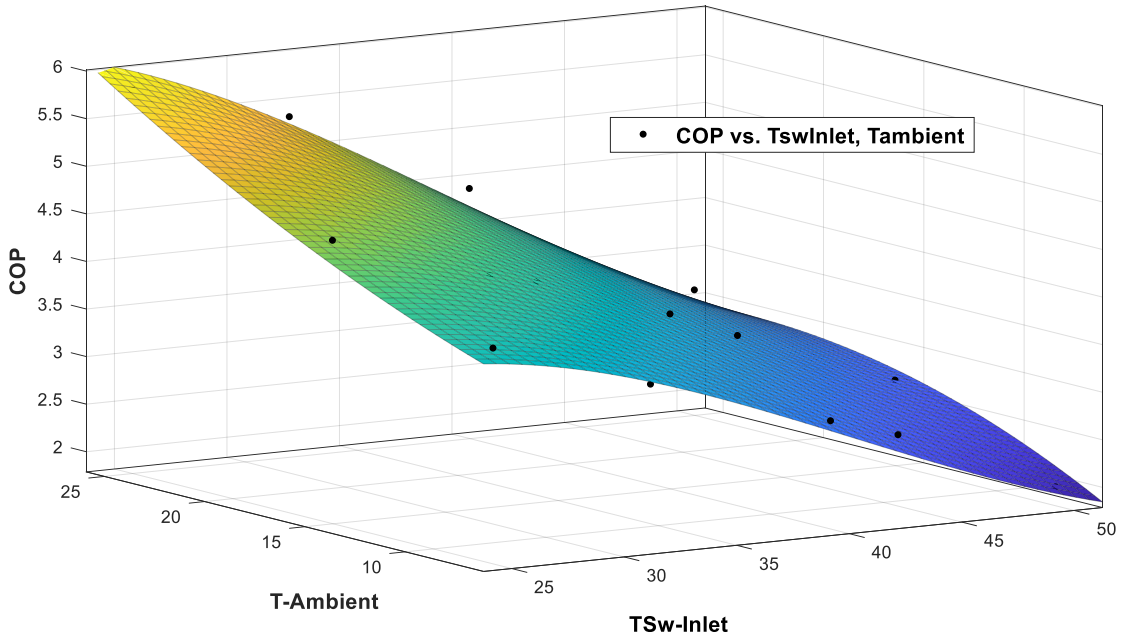

Figure 6-5 COP as a function of ambient and heat pump hot water tank temperature

6.6 Performance of hybrid PV/T Heat Pump at the different climatic conditions

For the comparison of different climatic conditions in tropical areas, Dire Dawa is selected to represent the hot climate of lowland and Addis Ababa for the mild climate of the high land. The comparison is performed for the hot season taking the solar irradiation and ambient temperature of May for Dire Dawa and Addis Ababa. Parameters that have a major influence on the system performance such as PV/T area, PV/T tank capacity, heat pump capacity, hot water tank capacity as well as, daily hot water consumption volume, and hot water consumption patterns were made the same for both cases. It shall be noted that the system designed for Dire Dawa was simulated for Addis Ababa to compare both sites with system and demand similarity. As for performance indicators, the coefficient of performance, hot water temperature in the storage tank as well as the hot water end-use efficiency are used for technical data input of the system stated in Table 6-2.

Table 6-2 Technical data of the hybrid PV/T Heat Pump system used for simulation

	Description	Unit	Value
Heat Pump	Model		FAR-01S
	Heating capacity	Kw	3.6
	Hot water supply	L/H	75
	Unit weight	Kg	35
	Refrigerant type		R410A
Water Storage	Capacity	Liter	500
	Color		Stainless steel
	Maximum Pressure	Kpa	1000
PV/T	Each module area	m^2	1.654
	Total area	m^2	20

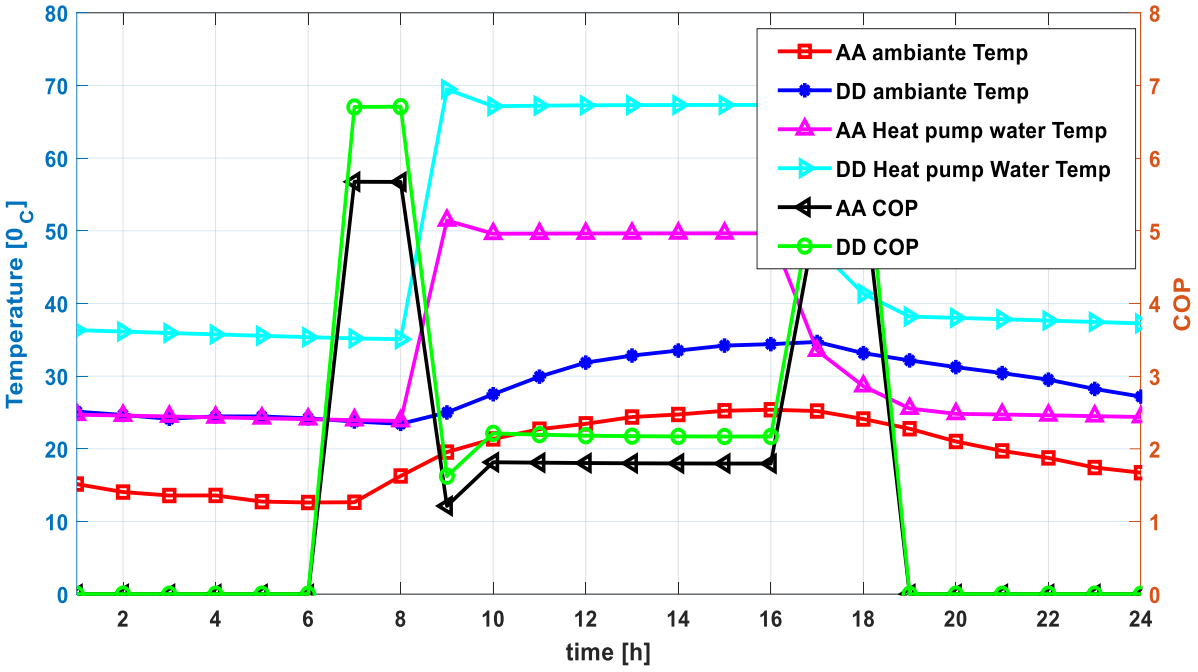

Figure 6-6 Comparison of performance of hybrid PV/T Heat Pump system in Dire Dawa and Addis Ababa under constant hot water supply condition during office hours

Figure 6-6 shows the results of the simulation of the hybrid PV/T Heat Pump water heating system for Dire Dawa and Addis Ababa for May. The hot water supply temperature of the Dire Dawa is higher than of Addis Ababa in all 24 hours of the day. At 9:00 h, the hot water temperature reached 70 ℃ and 52 ℃ respectively for Dire Dawa and Addis Ababa then both

started to decrease. This happened because the ambient temperature and other affecting parameters were better in Dire Dawa relative to Addis Ababa.

The COP of the heat pump at Dire Dawa was better than that of Addis Ababa due to the higher ambient temperature. It shall be noted that the Heat pump is not operating during the night as electric power is not generated by the PV/T unless the system is integrated with electrical battery storage.

The results show that Dire Dawa is a better and appropriate site for the application of a hybrid PV/T Heat Pump water heating system application than Addis Ababa. When the water temperature reached the highest temperature, the COP dropped to about 2 in Dire Dawa and 1.7 in Addis Ababa. The average COP during the Day was above 3.5 in Dire Dawa and about 3 in Addis Ababa.

Table 6-3 Annual hot water end-use efficacy of Dire Dawa and Addis Ababa

	Thermal efficiency of PV/T	**End-use efficiency**			
		Storage Volume 4.8m^3		**Storage Volume 2.4m^3**	
		PV/T	PV/T Heat Pump	PV/T	PV/T Heat Pump
Dire Dawa	51.34%	37.54%	63.69%	38.59%	66.77%
Addis Ababa	47.03%	29.01%	61.24%	29.81%	64.32%

The evaluation of annual end-use efficiency for a different storage volume is given in Table 6-3. The results show that an improvement of 3% is obtained by making the hot water supply tank half of the daily hot water consumption.

6.7 Effect of hot water consumption pattern on system performance

The effect of hourly hot water consumption patterns of the end-user for a restaurant, motel, and health center on the system performance was analyzed for Dire Dawa. The hourly hot water fraction pattern for the different cases is illustrated in Figure 6-7. Their effect on COP of heat pump, hot water supply temperature, and hot water end-use efficiency is discussed in the following paragraphs.

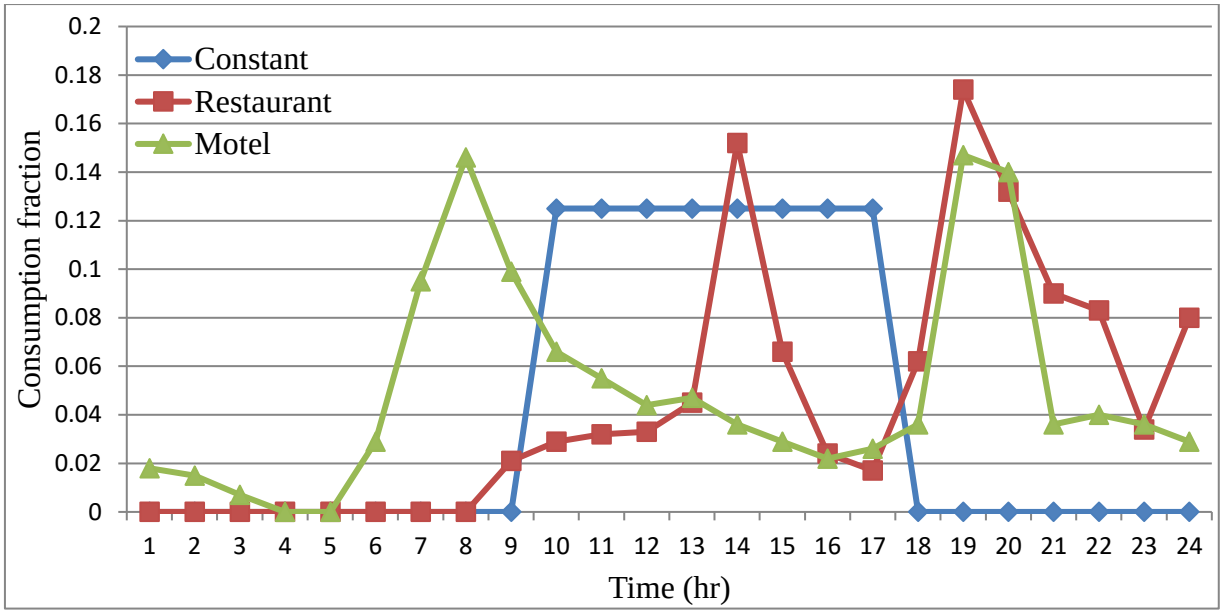

Figure 6-7 Hot water consumption pattern for three selected case

Table 6-4 shows the variation of COP for different hot water consumption patterns cases on directly supplied the PV/T system-generated electrical energy to the heat pump.

Table 6-4 COP of the heat pump on selected days by taking max and minimum

Fraction type	Constant		Restaurant		Motel	
	Maximum	Minimum	Maximum	Minimum	Maximum	Minimum
Selected month	June 11	January 17	June 11	January 17	June 11	January 17
Minimum	1.62	1.11	1.72	1.15	1.97	1.33
Maximum	6.85	6.06	6.78	6.06	6.78	6.07
Average	5.2	4.4	5.17	4.26	5.21	4.3

Similar to the COP of the heat pump, the hot water supply temperature was compared for three types of consumption pattern cases (constant, restaurant, and motel).

a. Constant consumption pattern case

In this case, the maximum hot water temperature generated by the heat pump and stored in the tank rose to 80℃ as shown in Figure 6-8. As the solar irradiation decreased between 13:00-17:00 hours of the day the end-user hot water temperature dropped between 40-50^{o}C during the evening the temperature further dropped.

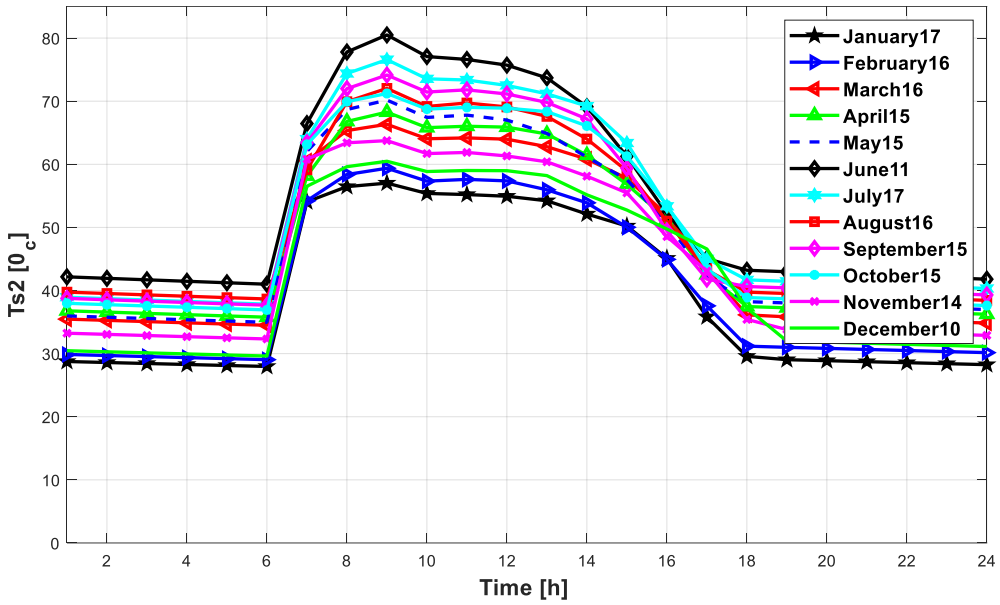

Figure 6-8 Storage water temperature in case of constant consumption pattern

b. Restaurant case

In a restaurant like consummation pattern, hot water at 55-80^{O}C is supplied from 8 to 13 hours to the end-user during the year as shown in Figure 6-9 and then hot water temperature dropped drastically from 13:00 to 17:00 hour reaching 42-50℃.

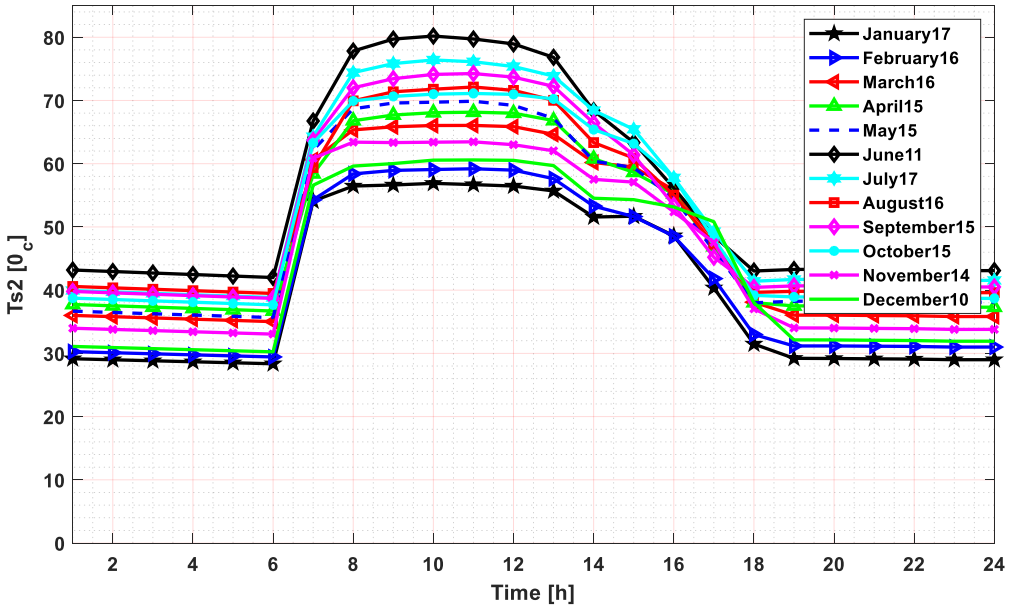

Figure 6-9 Storage water temperature at restaurant consumption pattern

c. Motel case

In the motel consumption pattern case, the hot water temperature was delivered at 55 – 80 ℃ to the end-user from 8 to 13 hours during the year as shown in Figure 6-10. At night time, the required hot water temperature was not achieved due to the absence of electric power to the heat pump. To eliminate this problem, the hot water tank with controlled mixing with make-up water with two levels can be considered to avoid thermal degradation can be considered. Another alternative using the battery for electrical energy.

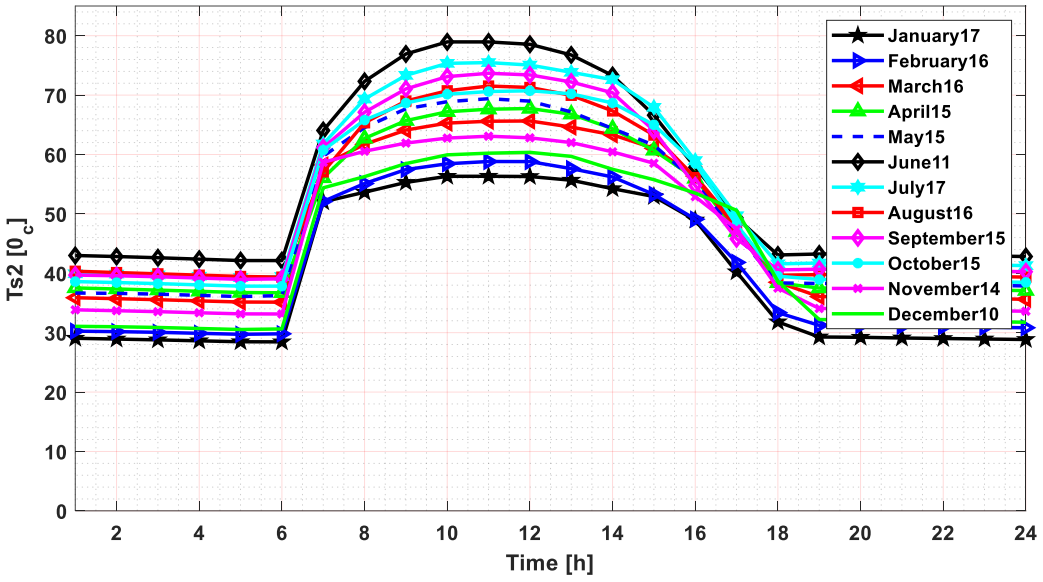

Figure 6-10 Storage water temperature for motel consumption pattern case

Table 6-5 shows a comparison of the hot water supply temperature of the three hot water hourly consummation patterns. Although the difference is insignificant, the restaurant case seems to have the best performance.

Table 6-5 Temperature summary of the heat pump by taking max and minimum

Fraction type	Constant		Restaurant		Motel	
	Maximum	Minimum	Maximum	Minimum	Maximum	Minimum
Selected month	June 11	January 17	June 11	January 17	June 11	January 17
Minimum (℃)	41.4	28.39	42.16	28.5	42.29	29.6
Maximum(℃)	80.83	57.16	80.52	57.04	79.33	56.5
Average (℃)	54.65	39.55	55.87	40.32	55.71	40.2

6.8 Effect of the electrical energy storage battery on hot water supply temperature

In this section, the option of storing electrical energy to level the variation of hot water temperature is investigated. The hourly hot water consumption pattern that is used for the simulation, is the constant consumption pattern case for 8 hours.

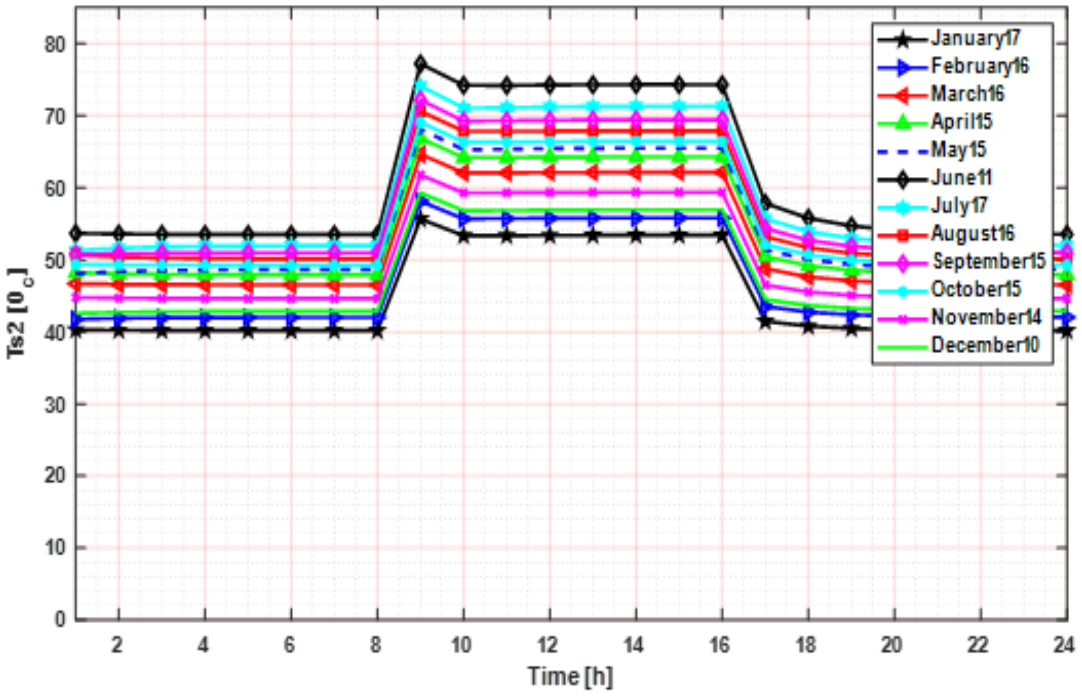

Figure 6-11 Water temperature with 75% electrical energy supply during 8 hours of water supply hours and 25 % during the rest

The first case is 75% of the electrical energy is utilized during 8 hours of hot water supply and 25% of the electrical energy is used for 16 hours of the day. Compared to the results of Dire Dawa in Figure 6-8 the results of this investigation in Figure 6-11 increased the hot temperature in the early morning and evening. Even in the coolest month, the hot water temperature was above 45^{o}C.

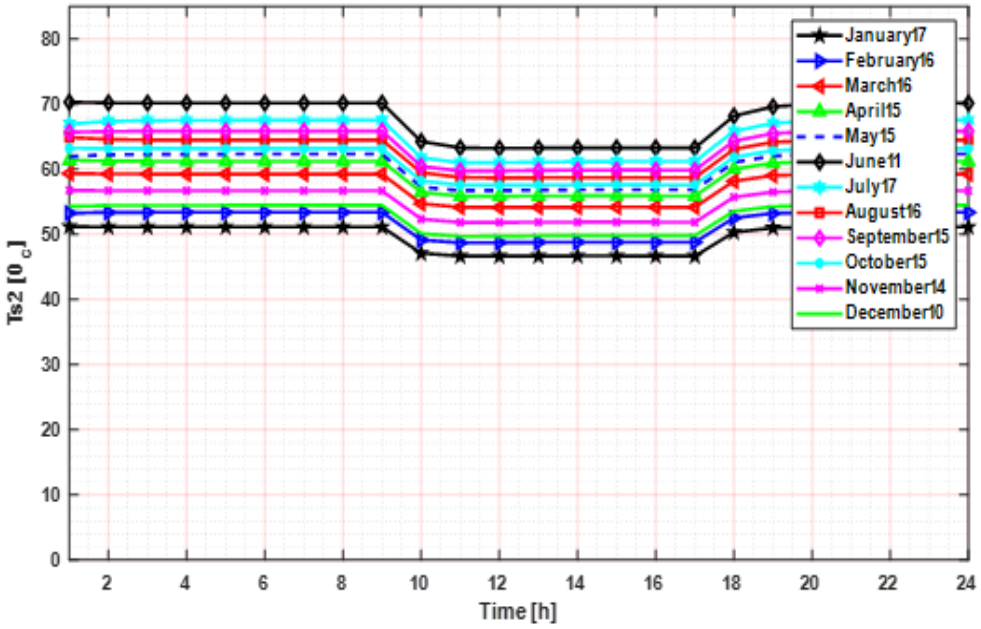

Figure 6-12 Water temperature for constant power supply energy option in 24 hours using battery storage and 8 hours of hot water consumption at a constant rate

Figure 6-12 shows got water temperature variation when the power supply to the compressor is made constant through 24 hours of the day and hot water is consumed during the day from 9-17 h at a constant rate. The conclusion is that the water temperature in the tank is leveled and such type of power supply is more suitable for the water heating system with considerable evening and early morning loads.

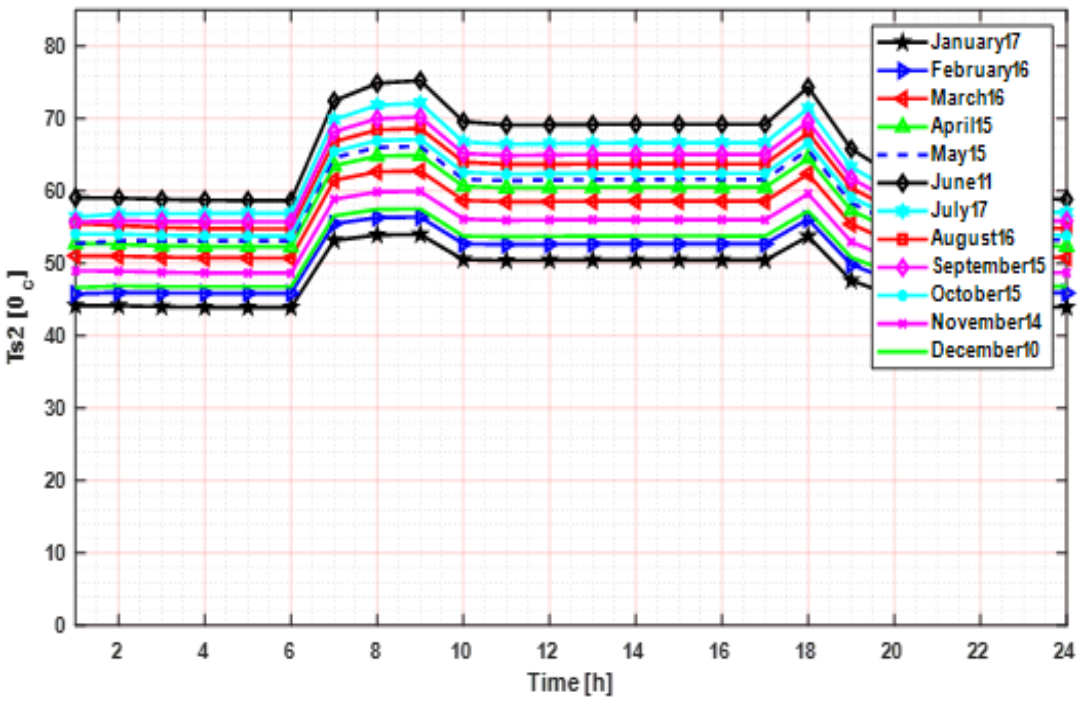

Figure 6-13 Water temperature with 75% electrical energy supply during 12 hours of the day and 25% during the rest

Figure 6-13 shows hot water temperature variation when the power supply to the compressor is made constant through 12 hours (6h- 18h) of the day using battery electrical storage for PV and hot water consumption from 9h to 17h at a constant rate. From the figure, it can be concluded that the water temperature in the tank is almost constant from 7 h to 20 h which is more appropriate for application with a considerable hot load during the day. The temperature summary of the three cases with the baseline data or no-electrical energy storage is given in Table 6-6.

Table 6-6 Temperature of selected days on different energy supply cases

General classification	**Energy supply**	**Selected days**	**Minimum (℃)**	**Maximum** (℃)
Baseline	No Battery	11-Jun	41	80
		17-Jan	28	57
75% in 8 hot water	25/75	11-Jun	53.5	77.2
supply hours		17-Jan	40.16	55.66
24-hour uniform		11-Jun	63.23	70.32
		17-Jan	46.67	51.2
75% in 12-hour day		11-Jun	58.68	75.26
time		17-Jan	43.93	54.00

For different cases of storage and supply of electricity, COP maximum and the minimum values for representative days of the hot and cool-season are given. In Table 6-7 the result shows, the gap between maximum and minimum COP values decreased when the electrical energy supply is made more uniform.

Table 6-7 COP Summary for different cases on a selected day

General classification	**Energy supply**	**Selected days**	**Minimum**	**Maximum**
Base Line	0%	11-Jun	2.00	6.94
		17-Jan	1.29	6.07
8 h/16h	75/25 %	11-Jun	2.4	5.94
		17-Jan	1.6	5.13
24 h uniform	100%	11-Jun	3.67	4.77
		17-Jan	2.88	3.96
12/12 h	75/25%	11-Jun	2.78	5.36
		17-Jan	2.1	4..51

In section 6.7, it was shown that for the motel case hot water consumption, the required hot water temperature was not meet especially in the cooled season due to considerable high hot water consumption during the night. Because of the electrical energy supplied to the HP compressor without stored in battery only on the PV/T working time. To solve this problem, integrate electrical battery storage into the system is considered as a solution.

After several trials, a PV/T Heat Pump system with an increase of 20% in size from the baseline and integration of battery system for storing about one-third of electrical energy generated hours for supply in the PV/T off-time or night time. delivered hot water temperature above 50 ℃ in the cold season as illustrated in Figure 6-14.

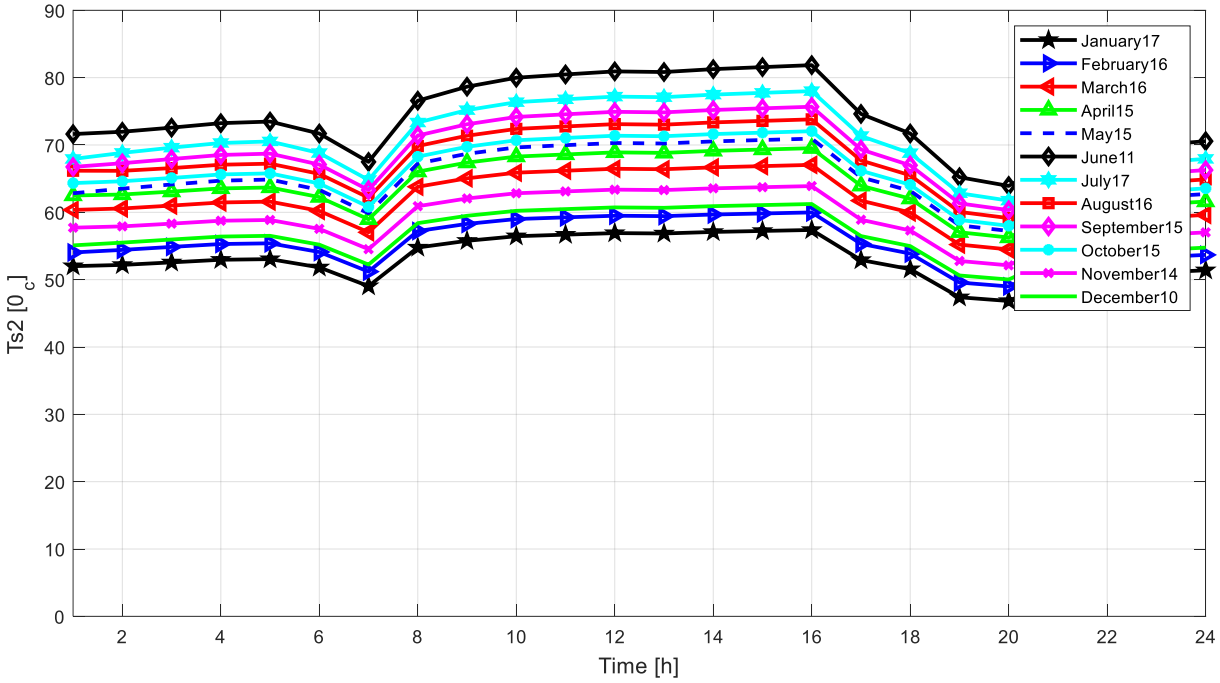

Figure 6-14 Water temperature in motel consumption with 1/3 of electrical energy storage in the battery for night time

6.9 Conclusion on the performance of hybrid PV/T Heat Pump water heater

The computational model of PV/T Heat Pump integrated hybrid system developed during the research was used to analyze the performance of hybrid PV/T Heat Pump systems for different applications and different tropical climate conditions. The computations were done using the MATLAB program considering different tropical climatic conditions, heat pump energy consumption options, and variability of the end-user (constant, restaurant, and motel) hourly hot water fraction pattern. The simulation results of the system consisted of s COP, hourly hot water temperature, and hot water end-use efficiency for selected days of each month.

Beyond the impact of hot water consumption patterns, using electrical storage, and supply hot water tank size, the effect of different climatic conditions within tropical areas such as lowland and moderate high land was seen. The nominated sites Addis Ababa and Dire Dawa

are representative of the moderate highland and lowland site of Ethiopia, respectively. According to the results, a hybrid PV/T Heat Pump hot water production system is highly recommended for hot sites like Dire Dawa relative to Addis Ababa.

As per the results, the hybrid PV/T Heat Pump water heater can deliver a maximum of 80 ℃ hot water and an average hot water temperature of 55 ℃ and above. The maximum value of hot water end-use efficiency of 66% was also obtained by making the hot water tank capacity about 50% of daily hot water consumption.

Whenever the hot water demand during the day working hours is constant, the hybrid PV/T heat hump system can supply hot water without a back-up system in all seasons. In some cases, the major consumptions are during the night and morning, the system has to be slightly oversized with a larger PV/T area and larger heat pump capacity and storing about one-third of electrical energy generated in a battery.

CHAPTER SEVEN

ECONOMIC ANALYSIS

7.1 Introduction

Economic analysis of the PV/T Heat Pump system is one of the vital parts of this paper since it reveals the system from a financial point of view whether as an investment project worthwhile or not. The economic viability analysis is established to show the system's benefits in addition to the environmental protection and functionality of the system in off-grid areas. In this regard, different researches have compared diverse types of sources of energy to bear out the user's need. Besides the capability of the technology meeting the energy demand the capability to the specific application's needs, more importantly, evaluate the cost-competitiveness of the system in comparison with other alternative solar technologies[120].

In line with the previous research reviewed paper, the comparison of alternative energy technology mostly stipulates energy and conversion efficacy perspectives. There was a huge limitation on considering the economic appraisal[120]. In the current research work, the economic viability study of the system is done based on the life cycle cost analysis (LCC) and payback time of the system. In all cases, account fuel inflation rate, market discount rate, annual maintenance cost, and the power consumed by the system were considered. The economic scenario analysis is implemented by assuming that all the costs of the system are paid at the beginning.

In recent years, techno-economic analysis and comparison developed for different categories of the hybrid system. From those systems photovoltaic assisted heat pump water heater, DHW heat pump without PV, an electrical heater, a boiler, and a boiler with solar thermal collectors evaluated the system[121]. Furthermore, other researchers reveal that the air-to-water heat pump system is the lowest operating cost, and the highest economic saving is obtained, and it is investigated by comparing with other types of water heating mechanisms [122]. The current economic analysis is carried out by considering both the overall costs and the annual operating cost over the system lifetime; then, it is compared to the current Ethiopian electric seal price.

To compare and complete the economic analysis of the system cost, it is necessary to know each component's initial investment cost.

Table 7-1 System component cost with a lifetime [123]–[125]

Component	Lifetime	Each cost ($)	Quantity	Total Cost ($)	Total cost (Birr)
PV/T	25 y	250	12	3000	96,500
Inverter	9 y	635	2	1270	40,640
Batteries seat	5 y	229	2	458	14,656
Storage tank	25 y	470	1	470	15,040
Structure	25 y	3.12	65	202.67	64,89.6
Tools	-	25	1	25	800
PV cables	25 y	0.51	200m	102	3264
Battery Cables	25 y	2.04	30m	61.2	1,958
Heat Pump		292	1	292	9344
Transportation	-	4.68	528.5kg	2473	79,148.16
Replacement (Batteries& Inverter)	-	-	-	4372	139,904
Tax (15%)	-	-	1	1908.96	61,081.62
O&M		-	-	503.09	16,098.87
LCC	-	-	-	**20,681.72**	**661,815.17**

7.2 Life cycle cost analysis

The investment cost of the PV/T Heat Hump system is determined from the FOB price of equipment, shipping cost, inland transportation cost, customs tax, installation cost, and supply and overhead cost as stated in Table 7-1. The life cycle cost includes the initial investment and the maintenance cost of the system with an interest rate of the cost throughout the lifetime of the system quantified in Eq 7.1 [126].

$$\mathrm{LCC} = \mathrm{C_i} + \mathrm{C_m}\,\frac{1+\mathrm{i}}{\mathrm{i}}\left(1 - \frac{1}{(1+\mathrm{i})^{\mathrm{n}}}\right) \tag{7.1}$$

Where C_I is the investment cost, C_m the operation and maintenance cost, n lifetime of the system, and i interest rate.

The present worth of maintenance cost distributed through the life of the project on the life cycle maintenance cost is determined as follows. Evaluate c_m taking 2.5% of the total capital cost including the replacement of spare parts cost [122], [127].

$$LCC_m = C_m \frac{1+i}{i}\left(1 - \frac{1}{(1+i)^n}\right) \tag{7.2}$$

While the hybrid PV/T Heat Pump water heater system has costs it also generates savings from the cost of hot water produced annually. From annually thermal energy produced by the system is f_a, Q_a, the annual savings from hot water production is $p_{e,}\, f_{a,} Q_a$. The life cycle cost saving, LCS, is defined as the present value of the total energy cost savings over the lifetime of the system considering inflation of energy price.

$$LCS = p_e f_a Q_a \frac{1+i}{i-i_e}\left(1 - \left(\frac{1+i_e}{1+i}\right)^n\right) \tag{7.3}$$

Where p_e the unit price of solar energy, f_a the annual fraction of contribution of solar energy, Q_a annual heating load and i_e the inflation rate of energy prices. For detailed analysis taking an interest rate of 0.1 and the inflation rate of energy price 5%.

Equating life cycle saving to the life cycle cost, the cost of a water heater per kWh of thermal energy is determined as follows.

$$p_e = \frac{C_i}{f_a Q_a} \frac{1+\frac{C_m}{C_i}\ \frac{1+i}{i-1}\left(1-\left(\frac{1}{1+i}\right)^n\right)}{\frac{1+i}{i-i_e}\left(1-\left(\frac{1-i_e}{1+i}\right)^n\right)} \tag{7.4}$$

The energy price for water heating is a key indicator of the power generation plant to compare them with each other during their lifetime of energy generation capacity with the required cost. Different equations and approaches were used to evaluate, and it is done by considering the life cycle of the system for 25 years.

The annual energy generation is assumed constant throughout the lifetime of the system. As per the above equation evaluated the system by considering the thermal to electrical conversion efficiency.

The cost of electrical energy generation of the system without electrical battery storage, 25% and 50% electrical battery storage were 2.16 $birr/kwh$, 2.23 $birr/kwh$ and 2.4 $birr/kwh$ respectively.

The unit energy price of the PV/T Heat Pump system is compared with the current Ethiopian electric supply tariff cost. The Ethiopian electric utility agency prepared different categories and blocks of cost to charge the user as per kWh/month usage. The electrical water heater is aligned in the category of residential of 7th block above 500kwh/month with the cost of 2.48 Birrs/kWh as of Dec 2021 onward[128]. The unit price of the PV/T Heat Pump system energy in all cases below that of an electric water heater.

7.3 Payback period of the system

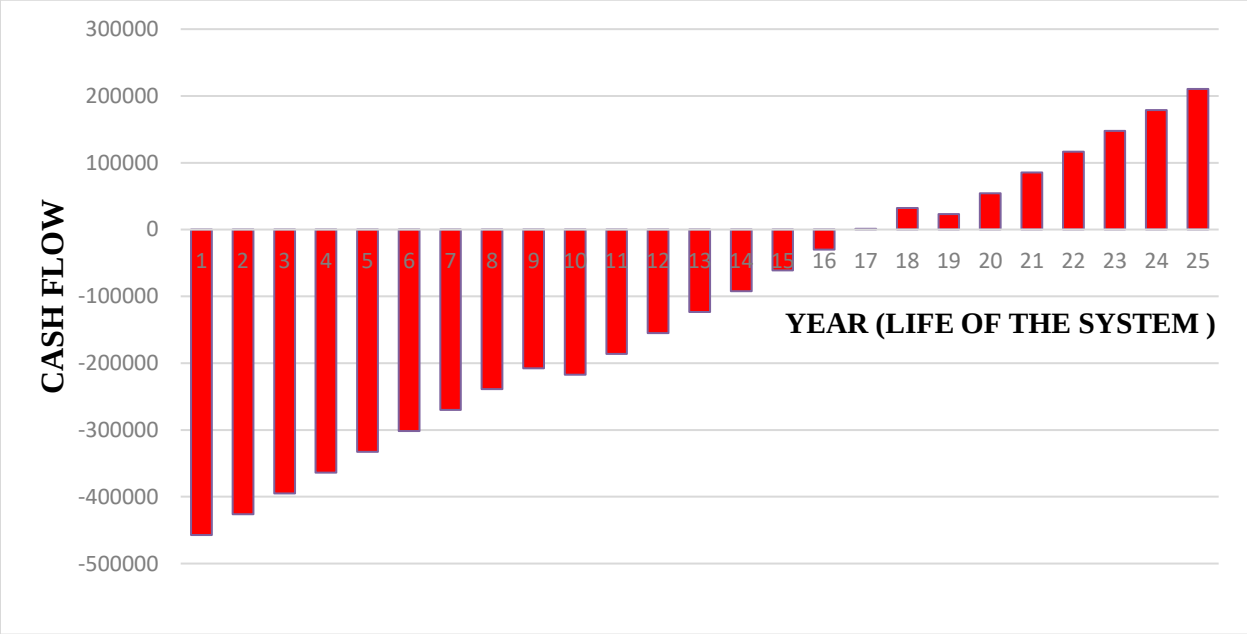

Figure 7-1 PV/T Heat Pump system cash flow

The payback period (PP) of the system is an indicator of the time when the initial investment is recovered[129].

$$PP = \frac{C_{inv}}{C_{Sav}} \quad (7.5)$$

Where C_{inv} is the cost of the investment and C_{sav} is the cost of the system saving.

Using the above equation and the system, 25 years lifetime cash flow is prepared, and the payback period scored 16.96 years as demonstrated in Figure 7-1. In the analysis, the system output is found out that it is constant throughout the life cycle and the payback period is more than half of the life cycle of the system. However, still, the system shows that in a good profitability stage.

CHAPTER EIGHT

CONCLUSION AND RECOMMENDATIONS

8.1 Conclusion

The demand for energy in Ethiopia and the entire world has been increasing drastically. To reply, such appeal, a renewable source, specifically solar, is one of the best solutions for the off-grid area in the Ethiopian context and other developing countries.

This research has been devoted to the study of the hybrid photovoltaic thermal and heat pump water heating system to deliver the required electrical energy and hot water to satisfy the end-user temperature. At first, the capacity of PV/T alone in the cogeneration of electricity and warm water in tropical areas was investigating considering the Dire Dawa site. The major findings were.

- A PV/T system can supply hot water up to a maximum of 45 ℃ and has a PV efficiency of 15%, the thermal efficiency of 50%, hot water end-use overall efficiency of 37.9%, and cogeneration efficiency of 65%.
- The fraction of the PV/ T system in meeting the hot water energy demand was 44.5%. There is about a 10% difference between thermal efficiency and overall end-use efficiency of hot water generation due to the time shift between generation and consumption of hot water.
- A PV/T system can be used only as a preheater for hot water generation systems meeting up to 50 % of the energy demand.

The hybrid PV/T Heat Pump system water heating system integration was studied and analyzed to see the performance variation with climate, hot water consumption pattern, storage tank volume, and using electrical battery storage keeping constant other design parameters. From which, the following conclusion is drawn.

- The hybrid PV/T-heat pump system is one of the best solutions to deliver electrical and thermal energy simultaneously in one system. Especially for an off-greed area of Ethiopian institutions like health center and lodge, which demand both heat and electrical energy of the

PV/T-heat pump, it is a perfect solution. The benefit of the system is not limited only to the end-users; also helpful for environmental protection in Ethiopia and the globe.

- For hot water consumption during the daytime such as health centers, a hybrid PV/T-heat pump system can deliver hot water at the required temperature.
- The effect of electrical energy storage using the battery on hot water temperature was investigated for operating the heat pump in the evening and night. It was found that the system has been oversized by about 20 % and one-third of the electrical energy has to be stored in batteries.
- The system can deliver hot water at end-use efficiency of 66% compared to 38% of PV/T alone using the 15% electrical energy generated by PV/T at COP of 1.9. End-use efficiency of 66 % is above solar water heaters.
- The system cannot meet hot water temperature requirements when early morning and night consumptions are considerably high without battery back-up. However, using a specialized type of hot water storage such as a stratified tank or two-level tank controller for the addition of make-up water and increasing the capacity of PV/T and heat pump will require thorough investigation before considering the battery back-up.

8.2 Recommendations

This research devoted and showed the system performance improvements and how the system delivers the thermal and electrical energy to end-user, and it is done by considering different system integration optimization. Further research work is needed in such an area. Hence the following are suggested as a future investigation area.

- The PV/T-heat pump is more appropriate in hot equatorial areas than the cold areas, so the researches to come should be more concentrated on such area considering the multifunctional of the system, for heating and cooling in one system functioning all variety of the season.
- This research is delimited to simulation and validation analysis work. It is necessary to manufacture a prototype system and evaluate it experimentally.
- The system simulation has considered only some parameters; Hence, it is better to include more parameters such as stratified the water storage tank.

REFERENCES

[1] A. M. Yonas Alem, Abebe D, Gunnar Köhlin, "Household Fuel Choice in Urban Ethiopia A Random Effects Multinomial Logit Analysis," 2013.

[2] G. E. Beyene, A. Kumie, R. Edwards, and K. Troncoso, "Opportunities for transition to clean household energy in Ethiopia Application of the WHO Household Energy Assessment Rapid Tool (HEART)," Geneva, 2018.

[3] International Energy Agency, "Renewables Information Overview," *IEA Stat.*, vol. 53, no. 9, pp. 1–12, 2019.

[4] National Planning Commission, "Federal Democratic Republic of Ethiopia Growth and Transformation Plan II (GTP II)," Addis Ababa, 2016.

[5] International Energy Agency, "Africa Energy Outlook 2019 World Energy Outlook Special Report," 2019.

[6] Rfassbind, "Price history of silicon PV cells since 1977," *Wikimedia Commons*. 2014.

[7] International Energy Agency (IEA), "Renewables 2O17 Analysis and Forecasts to 2O22," 2017.

[8] "Solar Price | EnergyTrend." [Online]. Available: https://www.energytrend.com/solar-price.html. [Accessed: 16-Jun-2020].

[9] D. Jonas, D. Theis, and G. Frey, "Implementation and Experimental Validation of a Photovoltaic-Thermal (PVT) Collector Model in TRNSYS," in *EuroSun 2018*, 2019, no. March 2019, pp. 1–12.

[10] A. L. Abdullah and et el., "Photovoltaic thermal /solar (PVT) collector (PVT) system based on fluid absorber design: A review," *J. Adv. Res. Fluid Mech. Therm. Sci.*, vol. 48, no. 2, pp. 196–208, 2018.

[11] T. T. Chow, "A review on photovoltaic/thermal hybrid solar technology," *Appl. Energy*,

vol. 87, no. 2, pp. 365–379, 2010.

[12] R. Daghigh and et el., “Review of solar assisted heat pump drying systems for agricultural and marine products,” *Renew. Sustain. Energy Rev.*, vol. 14, no. 9, pp. 2564–2579, 2010.

[13] Z. M. Amin and M. N. A. Hawlader, “A review on solar assisted heat pump systems in Singapore,” *Renew. Sustain. Energy Rev.*, vol. 26, pp. 286–293, 2013.

[14] A. Jamar and et el., “A review of water heating system for solar energy applications,” *Int. Commun. Heat Mass Transf.*, vol. 76, pp. 178–187, 2016.

[15] H. J. Gärtner and A. M. J. P. Stamps, “Ethiopian power grid Electrical Power Engineering & Environmen,” Netherland, 2014.

[16] “Ethiopia Energy Situation.” [Online]. Available: https://energypedia.info/wiki/Ethiopia_Energy_Situation. [Accessed: 16-Jun-2020].

[17] N. United, “Rural Electrification Project Framework Documents,” 2002.

[18] F. Obeidat, “A comprehensive review of future photovoltaic systems,” *Sol. Energy*, vol. 163, no. July 2017, pp. 545–551, 2018.

[19] M. Raugei and P. Frankl, “Life cycle impacts and costs of photovoltaic systems: Current state of the art and future outlooks,” *Energy*, vol. 34, no. 3, pp. 392–399, 2009.

[20] S. Abdelhady, M. S. Abd-Elhady, and M. M. Fouad, “An Understanding of the Operation of Silicon Photovoltaic Panels,” *Energy Procedia*, vol. 113, pp. 466–475, 2017.

[21] R. Deep, A. Agarwal, and A. Mishra, “A study and comparative analysis of various materials based solar photovoltaic module to improve the output performance,” *Mater. Today Proc.*, vol. 22, pp. 3203–3212, 2019.

[22] H. Chen and S. B. Riffat, “Development of photovoltaic thermal technology in recent years: A review,” *Int. J. Low-Carbon Technol.*, vol. 6, no. 1, pp. 1–13, 2011.

[23] M. S. Hossain *et al.*, "Review on solar water heater collector and thermal energy performance of circulating pipe," *Renew. Sustain. Energy Rev.*, vol. 15, no. 8, pp. 3801–3812, 2011.

[24] M. Raisul Islam, K. Sumathy, and S. Ullah Khan, "Solar water heating systems and their market trends," *Renew. Sustain. Energy Rev.*, vol. 17, pp. 1–25, 2013.

[25] S. Mekhilef, A. Safari, W. E. S. Mustaffa, R. Saidur, R. Omar, and M. A. A. Younis, "Solar energy in Malaysia: Current state and prospects," *Renew. Sustain. Energy Rev.*, vol. 16, no. 1, pp. 386–396, 2012.

[26] S. A. Kalogirou, *Solar Energy Engineering Processes and Systems*, Second edi. AE Amsterdam: Elsevier Inc, 2014.

[27] L. A. Chidambaram and et el., "Review of solar cooling methods and thermal storage options," *Renew. Sustain. Energy Rev.*, vol. 15, no. 6, pp. 3220–3228, 2011.

[28] S. I. Khan and A. Islam, "Performance Analysis of Solar Water Heater," *Smart Grid Renew. Energy*, vol. 02, no. 04, pp. 396–398, 2011.

[29] A. Gastli and Y. Charabi, "Solar water heating initiative in Oman energy saving and carbon credits," *Renew. Sustain. Energy Rev.*, vol. 15, no. 4, pp. 1851–1856, 2011.

[30] R. Shukla, K. Sumathy, P. Erickson, and J. Gong, "Recent advances in the solar water heating systems: A review," *Renew. Sustain. Energy Rev.*, vol. 19, pp. 173–190, 2013.

[31] H. Nam, C. Bai, and J. Sim, "A study on characteristics of thermal storage tank for varying thermal load in multi-use heat pump water heater," *Appl. Therm. Eng.*, vol. 66, no. 1–2, pp. 640–645, 2014.

[32] J. a. Duffie, W. a. Beckman, and W. M. Worek, *Solar Engineering of Thermal Processes, 4nd ed.*, vol. 116. 2003.

[33] K. K. Chong, K. G. Chay, and K. H. Chin, "Study of a solar water heater using stationary V-trough collector," *Renew. Energy*, vol. 39, no. 1, pp. 207–215, 2012.

[34] A. Tiwari and M. S. Sodha, “Performance evaluation of hybrid PV/thermal water/air heating system: A parametric study,” *Renew. Energy*, vol. 31, no. 15, pp. 2460–2474, 2006.

[35] C. Good, J. Chen, Y. Dai, and A. Grete, “Hybrid photovoltaic-thermal systems in buildings – a review,” *Energy Procedia*, vol. 70, no. 1876, pp. 683–690, 2015.

[36] L. W. Florschuetz, “Extension of the Hottel-Whillier model to the analysis of combined photovoltaic/thermal flat plate collectors,” *Sol. Energy*, vol. 22, no. 4, pp. 361–366, 1979.

[37] M. Wolf, “Performance analyses of combined heating and photovoltaic power systems for residences,” *Energy Convers.*, vol. 16, no. 1–2, pp. 79–90, 1976.

[38] C. H. Cox and P. Raghuraman, “Design considerations for flat-plate-photovoltaic/thermal collectors,” *Sol. Energy*, vol. 35, no. 3, pp. 227–241, 1985.

[39] T. Bergene and O. M. Løvvik, “Model calculations on a flat-plate solar heat collector with integrated solar cells,” *Sol. Energy*, vol. 55, no. 6, pp. 453–462, 1995.

[40] J. Prakash, “Transient analysis of a photovoltaic-thermal solar collector for co-generation of electricity and hot air/water,” *Energy Convers. Manag.*, vol. 35, no. 11, pp. 967–972, 1994.

[41] D. Vries, *Design of a photovoltaic / thermal combi-panel*, no. 1998. Eindhoven: Eindhoven Univeristy Press, 1998.

[42] T. Fujisawa and T. Tani, “Annual exergy evaluation on photovoltaic-thermal hybrid collector,” *Sol. Energy Mater. Sol. Cells*, vol. 47, no. 1–4, pp. 135–148, 1997.

[43] S. A. Kalogirou, “Use of TRNSYS for modelling and simulation of a hybrid pv – thermal solar system for Cyprus,” vol. 23, pp. 247–260, 2001.

[44] Y. Tripanagnostopoulos, M. Souliotis, R. Battisti, and A. Corrado, “Application aspects of hybrid PV/T solar systems,” *ISES Sol. World …*, no. January 2003, 2003.

[45] Y. Tripanagnostopoulos, T. Nousia, M. Souliotis, and P. Yianoulis, “Hybrid

photovoltaic/thermal solar systems," *Sol. Energy*, vol. 72, no. 3, pp. 217–234, 2002.

[46] T. T. Chow, J. W. Hand, and P. A. Strachan, "Building-integrated photovoltaic and thermal applications in a subtropical hotel building," *Appl. Therm. Eng.*, vol. 23, no. 16, pp. 2035–2049, 2003.

[47] H. A. Zondag, D. W. De Vries, W. G. J. Van Helden, R. J. C. Van Zolingen, and A. A. Van Steenhoven, "The thermal and electrical yield of a PV-thermal collector," *Sol. Energy*, vol. 72, no. 2, pp. 113–128, 2002.

[48] H. A. Zondag and et el., "The yield of different combined PV-thermal collector designs," *Sol. Energy*, vol. 74, no. 3, pp. 253–269, 2003.

[49] T. T. Chow, "Performance analysis of photovoltaic-thermal collector by explicit dynamic model," *Sol. Energy*, vol. 75, no. 2, pp. 143–152, 2003.

[50] W. He and et el., "Hybrid photovoltaic and thermal solar-collector designed for natural circulation of water," *Appl. Energy*, vol. 83, no. 3, pp. 199–210, 2006.

[51] "IEA SHC || Task 35 || Publications." [Online]. Available: https://task35.iea-shc.org/publications. [Accessed: 20-Jun-2020].

[52] A. K. Athienitis and et el., "A prototype photovoltaic/thermal system integrated with transpired collector," *Sol. Energy*, vol. 85, no. 1, pp. 139–153, 2011.

[53] T. T. Chow and et el., "Energy and exergy analysis of photovoltaic-thermal collector with and without glass cover," *Appl. Energy*, vol. 86, no. 3, pp. 310–316, 2009.

[54] L. T. Kostić, T. M. Pavlović, and Z. T. Pavlović, "Optimal design of orientation of PV/T collector with reflectors," *Appl. Energy*, vol. 87, no. 10, pp. 3023–3029, 2010.

[55] Z. Jiafei and et el., "Solar Radiation Transfer and Performance Analysis for a Low Concentrating Photovoltaic/Thermal System," *Environ. Sci. Technol.*, vol. 33, no. 2, pp. 482–489, 2015.

[56] T. Jessa B and R. Valerie, “New Solar Technology Deployed at the UA Tech Park ’ s Solar Zone Gains Momentum,” Arizona, pp. 1–2, Sep-2013.

[57] A. S. C. AB, “Sun provides heating and cooling to the hospital,” Harnosand, p. 1, Apr-2010.

[58] X. Fang and D. Li, “Solar photovoltaic and thermal technology and applications in China,” *Renew. Sustain. Energy Rev.*, vol. 23, pp. 330–340, 2013.

[59] K. Kramer and H. Helmers, “The interaction of standards and innovation: Hybrid photovoltaic-thermal collectors,” *Sol. Energy*, vol. 98, no. PC, pp. 434–439, 2013.

[60] S. M. Sultan, C. P. Tso, and M. N. E. Efzan, “Comments on ‘Performance evaluation of photovoltaic thermal solar air collector for composite climate of India,’” *Sol. Energy Mater. Sol. Cells*, vol. 198, pp. 63–64, 2019.

[61] A. Ibrahim, K. Sopian, and M. Othman, “Simulation of different configuration of hybrid Photovoltaic Thermal Solar Collector (PVTS) Designs,” *Sel. Pap. from Commun. Inf. Technol.*, no. 1976, pp. 1–3, 2008.

[62] J. K. Tonui and Y. Tripanagnostopoulos, “Improved PV/T solar collectors with heat extraction by forced or natural air circulation,” *Renew. Energy*, vol. 32, no. 4, pp. 623–637, 2007.

[63] T. N. Anderson, “Investigation of Thermal Aspects of Building Integrated Photovoltaic/Thermal Solar Collectors,” The University of Waikato by, 2009.

[64] M. Tom and C. Luis, *Practical Handbook of Photovoltaics Fundamentals and Application*. Oxford: Elsevier, 2003.

[65] S. A. Kalogirou and Y. Tripanagnostopoulos, “Industrial application of PV/T solar energy systems,” *Appl. Therm. Eng.*, vol. 27, no. 8–9, pp. 1259–1270, 2007.

[66] M. Bosanac, B. Sørensen, I. Katic, H. Sørensen, B. Nielsen, and J. Badran, “Photovoltaic / Thermal Solar Collectors and Their Potential in Denmark,” 2003.

[67] A. Kumar, P. Baredar, and U. Qureshi, “Historical and recent development of photovoltaic thermal (PVT) technologies,” *Renew. Sustain. Energy Rev.*, vol. 42, pp. 1428–1436, 2015.

[68] M. Azly and et el., “Technology Review of Solar Assisted Heat Pump System for Hot Water Production,” *Latest Trends Renew. Energy Environ. Informatics*, pp. 65–75, 2013.

[69] A. Hepbasli and Y. Kalinci, “A review of heat pump water heating systems,” *Renew. Sustain. Energy Rev.*, vol. 13, no. 6–7, pp. 1211–1229, 2009.

[70] “Heat Pump Types Archives - Heat Pump Reviews.” [Online]. Available: https://www.heatpumpreview.net/category/heat-pump-types/. [Accessed: 20-Jun-2020].

[71] M. Forsén, “Heat pumps: Technology and environmental impact,” Bengt Sandstrom, 2005.

[72] M. Inalli and H. Esen, “Experimental thermal performance evaluation of a horizontal ground-source heat pump system,” *Appl. Therm. Eng.*, vol. 24, no. 14–15, pp. 2219–2232, 2004.

[73] Y. J. Nam, X. Y. Gao, S. H. Yoon, and K. H. Lee, “Study on the performance of a ground source heat pump system assisted by solar thermal storage,” *Energies*, vol. 8, no. 12, pp. 13378–13394, 2015.

[74] O. Kara, K. Ulgen, and A. Hepbasli, “Exergetic assessment of direct-expansion solar-assisted heat pump systems: Review and modeling,” *Renew. Sustain. Energy Rev.*, vol. 12, no. 5, pp. 1383–1401, 2008.

[75] S. Ito, N. Miura, and K. Wang, “Performance of a heat pump using direct expansion solar collectors,” *Sol. Energy*, vol. 65, no. 3, pp. 189–196, 1999.

[76] B. J. Ã. Huang and C. P. Lee, “Long-term performance of solar-assisted heat pump water heater,” vol. 29, pp. 633–639, 2003.

[77] J. Ji, K. Liu, T. tai Chow, G. Pei, W. He, and H. He, “Performance analysis of a photovoltaic heat pump,” *Appl. Energy*, vol. 85, no. 8, pp. 680–693, 2008.

[78] J. Ji *et al.*, "Experimental study of photovoltaic solar assisted heat pump system," *Sol. Energy*, vol. 82, no. 1, pp. 43–52, 2008.

[79] A. Hazi and G. Hazi, "Comparative study of indirect photovoltaic thermal solar-assisted heat pump systems for industrial applications," *Appl. Therm. Eng.*, vol. 70, no. 1, pp. 90–99, 2014.

[80] H. D. Fu, G. Pei, J. Ji, H. Long, T. Zhang, and T. T. Chow, "Experimental study of a photovoltaic solar-assisted heat-pump/heat-pipe system," *Appl. Therm. Eng.*, vol. 40, pp. 343–350, 2012.

[81] Y. Bai, T. T. Chow, C. Ménézo, and P. Dupeyrat, "Analysis of a hybrid PV/thermal solar-assisted heat pump system for sports center water heating application," *Int. J. Photoenergy*, vol. 2012, 2012.

[82] E. Fuentes, L. Arce, and J. Salom, "A review of domestic hot water consumption profiles for application in systems and buildings energy performance analysis," *Renewable and Sustainable Energy Reviews*, vol. 81. pp. 1530–1547, 2018.

[83] A. A. Mermoud and B. Wittmer, "Pvsyst User's Manual," *PVSyst SA*, no. January, 2014.

[84] S. S. Dual, "A revolutionary hybrid solar panel," Marseille, 13013, 2018.

[85] H. B. C. El Hocine, K. Touafek, F. Kerrour, H. Haloui, and A. Khelifa, "Model Validation of an Empirical Photovoltaic Thermal (PV/T) Collector," *Energy Procedia*, vol. 74, pp. 1090–1099, 2015.

[86] A. D. Jones and C. P. Underwood, "A thermal model for photovoltaic systems," *Fuel Energy Abstr.*, vol. 43, no. 3, p. 199, 2002.

[87] K. Touafek and et el, "Model Validation of an Empirical Photovoltaic Thermal (PV / T) Collector," *Energy Procedia*, vol. 74, pp. 1090–1099, 2015.

[88] S. Bhattarai and et el, "Simulation and model validation of sheet and tube type photovoltaic thermal solar system and conventional solar collecting system in transient states," *Sol.*

Energy Mater. Sol. Cells, vol. 103, no. August 2012, pp. 184–193, 2012.

[89] M. Roger A and V. Jerry, *Photovoltaic Systems Engineering*, Second Edi. New York: Taylor & Francis, 2005.

[90] A. Bekele, D. Alemu, and M. Mishra, "Large-scale solar water heating systems analysis in Ethiopia: a case study," *Int. J. Sustain. Energy*, vol. 32, no. November, pp. 1–22, 2011.

[91] H. A. Zondag, "Flat-plate PV-Thermal collectors and systems: A review," *Renew. Sustain. Energy Rev.*, vol. 12, no. 4, pp. 891–959, 2008.

[92] M. Sardarabadi, "Computer Modelling and Experimental Validation of a Photovoltaic Thermal (PV/T) Water Based Collector System," *2nd Int. Conf. Power Energy Syst. (ICPES 2012)*, vol. 56, no. Icpes, pp. 75–79, 2012.

[93] A. S. Abdelrazik and et el, "A review on recent development for the design and packaging of hybrid photovoltaic / thermal (PV / T) solar systems Design of PV," *Renew. Sustain. Energy Rev.*, vol. 95, no. December 2017, pp. 110–129, 2018.

[94] A. Kazemian, M. Hosseinzadeh, and M. Sardarabadi, "Effect of glass cover and working fl uid on the performance of photovoltaic thermal (PVT) system : An experimental study," vol. 173, no. August, pp. 1002–1010, 2018.

[95] N. M.-A. Mutombo, F. Inambao, and G. Bright, "Performance analysis of thermosyphon hybrid photovoltaic thermal collector," *J. Energy South. Africa*, vol. 27, no. 1, pp. 28–38, 2016.

[96] L. Yalçin and R. Öztürk, "Performance comparison of c-Si, mc-Si and a-Si thin film PV by PVsyst simulation," *J. Optoelectron. Adv. Mater.*, vol. 15, no. 3–4, pp. 326–334, 2013.

[97] C.-Y. Huang, "A study of photovoltaic thermal (PV/T) hybrid system with computer modeling," *Int. J. Smart Grid Clean Energy*, vol. 3, no. 1, pp. 75–79, 2014.

[98] L. pauly, L. Rekha, C. V. Vazhappilly, and C. R. Melvinraj, "Numerical Simulation for Solar Hybrid Photovoltaic Thermal Air Collector," *Procedia Technol.*, vol. 24, pp. 513–

522, 2016.

[99] S. M. Sultan and M. N. E. Efzan, “Review on recent Photovoltaic / Thermal (PV / T) technology advances and applications,” *Sol. Energy*, vol. 173, no. August, pp. 939–954, 2018.

[100] B. Du, E. Hu, and M. Kolhe, “Performance analysis of water cooled concentrated photovoltaic (CPV) system,” *Renew. Sustain. Energy Rev.*, vol. 16, no. 9, pp. 6732–6736, 2012.

[101] M. Kolhe, D. Bin, and E. Hu, “Water Cooled Concentrated Photovoltaic System,” pp. 2–6, 2012.

[102] R. Daneshazarian, E. Cuce, P. Mert, and F. Sher, “Concentrating photovoltaic thermal (CPVT) collectors and systems : Theory , performance assessment and applications,” *Renew. Sustain. Energy Rev.*, vol. 81, no. August 2017, pp. 473–492, 2018.

[103] T. T. Chow, W. He, J. Ji, and A. L. S. Chan, “Performance evaluation of photovoltaic – thermosyphon system for subtropical climate application,” vol. 81, pp. 123–130, 2007.

[104] M. Ben Ammar, M. Ben Ammar, and M. Chaabene, “A dynamic model of hybrid photovoltaic / thermal panel,” *Int. Renew. Energy Congr.*, pp. 19–24, 2009.

[105] I. Guarracino and et el, “Dynamic coupled thermal-and-electrical modelling of sheet-and-tube hybrid photovoltaic / thermal (PVT) collectors,” *Appl. Therm. Eng.*, vol. 101, pp. 778–795, 2016.

[106] M. S. Hossain and et el, “Thermal performance analysis of parallel serpentine flow based photovoltaic / thermal (PV / T) system under composite climate of Malaysia,” *Appl. Therm. Eng.*, no. January, pp. 1–11, 2019.

[107] B. Theodore L and et el, *Fundamentals of Heat and Mass Transfer*, Seven., vol. 39, no. 5. John Wiley & Sons, 2008.

[108] A. H. A. Al-waeli and et el, “Photovoltaic / Thermal (PV / T) systems : Status and future

prospects," *Renew. Sustain. Energy Rev.*, vol. 77, no. February, pp. 109–130, 2017.

[109] S. M. Sultan, M. I. Fadhel, and S. A. Alkaff, "Performance Analysis of the Photovoltaic / Thermal Collector (PV / T) System for Different Malaysian Climatic Conditions," vol. 467, pp. 522–527, 2014.

[110] J. I. Bilbao and A. B. Sproul, "Detailed PVT-water model for transient analysis using RC networks," *Sol. Energy*, vol. 115, pp. 680–693, 2015.

[111] P. Dupeyrat, C. Ménézo, and S. Fortuin, "Study of the thermal and electrical performances of PVT solar hot water system," *Energy Build.*, vol. 68, no. PART C, pp. 751–755, 2014.

[112] W. Stephan *et al.*, "Design Handbook for Reversible Heat Pump Systems with and without Heat Recovery," Mines Paritech, 2011.

[113] D. Zogg, "Fault diagnosis for heat pump systems," Swiss Federal Institute of Technology Zurich, 2002.

[114] K. Gram-Hanssen, T. H. Christensen, and P. E. Petersen, "Air-to-air heat pumps in real-life use: Are potential savings achieved or are they transformed into increased comfort?," *Energy Build.*, vol. 53, pp. 64–73, 2012.

[115] S. Poppi and et el, "Techno-economic review of solar heat pump systems for residential heating applications," *Renewable and Sustainable Energy Reviews*. 2018.

[116] T. T. Chow and et el, "Potential use of photovoltaic-integrated solar heat pump system in Hong Kong," *Appl. Therm. Eng.*, vol. 30, no. 8–9, pp. 1066–1072, 2010.

[117] S. Lu, R. Liang, J. Zhang, and C. Zhou, "Performance improvement of solar photovoltaic/thermal heat pump system in winter by employing vapor injection cycle," *Appl. Therm. Eng.*, vol. 155, no. September 2018, pp. 135–146, 2019.

[118] H. Ben Nejma *et al.*, "In-situ performance evaluation by simulation of a coupled air source heat pump/PV-T collector system," *Proc. BS2013*, vol. BS2013, no. 13 th, pp. 1927–1935, 1927.

[119] H. Chen, S. B. Riffat, and Y. Fu, “Experimental study on a hybrid photovoltaic/heat pump system,” *Appl. Therm. Eng.*, vol. 31, no. 17–18, pp. 4132–4138, 2011.

[120] K. Wang, M. Herrando, A. M. Pantaleo, and C. N. Markides, “Technoeconomic assessments of hybrid photovoltaic-thermal vs . conventional solar-energy systems : Case studies in heat and power provision to sports centres,” *Appl. Energy*, vol. 254, no. July, p. 113657, 2019.

[121] F. Aguilar and P. V Quiles, “Environmental bene fi ts and economic feasibility of a photovoltaic assisted heat pump water heater,” *Sol. Energy*, vol. 193, no. July, pp. 20–30, 2019.

[122] R. Simonetti, L. Moretti, L. Molinaroli, and G. Manzolini, “Energetic and economic optimization of the yearly performance of three different solar assisted heat pump systems using a mixed integer linear programming algorithm,” *Energy Convers. Manag.*, vol. 206, no. December 2019, p. 112446, 2020.

[123] C. Invoice, “Suzhou sharesun photovoltaic technology co.,ltd,” Wangting, PI-12 panels, 2020.

[124] Z. Zhao, “Eitai New Energy Technology Co.Ltd,” *Quotation*, vol. 53, no. 9, p. 287, 2020.

[125] FAR.S, *AIR to water heat pump water heater (Split series)*. 2020, pp. 1–2.

[126] D. Alemu, “Optimal design of solar water heating systems,” *J. EAEA*, vol. 15, pp. 53–60, 1998.

[127] J. A. Aguilar-jiménez, N. Velázquez, A. Acuña, R. Cota, E. González, and L. González, “Techno-economic analysis of a hybrid PV-CSP system with thermal energy storage applied to isolated microgrids,” *Sol. Energy*, vol. 174, no. August, pp. 55–65, 2018.

[128] E. E. Authority, “Energy Tariff amendment study according to consumers class Service Charge rates amendment study for four years , starting 2018 GC,” pp. 2–3, 2018.

[129] C. Rubio-maya and A. L. Soto-sánchez, “Feasibility Analysis of Hybrid Photovoltaic /

Thermal Cogeneration System for DOMESTIC APPLICATIONS," no. November 2016, 2016.

APPENDIX

Appendix A**:** Hourly electrical energy consumption distribution for different cases

	For Heat pump								**Domestic Appliance**
No	Percentage distributed all generated electrical energy for 8 working with the rest of 16 hours respectively					Night and day time distribution respectively			Addis and Dire Dawa
	5/95%	10/90%	15/85%	20/90	25/75%	50/50%	25/75%	10/90%	
1	35.418	70.8375	106.25625	141.675	177.09375	472.25	236.125	94.45	234
2	35.418	70.8375	106.25625	141.675	177.09375	472.25	236.125	94.45	234
3	35.418	70.8375	106.25625	141.675	177.09375	472.25	236.125	94.45	234
4	35.418	70.8375	106.25625	141.675	177.09375	472.25	236.125	94.45	234
5	35.418	70.8375	106.25625	141.675	177.09375	472.25	236.125	94.45	234
6	35.418	70.8375	106.25625	141.675	177.09375	472.25	236.125	94.45	234
7	35.418	70.8375	106.25625	141.675	177.09375	472.25	708.375	850.05	234
8	35.418	70.8375	106.25625	141.675	177.09375	472.25	708.375	850.05	234
9	1345.9125	1275.075	1204.2375	1133.4	1062.5625	472.25	708.375	850.05	234
10	1345.9125	1275.075	1204.2375	1133.4	1062.5625	472.25	708.375	850.05	234
11	1345.9125	1275.075	1204.2375	1133.4	1062.5625	472.25	708.375	850.05	234
12	1345.9125	1275.075	1204.2375	1133.4	1062.5625	472.25	708.375	850.05	700
13	1345.9125	1275.075	1204.2375	1133.4	1062.5625	472.25	708.375	850.05	700
14	1345.9125	1275.075	1204.2375	1133.4	1062.5625	472.25	708.375	850.05	700
15	1345.9125	1275.075	1204.2375	1133.4	1062.5625	472.25	708.375	850.05	700
16	1345.9125	1275.075	1204.2375	1133.4	1062.5625	472.25	708.375	850.05	700
17	35.418	70.8375	106.25625	141.675	177.09375	472.25	708.375	850.05	700
18	35.418	70.8375	106.25625	141.675	177.09375	472.25	708.375	850.05	700
19	35.418	70.8375	106.25625	141.675	177.09375	472.25	236.125	94.45	641
20	35.418	70.8375	106.25625	141.675	177.09375	472.25	236.125	94.45	641
21	35.418	70.8375	106.25625	141.675	177.09375	472.25	236.125	94.45	641
22	35.418	70.8375	106.25625	141.675	177.09375	472.25	236.125	94.45	641
23	35.418	70.8375	106.25625	141.675	177.09375	472.25	236.125	94.45	641
24	35.418	70.8375	106.25625	141.675	177.09375	472.25	236.125	94.45	641

Appendix B**:** Solar Data for representative days for Dire Dawa site

Month	Hour	I_{total}	I_d	I_b	T_{amb}
17-Jan	1	0	0	0	18.93
	2	0	0	0	18.28
	3	0	0	0	17.53
	4	0	0	0	17.18
	5	0	0	0	17.04
	6	0	0	0	16.78
	7	0	0	0	16.43
	8	355.9	59.3	296.6	16.06
	9	548.4	91.4	457.1	17.09
	10	687.6	115	573.1	20.74
	11	811	135	675.9	22.49
	12	770	128	641.7	23.42
	13	715	119	595.9	25.07
	14	600	100	500	26.24
	15	401.6	66.9	334.7	27.29
	16	299.7	49.9	249.7	27.88
	17	149	24.8	124.2	28.03
	18	29.27	4.88	24.39	28.08
	19	0	0	0	27.01
	20	0	0	0	24.93
	21	0	0	0	22.85
	22	0	0	0	21.43
	23	0	0	0	20.42
	24	0	0	0	19.23

Month	Hour	I$total$	Id	Ib	Tamb
16-Feb	1	0	0	0	20.181
	2	0	0	0	19.688
	3	0	0	0	18.925
	4	0	0	0	18.563
	5	0	0	0	18.294
	6	0	0	0	17.725
	7	0	0	0	17.394
	8	326.56	76.95	249.6	16.906
	9	497.13	117.1	380	17.925
	10	663.34	156.3	507	21.656
	11	735	173.2	561.8	24.406
	12	781	184	597	26.513
	13	731	172.2	558.8	27.888
	14	539.46	127.1	412.3	29.356
	15	382.06	90.03	292	30.319
	16	226.83	53.45	173.4	30.913
	17	124.31	29.29	95.02	31.45
	18	40.345	9.507	30.84	31.463
	19	0	0	0	30.644
	20	0	0	0	28.981
	21	0	0	0	26.588
	22	0	0	0	25.069
	23	0	0	0	23.7
	24	0	0	0	22.606

Month	Hour	I$total$	Id	Ib	Tamb
16-Mar	1	0	0	0	23.2
	2	0	0	0	23.065
	3	0	0	0	23.155
	4	0	0	0	24.025
	5	0	0	0	23.615
	6	0	0	0	23.185
	7	0	0	0	23
	8	376.06	62.14	313.9	22.88
	9	553.48	91.46	462	23.82
	10	696.22	115.1	581.2	25.98
	11	773	127.7	645.3	27.4
	12	790	130.6	659.4	29.175
	13	752	124.3	627.7	30.355
	14	599.22	99.02	500.2	31.065
	15	442.97	73.2	369.8	32.06
	16	301.1	49.76	251.3	32.36
	17	157.23	25.98	131.2	32.595
	18	50.375	8.325	42.05	31.935
	19	0	0	0	31.64
	20	0	0	0	30.145
	21	0	0	0	28.2
	22	0	0	0	27.025
	23	0	0	0	25.72
	24	0	0	0	24.805

Month	Hour	I$total$	Id	Ib	Tamb
15-Apr	1	0	0	0	23.775
	2	0	0	0	24.1
	3	0	0	0	23.675
	4	0	0	0	23.475
	5	0	0	0	23
	6	0	0	0	22.525
	7	0	0	0	21.675
	8	307.79	101.2	206.6	22.875
	9	513.93	169	345	25.325
	10	642.65	211.3	431.4	26.625
	11	727	239	488	27.65
	12	751	246.9	504.1	29.725
	13	726	238.7	487.3	31.25
	14	602	197.9	404.1	32.275
	15	380	124.9	255.1	33.675
	16	230	75.62	154.4	34
	17	134.11	44.09	90.01	33.65
	18	36.66	12.05	24.61	32.775
	19	0	0	0	30.75
	20	0	0	0	28.4
	21	0	0	0	27.075
	22	0	0	0	26.075
	23	0	0	0	24.5
	24	0	0	0	23.45

Month	Hour	I$total$	Id	Ib	Tamb
15-May	1	0	0	0	25.115
	2	0	0	0	24.66
	3	0	0	0	24.13
	4	0	0	0	24.465
	5	0	0	0	24.45
	6	0	0	0	24.195
	7	0	0	0	23.76
	8	422.42	70.53	351.9	23.435
	9	586.44	97.92	488.5	25.005
	10	758.14	126.6	631.5	27.51
	11	810	135.3	674.7	29.93
	12	851.48	142.2	709.3	31.865
	13	728	121.6	606.4	32.83
	14	524.62	87.6	437	33.52
	15	333.91	55.76	278.2	34.205
	16	238.37	39.8	198.6	34.405
	17	116.17	19.4	96.77	34.705
	18	33.275	5.556	27.72	33.165
	19	0	0	0	32.165
	20	0	0	0	31.24
	21	0	0	0	30.42
	22	0	0	0	29.515
	23	0	0	0	28.24
	24	0	0	0	27.18

Month	Hour	I$total$	Id	Ib	Tamb
11-Jun	1	0	0	0	28.35
	2	0	0	0	28.155
	3	0	0	0	28.075
	4	0	0	0	27.73
	5	0	0	0	27.695
	6	0	0	0	27.435
	7	0	0	0	27.02
	8	375.79	79.9	295.9	26.325
	9	571.27	121.5	449.8	26.105
	10	738.59	157	581.6	26.91
	11	823.24	175	648.2	27.815
	12	766	162.9	603.1	29
	13	678	144.2	533.8	30.31
	14	540	114.8	425.2	31.95
	15	348.15	74.02	274.1	32.675
	16	174.65	37.13	137.5	32.85
	17	71.73	15.25	56.48	32.79
	18	29.6	6.293	23.31	32.56
	19	0	0	0	31.27
	20	0	0	0	29.57
	21	0	0	0	28.74
	22	0	0	0	28.365
	23	0	0	0	28.12
	24	0	0	0	27.88

Month	Hour	I_{total}	I_d	I_b	T_{amb}
July 17	1	0	0	0	26.99
	2	0	0	0	27.08
	3	0	0	0	26.64
	4	0	0	0	26.41
	5	0	0	0	26.2
	6	0	0	0	25.81
	7	0	0	0	24.9
	8	373.8	64.52	309.3	24.02
	9	558.5	96.39	462.1	23.91
	10	703	121.3	581.7	24.72
	11	806	139.1	666.9	26.04
	12	769	132.7	636.3	27.15
	13	673	116.2	556.8	28.38
	14	567.9	98.01	469.8	29.76
	15	459.7	79.34	380.3	30.56
	16	259.1	44.72	214.4	30.93
	17	92.39	15.95	76.44	31.11
	18	33.2	5.73	27.47	31.27
	19	0	0	0	30.64
	20	0	0	0	29.69
	21	0	0	0	28.89
	22	0	0	0	28.22
	23	0	0	0	27.77
	24	0	0	0	27.5

Month	Hour	I$total$	Id	Ib	Tamb
16-Aug	1	0	0	0	26.21
	2	0	0	0	25.71
	3	0	0	0	25.51
	4	0	0	0	25.17
	5	0	0	0	24.73
	6	0	0	0	24.4
	7	0	0	0	23.22
	8	282.8	79.93	202.8	22.46
	9	487	137.7	349.3	22.02
	10	610.9	172.7	438.2	23.21
	11	681	192.5	488.5	24.72
	12	741	209.5	531.5	26.32
	13	666	188.3	477.7	27.62
	14	538.8	152.3	386.5	29.12
	15	354.3	100.2	254.2	29.87
	16	216.4	61.18	155.2	30.08
	17	94.54	26.72	67.81	29.81
	18	33.07	9.349	23.72	29.96
	19	0	0	0	28.7
	20	0	0	0	27.63
	21	0	0	0	26.85
	22	0	0	0	25.5
	23	0	0	0	24.5
	24	0	0	0	24.29

Month	Hour	I$total$	Id	Ib	Tamb
15-Sep	1	0	0	0	26.09
	2	0	0	0	26.35
	3	0	0	0	25.37
	4	0	0	0	24.99
	5	0	0	0	24.79
	6	0	0	0	24.86
	7	0	0	0	24.34
	8	324.9	77.74	247.2	23.72
	9	478.2	114.4	363.8	24.29
	10	629.7	150.7	479	25.8
	11	747.5	178.9	568.7	27
	12	782	187.1	594.9	28.41
	13	697	166.8	530.2	29.52
	14	574.6	137.5	437.1	30.14
	15	418.9	100.2	318.7	29.81
	16	184.7	44.18	140.5	30.42
	17	59.48	14.23	45.25	28.98
	18	16.42	3.929	12.49	28.52
	19	0	0	0	28.91
	20	0	0	0	27.88
	21	0	0	0	26.94
	22	0	0	0	26.47
	23	0	0	0	26.47
	24	0	0	0	26.3

Month	Hour	I$total$	Id	Ib	Tamb
15-Oct	1	0	0	0	25.61
	2	0	0	0	25.08
	3	0	0	0	24.82
	4	0	0	0	24.41
	5	0	0	0	24.14
	6	0	0	0	23.74
	7	0	0	0	23.3
	8	322.6	58.09	264.6	22.89
	9	527.9	95.03	432.8	24.57
	10	679.4	122.3	557.1	27.15
	11	781.2	140.6	640.6	28.7
	12	820.2	147.7	672.5	29.86
	13	795	143.1	651.9	30.88
	14	714.8	128.7	586.1	31.17
	15	500.5	90.1	410.4	30.98
	16	280.6	50.51	230.1	30.7
	17	122.1	21.98	100.1	30.44
	18	23.26	4.187	19.07	29.8
	19	0	0	0	28.87
	20	0	0	0	27.58
	21	0	0	0	27.54
	22	0	0	0	27.42
	23	0	0	0	27.05
	24	0	0	0	26.56

Month	Hour	I$total$	Id	Ib	Tamb
14-Nov	1	0	0	0	21.96
	2	0	0	0	21.64
	3	0	0	0	21.59
	4	0	0	0	20.84
	5	0	0	0	20.27
	6	0	0	0	19.34
	7	0	0	0	18.76
	8	434	161.2	272.8	18.21
	9	684	254.1	429.9	19.02
	10	789	293.1	495.9	21.59
	11	859	319.1	539.9	23.98
	12	898	333.6	564.4	25.49
	13	773	287.2	485.8	25.93
	14	630.3	234.2	396.2	26.33
	15	425.9	158.2	267.7	26.98
	16	296.9	110.3	186.6	27.45
	17	125.2	46.52	78.71	27.51
	18	66.45	24.69	41.76	27.11
	19	0	0	0	25.66
	20	0	0	0	23.64
	21	0	0	0	22.94
	22	0	0	0	22.92
	23	0	0	0	22.71
	24	0	0	0	22.66

Month	Hour	I$total$	Id	Ib	Tamb
10-Dec	1	0	0	0	20.26
	2	0	0	0	20.33
	3	0	0	0	20.74
	4	0	0	0	20.54
	5	0	0	0	20.18
	6	0	0	0	19.46
	7	0	0	0	18.79
	8	328.7	103.1	225.6	18.24
	9	475.8	149.3	326.6	18.84
	10	618.6	194.1	424.5	21.28
	11	784	246	538	23.56
	12	812	254.8	557.2	24.83
	13	799	250.7	548.3	25.58
	14	658	206.4	451.6	26.26
	15	380	119.2	260.8	26.35
	16	273.5	85.79	187.7	26.49
	17	187	58.66	128.3	26.53
	18	118.6	37.21	81.4	26.35
	19	0	0	0	25.46
	20	0	0	0	23.66
	21	0	0	0	22.39
	22	0	0	0	22.4
	23	0	0	0	21.8
	24	0	0	0	21.04

Appendix C Loss diagram over whole year Dire Dawa (Top) and Addis Ababa (Bottom)

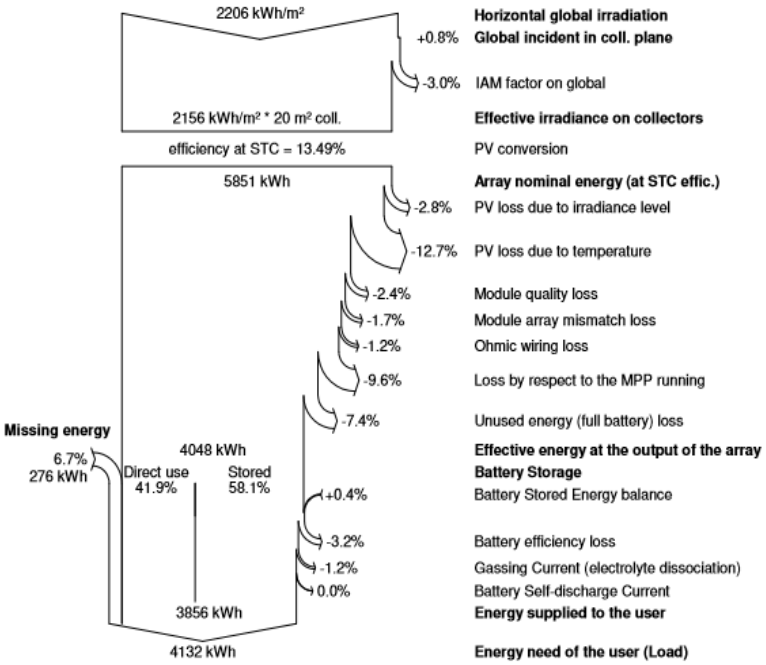

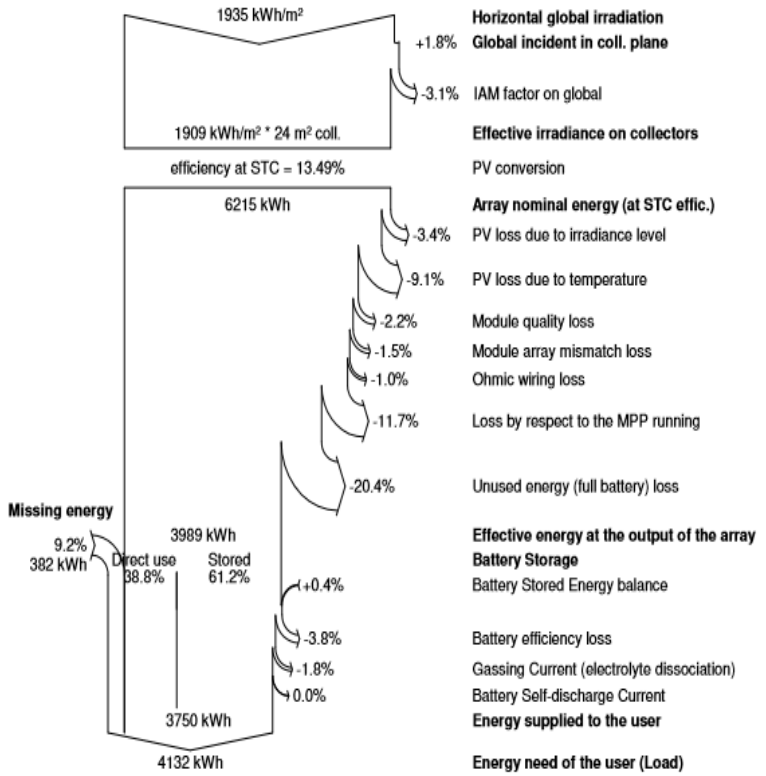

Appendix D: PV/T Heat Pump MATLAB program

```
%Photovoltaic Thermal Heat Pump MATLAB PROGRAM
clc
clear all
Ac=1.654; %one module collector area
Vs=0.4;   %Volume of storage for PV/T per one module
Vsh=0.2;  %Volume of Storage of Heat pump per one module
DWC=0.4;  %daily water consumption per module area
d=nthroot((2*Vs/3.14),3); %Diameter of the storage PV/T
dh=nthroot((2*Vsh/3.14),3);%Diameter of the storage heat pump
Ls=2*d;  % Length of PV/T storage
Lsh=2*dh;% Length of Heat pump storage
As=(3.1416*d^2)+(3.1416*d*Ls);     %Total Area of the PV/T storage
Ash=(3.1416*dh^2)+(3.1416*dh*Lsh); %Total Area of the Heat pump storage
ff=[0,0,0,0,0,0,0,0,0,0.125,0.125,0.125,0.125,0.125,0.125,0.125,0.125,0,0,0,0
,0,0,0]; %Constant water consumption
%
ff=[0,0,0,0,0,0,0,0,0.021,0.029,0.032,0.033,0.045,0.152,0.066,0.024,0.017,0.0
62,0.174,0.132,0.09,0.083,0.034,0.08];%Restaurant water consumption
%
ff=[0.018,0.015,0.007,0,0,0.029,0.095,0.146,0.099,0.066,0.055,0.044,0.047,0.0
36,0.029,0.022,0.026,0.036,0.147,0.14,0.036,0.04,0.036,0.029];%MOTEL
mfw=(Vs/(8*60*60))*998; %mass flow of water
mdot=mfw;
Rhow=998;  %Density of water
Rhoa=1.226;%Density of air
Twb=22;    %Back up water in to the storage
P=5.334;   %Perimeter of the collector
de=0.05;   %Depth of the edge of the collector
Al=P*de;   %Collector side area
do=0.015;  %Outer dimeter of the pipe
di=0.013;  %Inner dimeter of the pipe
w=0.088;   %Center to center b/n tubes
Ap=0.78;   %Absorbing area of the PV module from one square area
no=10;     %Number of riser
Lr=16;     %Length of the Pipe
tpv=0.3;   %Thickness of the PV module
ti=0.05;   %Back insulation thickness and storage the same thickness
tei=0.025; %EDGE INSULATION THICKNESS
tab=0.0035;%Absorber Thickness
eg=0.88;   %Emissivity of the glass
Gtg=0.9;   %Transmissivity of glass
Trpv=0.1;  %Transitivity of the PV module
epv=0.83;  %Emissivity of the PV module
apv=0.9;   %Absorbability of PV module
tapv=0.87; %Difference b/n Absorptivity and Transitivity of Module
eef=((1/epv)+(1/eg)-1)^-1; %Effective emissivity of PV and Glass
pf=0.88;     %Packing Factor
Tfp=0.92;    %Temperature coefficient of PV module
Nepv=0.1687; %Nominal efficiency of PV module
Trf=25;      %Reference Temperature
ka=0.026;    %Thermal conductivity of air
kw=0.625;    %Thermal conductivity of water
kp=0.158;    %Thermal conductivity of PV
```

```
kab=65;       %Thermal conductivity of absorber
kg=0.93;      %Glass Thermal Conductivity
ki=0.045;     %Insulation Thermal conductivity
rho=0.2;      %Ground reflection
spg=0.05;     %Distance between glass and PV module
cg=670;       %Glass specific heat ;
Ca=1.005;     %Specific heat capacity of air
cw=4186;      %Specific Heat of Water
cp=677;       %PV specific heat
ci=670;       %Insulation Specific Heat
ca=903;       %Absorber plate specific heat
mg=11.7;      %Mass of glass;
mp=9.47;      %mass of PV ;
ma=10.62;     %Mass of absorber and Tube;
mw=1.32;      %Mass of water in one module meter square area;
mic=1;        %collector insulation mass
mis=0.2908;   %storage insulation mass
mcpw=mw*cw;   %Mass and specific heat of water collector
mcpp=mp*cp;   %Mass*CP of PV module
mcpc=ma*ca;   %MASS*CP OF ABSORBER
mcpg=mg*cg;   %mass*Cp of Glass
mcps=Rhow*Vs*cw; %Storage Mass*Cp
mcpi=mic*ci;      %mass of insulation for collector
Vw=3;             %wind speed
beta=pi/18;       %collector slop
phi=9.7*pi/180;   %Latitude of the site
pr=4.772;         %Pranditile Number for water
pra=0.72;         %Pranditle number for air
Re=733;           %Reynoldos Number
dvi=1.81e-5;      %dynamic viscosity of air
kvis=dvi/Rhoa;    %Kinematic viscosity of air
sigma=5.67e-8;    %Boltzmann constant
vis=pr*sigma;     %Viscosity
Tai=20;           %Initial Temperature of the atmosphere
TIQsolar=0;       %Initialization of solar irradiation
TQucl=0;
TQstorage=0;
FQstorage=0;
TQuseful=0;
Qwuhp=0;
TElec=0;
TQloss=0;
Vdot=mfw/1000;
PHp=0;
Thp2=40;
Thp2i=Thp2;
deltt=7.5;
Aat=pi*do*Lr/2; %Contact area b/n pipe and absorber
Aai=Ac;         %Contact area b/n absorber and insulation
Ati=pi*di*Lr;   %Internal surface area of the pipe
Act=pi*di^2/4;  %Cross cection area of the tube
open=('FinalRN.xlsx');
Z=xlsread(open);
for j=1:365
```

```
data1(:,:,j)=Z(j+(23*(j-1)):j*24,:); %Data formulate for 24 hours of each day
for all day in the year
end
for n=1:365
decl(n)=(pi/180)*(23.45*sin((2*pi/365)*(284+n))); %Calculation of the
declination angle )))
end
for ii=1:24
omega(ii)=(ii-12)*pi/12; % Calculation of the hourangle for each hour of the
day. )))
end
for i=1
Grr=data1(:,1,i);
Drr=data1(:,2,i);
Taa=data1(:,3,i);
for j=1
Gr=Grr(1);
Dr=Drr(1);
T=Taa(1);
Ta=T;
Tpi=T+3;
Tgi=T+2;
Tci=T+2.5;
Tsky=Ta-6;
Twi=Ta+2;
Two=Twi+2;
Tsi=Twi+15;
Twba=Ta;
Rb=((cos(phi-beta))*cos(decl(i))*cos(omega(j))+sin(decl(i))*(sin(phi-
beta)))/(cos(phi)*cos(decl(i))*cos(omega(j))+(sin(decl(i))*sin(phi)));
In=Rb*(Gr-Dr)+(Dr*0.5*(1+cos(beta)))+(0.5*rho*((1-cos(beta))*Gr));
Ic=In*apv;
Tf=(Tai+T)/2;
Ve=2/(Tai+T);
Gr=(9.81*Ve*(Tpi-Tgi)*spg^3)/kvis^2;
Nu=2.5+0.0133*(90-beta);
hc2=Nu*ka/spg;
Ub=ki/ti ;
Ue=Ub*(Al/Ac);
hc1=2.8+3*Vw;
hr1=eg*sigma*((Tgi^4-Tsky^4)/(Tgi-Ta));
hr2=eef*sigma*((Tpi^4-Tgi^4)/(Tpi-Tgi));
Ut=((1/(hc2+hr2))+(1/(hc1+hr1)))^-1;
Ul=Ut+Ub+Ue;
Uls=ki/ti;
hf=kw/di;
hap=kp/tpv;
hia=Ub;
Tpm = 30 + 0.0175.*(Ic-150) + 1.14*(Ta -25);
E=Ic*tapv.*pf.*Nepv*((1-Tfp).*(Tpm-Trf));
a12=hc1+hr1;
a13=hc2+hr2;
a11=a12+a13;
b11=hap;
b12=a13+b11;
```

```
m=(Ul/(kp*tpv))^1/2;
fe=tanh(m*((w-do)/2))/(m*((w-do)/2));
Fw=fe*2-1;
de=0.035;
zzz=1/Ul;
zz=1/(Ul*(de+(w-de)*fe));
cb=15;
zx=1/cb;
zc=1/(pi*di*hf);
Upw=zzz/(w*(zz+zx+zz));
c11=Ac*b11+Upw*Ati*Fw+Aai*hia*fe;
c12=Upw*Ati*2;
c13=Aai*hia*fe;
d11=(Ati*Upw*Fw*12);
d12=(((Ati*Upw)/2)+mdot*cw);
d13=(Ati*Upw)-(mdot*cw);
e11=mdot*cw;
e12=mdot*cw+Rhow*DWC*ff(j)*cw+Uls*As;
e13=Rhow*DWC*ff(j)*cw;
e14=Uls*As;
Tg1=Tgi+(deltt/mcpg)*Ac*((Ic*(1-Gtg))-a11*Tgi+a12*Ta+a13*Tpi);
Tp1=Tpi+((deltt/mcpp)*Ac*(Ic-E+a13*Tg1-b12*Tpi+Tci*b11));
Tc1=Tci+((deltt/mcpc*fe)*((b11*Tp1)-(c11*Tci)+(c12*Two)+(c12*Twi)+(c13*Ta)));
Tw1=Two+(deltt/mcpw)*((d11*Tc1)-(d12*Two)-(d13*Twi));
Ts1=Tsi+((deltt/mcps)*(e11*Tw1-e12*Tsi+e13*Twba+e14*Ta));
end
end
for i=1:365
Grr=data1(:,1,i);
Drr=data1(:,2,i);
Taa=data1(:,3,i);
T=Taa(1);
for j=1:24
Gr=Grr(j);
Dr=Drr(j);
Tamb=Taa(j);
Ta=T;
Rb=((cos(phi-beta))*cos(decl(i))*cos(omega(j))+sin(decl(i))*(sin(phi-
beta)))/(cos(phi)*cos(decl(i))*cos(omega(j))+(sin(decl(i))*sin(phi)));
if Rb<0
Rb=0.5;
end
In=Rb*(Gr-Dr)+(Dr*0.5*(1+cos(beta)))+(0.5*rho*((1-cos(beta))*Gr));
Ic=In*apv*Gtg;
if Ic<0
Ic=0;
end
TIQsolar=TIQsolar+In/1000;
for jj=1:480
Tf=(Tai+Ta)/2;
Ve=2/(Tai+Ta);
Tsky=Ta-6;
Twba=T+2;
Gr=(9.81*Ve*(Tp1-Tg1)*spg^3)/kvis^2;
Nu=2.5+0.0133*(90-beta);
```

```
hc2=Nu*ka/spg;
Ub=ki/ti;
Ue=Ub*(Al/Ac);
hc1=2.8+3*Vw;
hr1=eg*sigma*((Tg1^4-Tsky^4)/(Tg1-Ta));
hr2=eef*sigma*((Tp1^4-Tgi^4)/(Tp1-Tg1));
Ut=((1/(hc2+hr2))+(1/(hc1+hr1)))^-1;
Ul=Ut+Ub+Ue;
Uls=ki/ti;
hf=kw/di;
hia=Ub;
Tpm = 30 + 0.0175.*(Ic-150) + 1.14*(Ta -25);
a12=(hc1+hr1);
a13=(hc2+hr2);
a11=(a12+a13);
b11=hap;
b12=a13+b11;
m=(Ul/(kp*tpv))^1/2;
fe=tanh(m*((w-do)/2))/(m*((w-do)/2));
Fw=fe*2-1;
de=0.035;
zzz=1/Ul;
zz=1/(Ul*(de+(w-de)*fe));
cb=15;
zx=1/cb;
zc=1/(pi*di*hf);
Upw=zzz/(w*(zz+zx+zz));
c11=(Ac*b11+Upw*Ati*Fw+Ac*hia*fe);
c12=Upw*Ati/2;
c13=Aai*hia*fe;
d11=(Ati*Upw*Fw);
d12=(((Ati*Upw)/2)+(mdot*cw));
d13=((Ati*Upw)/2)-(mdot*cw);
e11=mdot*cw;
e12=mdot*cw+(Rhow*DWC*ff(j)*(deltt/3600)*cw)+Uls*As;
e13=Rhow*DWC*ff(j)*(deltt/3600)*cw;
e14=Uls*As;
Tg1=Tgi+((deltt/mcpg)*Ac)*((In*(1-Gtg))-(a11*Tgi)+(a12*Ta)+(a13*Tpi));
Tp1=Tpi+((deltt/mcpp)*Ac*(Ic-E+a13*Tg1-b12*Tpi+Tci*b11));
Tc1=Tci+((deltt/mcpc)*((b11*Tp1)-(c11*Tci)+(c12*Two)+(c12*Twi)+(c13*Ta)));
Tw1=Two+(deltt/mcpw)*((d11*Tc1)-(d12*Two)-(d13*Twi));
E=Ac*Ic*tapv*pf*Nepv*((1-0.0045*(Tp1-Trf)));
if E<0
E=0;
end
Eff=tapv.*pf.*Nepv.*((1-0.0045.*(Tpm-25)));
TElec=TElec+E*deltt/3600000;
Qu=Ac*(Upw*(Ic*(apv*Gtg)-Ul*(Tp1-Ta)));
if Qu<0.1
Qu=0;
mdot=0;
else
mdot=mfw;
end
if jj>18
```

```
mdot=0;
else if jj<6;
mdot=0;
end
end
TQucl=TQucl+Qu*deltt/3600000;
Aload=(Rhow*cw*DWC*ff(j)*(Tsi-Twba))*deltt;
TQstorage=TQstorage+Aload/3600000;
Fload=(Rhow*cw*DWC*ff(j)*(50-Twba))*deltt;
FQstorage=FQstorage+Fload/3600000;
A12=Uls*As*(Tsi-Ta)*deltt;
TQloss=TQloss+A12/900000;
if Qu<0.0
Qu=0;
mdot=0;
else
mdot=mfw;
end
A11=(Ac*mdot*cw*(Tw1-Twi))/2;
if A11<0
A11=0;
end
TQuseful=TQuseful+A11*deltt/9600000;
Ts1=Tsi+((deltt/mcps)*(e11*Tw1-e12*Tsi+e13*Twba-e14*Ta));
Tgi=Tg1;
Tpi=Tp1;
Tci=Tc1;
Two=Tw1;
Twi=Ts1;
Tsi=Ts1;
COP=(0.4641+((0.36538*Thp2i)-(0.13596*Ta)-
(0.01164*Thp2i.^2)+(0.004564*Ta*Thp2i)+(0.009122*Ta.^2)+(0.00009655*Thp2i.^3*
(deltt/480))+(0.0003286.*Thp2i.^2*Ta)-(0.02829*Thp2i*Ta.^2*(deltt/480))));
Ph=E;
% Pcomp=Phf(j);
Pcomp=Ph;
PHp=PHp+Pcomp/1000;
% Qhp= COP*Phf(j);
Qhp= COP*Ph;
Thp2=Thp2i+((Qhp-(DWC*cw*ff(j)*(Thp2-Ts1))*(deltt/480)-Uls*Ash*(Thp2-
Ta))*(deltt/480)/(Rhow*Vdot*cw));
if Thp2<Ts1
Thp2=Ts1;
else
end
Thp2i=Thp2;
Qwu=(Rhow*cw*DWC*ff(j)*(Thp2-Twba))/360000;
Qwuhp=Qwuhp+Qwu/240;
COP_1(i,j)=COP;
Pcomp_1(i,j)=Pcomp;
Thp_2(i,j)=Thp2;
QHP_1(i,j)=Qhp;
use(i,j)=A11;
Ict(i,j)=In;
Tgt(i,j)=Tg1;
```

```
Tpt(i,j)=Tp1;
Tc111(i,j)=Tc1;
Tw111(i,j)=Tw1;
Ts111(i,j)=Ts1;
Tsw1=Ts1;
Eff111(i,j)=E;
out=Eff111(:);
Tam(i,j)=Tamb;
EEe(i,j)=Eff;
Qu111(i,j)=Qu;
end
end
end
Tqsolar=sum(sum(TIQsolar))
Tqucoll=sum(sum(TQucl))
Tqstored=sum(sum(TQstorage))
Tqusefull=sum(sum(TQuseful))
Telec=sum(sum(TElec))
Tqloss=sum(sum(TQloss))
Fqload=sum(sum(FQstorage))
Tqwuhp=sum(sum(Qwuhp))
Eef=Telec/Tqsolar;
Tef=Tqucoll/Tqsolar
Thotwater=Tqusefull/Tqsolar
% PtHp=sum(sum(PHp))
PVTHPseffan=Tqwuhp/Tqsolar
Tpvtend=Tqusefull/Tqucoll;
rr=1:24;
solf=Tqstored/Fqload;
IclJ17=Ict(17,:);IclF16=Ict(47,:);IclM16=Ict(75,:);IclA15=Ict(105,:);...
IclM15=Ict(135,:);IclJ11=Ict(162,:);IclJu17=Ict(198,:);IclA16=Ict(228,:);...
IclS15=Ict(258,:);IclO15=Ict(288,:);IclN14=Ict(318,:);IclD10=Ict(344,:);...
IclOct15=Ict(288,:);
plot(rr,IclJ17,'k-p',rr,IclF16,'b->',rr,IclM16,'r-<',rr,IclA15,'g-
^',rr,IclM15,'b-',...
rr,IclJ11,'k-d',rr,IclJu17,'c-h',rr,IclA16,'r-s',rr,IclS15,'m--
d',rr,IclOct15,'c-*',...
rr,IclN14,'m-x',rr,IclD10,'g-','linewidth',2,'MarkerSize',6);
xlabel(' time [h]','FontSize',20);
ylabel(' G [w/m-2]','FontSize',20);
% title('monthly average solar irradiation on incliend surface ')
legend('January17','February16','March16','April15','May15','June11','July17'
,.....
'August16','September15','October15','November14','December10')
grid on
xlim([1 24])
pause
clf
%%%Temperature of the glass
Tgaj=Tgt(17,:)';Tgaf=Tgt(47,:);Tgam=Tgt(75,:);
Tgaa=Tgt(105,:);Tgm=Tgt(135,:);TgaJ=Tgt(162,:);Tgaju=Tgt(198,:);TgaU=Tgt(228,
:);Tgas=Tgt(258,:);Tgao=Tgt(288,:);Tgan=Tgt(318,:);Tgad=Tgt(344,:);
plot(rr,Tgaj,'k-p',rr,Tgaf,'b->',rr,Tgam,'r-<',rr,Tgaa,'g-^',rr,Tgm,'b-
',rr,TgaJ,'k-d',rr,Tgaju,'c-h',rr,TgaU,'r-s',rr,Tgas,'m--d',rr,Tgao,'c-
*',rr,Tgan,'m-x',rr,Tgad,'g-','linewidth',2,'MarkerSize',6);
```

```
grid on
legend('January','February','March','April','May','June','July','August','Sep
tember','Octowber','November','December')
ylim([0 40])
xlim([1 24])
xlabel('time [h]','FontSize',20);
ylabel('Tg [o_C]','FontSize',20);
pause
clc
%%%PVT Surface Temprature
TpJ=Tpt(17,:)'; Tpf=Tpt(47,:);Tpm=Tpt(75,:);
Tpap=Tpt(105,:);Tpma=Tpt(135,:);TpJl=Tpt(162,:);Tpju=Tpt(198,:);TpAu=Tpt(228,
:);Tps=Tpt(258,:);Tpo=Tpt(288,:);Tpn=Tpt(318,:);Tpd=Tpt(344,:);
plot(rr,TpJ,'k-p',rr,Tpf,'b->',rr,Tpm,'r-<',rr,Tpap,'g-^',rr,Tpma,'b-
',rr,TpJl,'k-d',rr,Tpju,'c-h',rr,TpAu,'r-s',rr,Tps,'m--d',rr,Tpo,'c-
*',rr,Tpn,'m-x',rr,Tpd,'g-','linewidth',2,'MarkerSize',6);
grid on
legend('January','February','March','April','May','June','July','August','Sep
tember','Octowber','November','December')
xlim([1 24])
ylim([0 60])
xlabel('time [h]','FontSize',20);
ylabel('Tpv [o_C]','FontSize',20);
pause
clf
%%%% Absorber temperature
TclJ17=Tc111(17,:);TclF16=Tc111(47,:);TclM16=Tc111(75,:);TclA15=Tc111(105,:);
...
TclM15=Tc111(135,:);TclJ11=Tc111(162,:);TclJu17=Tc111(198,:);TclA16=Tc111(228
,:);...
TclS15=Tc111(258,:);TclO15=Tc111(288,:);TclN14=Tc111(318,:);TclD10=Tc111(344,
:);...
TclOct15=Tc111(288,:);
plot(rr,TclJ17,'k-p',rr,TclF16,'b->',rr,TclM16,'r-<',rr,TclA15,'g-
^',rr,TclM15,'b--',...
rr,TclJ11,'k-d',rr,TclJu17,'c-h',rr,TclA16,'r-s',rr,TclS15,'m-
d',rr,TclOct15,'c-*',...
rr,TclN14,'m-x',rr,TclD10,'g--','linewidth',2,'MarkerSize',6);
xlabel(' time [h]','FontSize',20);
ylabel(' Tp [o_C]','FontSize',20);
xlim([1 24])
ylim([0 55])
legend('January17','February16','March16','April15','May15','June11','July17'
,.....
'August16','September15','October15','November14','December10')
grid on
pause
clf
%%%water temperature in the PV/T
TwlJ17=Tw111(17,:);TwlF16=Tw111(47,:);TwlM16=Tw111(78,:);
TwlA15=Tw111(105,:);....
TwlM15=Tw111(135,:);TwlJ11=Tw111(162,:);
TwlJu17=Tw111(198,:);TwlA16=Tw111(228,:);....
TwlS15=Tw111(258,:);TwlO15=Tw111(288,:);TwlN14=Tw111(318,:);TwlD10=Tw111(344,
:);
```

```
TwlOct15=Tw111(288,:);
plot(rr,TwlJ17,'k-p',rr,TwlF16,'b->',rr,TwlM16,'r-<',rr,TwlA15,'g-
^',rr,TwlM15,'b--',...
rr,TwlJ11,'k-d',rr,TwlJu17,'c-h',rr,TwlA16,'r-s',rr,TwlS15,'m-
d',rr,TwlOct15,'c-*',...
rr,TwlN14,'m-x',rr,TwlD10,'g--','linewidth',2,'MarkerSize',6);
xlabel(' time [h]','FontSize',20)
ylabel(' Two [o_C]','FontSize',20)
ylim([30 55])
legend('January17','February16','March16','April15','May15','June11','July17'
,.....
'August16','September15','October15','November14','December10')
grid on
xlim([1 24])
ylim([0 55])
pause
clf
%%%hot water PV/T storage tank temperature
Ts1J17=Ts111(17,:);Ts1F16=Ts111(47,:);Ts1M16=Ts111(75,:);Ts1A15=Ts111(105,:);
....
Ts1M15=Ts111(135,:);Ts1J11=Ts111(162,:);
Ts1Ju17=Ts111(198,:);Ts1A16=Ts111(228,:);....
Ts1S15=Ts111(258,:);Ts1O15=Ts111(288,:);Ts1N14=Ts111(318,:);Ts1D10=Ts111(344,
:);
Ts1Oct15=Ts111(288,:);
plot(rr,Ts1J17,'k-p',rr,Ts1F16,'b->',rr,Ts1M16,'r-<',rr,Ts1A15,'g-
^',rr,Ts1M15,'b--',...
rr,Ts1J11,'k-d',rr,Ts1Ju17,'c-h',rr,Ts1A16,'r-s',rr,Ts1S15,'m-
d',rr,Ts1Oct15,'c-*',...
rr,Ts1N14,'m-x',rr,Ts1D10,'g--','linewidth',2,'MarkerSize',6);
xlabel(' time [h]','FontSize',20)
ylabel(' Tsw [o_C]','FontSize',20)
% title('monthly average hotwater storage temeprature ')
legend('January17','February16','March16','April15','May15','June11','July17'
,.....
'August16','September15','October15','November14','December10')
grid on
xlim([1 24])
ylim([0 55])
pause
clf
%%% Electrical Energy
EEJ=Eff111(17,:)';EEF=Eff111(47,:);EEM=Eff111(75,:);EEA=Eff111(105,:);EEMa=Ef
f111(135,:);EEJu=Eff111(162,:);EEj=Eff111(198,:);EEAg=Eff111(228,:);EES=Eff11
1(258,:);EEO=Eff111(288,:);EEN=Eff111(318,:);EED=Eff111(344,:);
plot(rr,EEJ,'k-p',rr,EEF,'c-h',rr,EEM,'r-<',rr,EEA,'g-^',rr,EEMa,'b--
',rr,EEJu,'k-d',rr,EEj,'b->',rr,EEAg,'c-*',rr,EES,'m-d',rr,EEO,'r-
s',rr,EEN,'m-x',rr,EED,'g-','linewidth',2,'MarkerSize',6)
grid on
legend('January','February','March','April','May','June','July','August','Sep
tember','Octowber','November','December')
% title ('Electrical Energy of the system ');
xlabel('Time [h]');
xlim([1 24])
ylabel('Electrical Energy [w/_m2]');
```

```
pause
clf
%%% COP plot
COPJ17=COP_1(17,:);COPF16=COP_1(47,:);COPM16=COP_1(75,:);COPA15=COP_1(105,:);
....
COPM15=COP_1(135,:);COPJ11=COP_1(162,:);
COPJu17=COP_1(198,:);COPA16=COP_1(228,:);....
COPS15=COP_1(258,:);COPO15=COP_1(288,:);COPN14=COP_1(318,:);COPD10=COP_1(344,
:);
plot(rr,COPJ17,'k-p',rr,COPF16,'b->',rr,COPM16,'r-<',rr,COPA15,'g-
^',rr,COPM15,'b--',...
rr,COPJ11,'k-d',rr,COPJu17,'c-h',rr,COPA16,'r-s',rr,COPS15,'m-
d',rr,COPO15,'c-*',...
rr,COPN14,'m-x',rr,COPD10,'g-','linewidth',2,'MarkerSize',6);
xlabel(' Time [h]','FontSize', 12)
ylabel(' COP ','FontSize',12)
title('monthly average Heat Pump COP ')
legend('January17','February16','March16','April15','May15','June11','July17'
,.....
'August16','September15','October15','November14','December10')
grid on
xlim([1 24])
ylim([0 7])
pause
clf
% %%Heat pump Storage water Temperature
TS2J17=Thp_2(17,:);TS2F16=Thp_2(47,:);TS2M16=Thp_2(75,:);TS2A15=Thp_2(105,:);
....
TS2M15=Thp_2(135,:);TS2J11=Thp_2(162,:);
Ts2Ju17=Thp_2(198,:);Ts2A16=Thp_2(228,:);....
Ts2S15=Thp_2(258,:);Ts2O15=Thp_2(288,:);Ts2N14=Thp_2(318,:);Ts2D10=Thp_2(344,
:);
plot(rr,TS2J17,'k-p',rr,TS2F16,'b->',rr,TS2M16,'r-<',rr,TS2A15,'g-
^',rr,TS2M15,'b--',...
rr,TS2J11,'k-d',rr,Ts2Ju17,'c-h',rr,Ts2A16,'r-s',rr,Ts2S15,'m-
d',rr,Ts2O15,'c-*',...
rr,Ts2N14,'m-x',rr,Ts2D10,'g-','linewidth',2,'MarkerSize',6);
xlabel('Time [h]','FontSize',12)
ylabel('Ts2 [0_c]','FontSize',12)
% title('monthly average hot water storage temperature at tank 2 ')
legend('January17','February16','March16','April15','May15','June11','July17'
,.....
'August16','September15','October15','November14','December10')
grid on
xlim([1 24])
ylim([0 90])
pause
clf

%%%% HEAT ABSORBED FROM THE HEAT PUMP
QHPJ17=QHP_1(17,:);QHPF16=QHP_1(47,:);QHPM16=QHP_1(75,:);QHPA15=QHP_1(105,:);
....
QHPM15=QHP_1(135,:);QHPJ11=QHP_1(162,:);
QHPJu17=QHP_1(198,:);QHPA16=QHP_1(228,:);....
```

```
QHPS15=QHP_1(258,:);QHPO15=QHP_1(288,:);QHPN14=QHP_1(318,:);QHPD10=QHP_1(344,
:);
plot(rr,QHPJ17,'k-p',rr,QHPF16,'b->',rr,QHPM16,'r-<',rr,QHPA15,'g-
^',rr,QHPM15,'b--',...
rr,QHPJ11,'k-d',rr,QHPJu17,'c--+',rr,QHPA16,'r-s',rr,QHPS15,'m-
d',rr,QHPO15,'c-*',...
rr,QHPN14,'m-x',rr,QHPD10,'g-+','linewidth',2,'MarkerSize',6);
xlabel(' Time [h]','FontSize',12)
ylabel('Useful Heat of Heat Pump [w/_m2]','FontSize',12)
% title('monthly average Heat Pump Heat Absorbed')
legend('January17','February16','March16','April15','May15','June11','July17'
,.....
'August16','September15','October15','November14','December10')
grid on
xlim([1 24])
ylim([0 250])
```

Appendix E**:** Heat generated by the heat pump on direct electric supply

Fraction type	Constant		Restaurant		Motel	
Selected month	Maximum	Minimum	Maximum	Minimum	Maximum	Minimum
hours	June 11	January 17	June 11	January 17	June 11	January 17
1	0	0	0	0	0	0
2	0	0	0	0	0	0
3	0	0	0	0	0	0
4	0	0	0	0	0	0
5	0	0	0	0	0	0
6	0	0	0	0	0	0
7	226.994	155.072	225.139	154.8784	248.2373	200.9602
8	187.908	131.403	187.623	131.4009	276.9934	216.8928
9	181.555	132.595	199.215	146.862	259.4977	195.2952
10	282.404	214.836	207.853	153.6896	237.7205	177.2699
11	278.471	212.554	208.262	154.9151	226.0801	169.2598
12	270.746	210.096	205.471	154.5373	213.5767	161.159
13	255.184	204.943	205.184	159.3975	206.1995	160.2336
14	217.281	189.84	224.441	201.0748	175.8092	145.7013
15	146.98	176.493	138.277	154.2941	124.0132	135.0567
16	72.641	130.798	67.5321	107.002	65.21755	104.4902
17	30.3758	40.4234	29.1748	36.33771	28.90481	36.48745
18	0	0	0	0	0	0
19	0	0	0	0	0	0
20	0	0	0	0	0	0
21	0	0	0	0	0	0
22	0	0	0	0	0	0
23	0	0	0	0	0	0
24	0	0	0	0	0	0
Total	2150.541	1799.05	1898.172	1554.389	2062.2498	1702.806
Maximum	282.4044	214.836	225.1388	201.07479	276.99338	216.89282
Average	89.60586	74.96061	79.09048	64.766222	85.927073	70.950256